Physiology and Pathology of Neutral Amino Acid Transporters in Renal and Intestinal Epithelial Cells

Thesis submitted for the degree of

Doctor of Philosophy

at the Australian National University

(Research School of Biology)

by

Nadine Tietze

May 26, 2010

Declaration

This thesis is my own work and does not contain results that have been generated by persons other than myself, except where acknowledgment has been made. The results presented in this thesis have not been used for the award of any other degree.

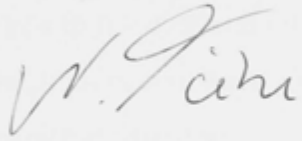

Nadine Tietze

May 26, 2010

Acknowledgements

My first thanks must go to my supervisor Professor Stefan Broer, who provided the grant funding for this PhD research and thesis and helped me with his ideas and support.

I would also like to express my sincerest gratitude to Professor Kiaran Kirk and Professor John Rasko, my co-supervisors, who supported and believed in me during my thesis.

Special thanks to Dr Susan Howitt for her role in providing moral support, guidance and supervision, even though I was not a student of hers.

Many thanks to my past and present fellow members of the Broer lab, who shared knowledge and friendship, some great discussions, fun out-of-lab activities and lots of support. A big thank you especially to Sarojini, my longest lab buddy, for all of this and much more beyond it.

Thank you to the past and present members of the Kirk lab, for being such good next door neighbours, and Rosa and Simon, for sharing the grief and happiness of PhD life and having birthday drinks.

I would like to thank all students and staff at the former BaMBi, which has been an awesome work environment where there is nothing that cannot be discussed and everybody feels welcomed.

Thanks to Dr Carsten Wagner of the University of Zurich, who gave me the opportunity to visit and learn about vesicles and Mrs Gerti Stange, who looked after me, shared her knowledge with me and introduced me to stunning Zurich and her fabulous cooking skills. I also need to thank the whole Physiology Department at the University of Zurich for such a warm welcome.

Special thanks to Mrs Cathy Gillespie, for her huge knowledge and expertise and unending help at the confocal microscopy and Mrs Anne Prins for making beautiful tissue slides and sharing her extensive knowledge of anatomy with me.

Many thanks also go to Jessica Vanslambrouck, for introducing me to immunofluorescence and kindly providing the ASCT2 staining needed for this work.

A big thank you to my friends including but not limited to, Corinna, Michael, Britta, Sarah, Silke, Nicole, Val and the Breakfast Club (Ivana, Steph and Anthie), for proof reading, moral support, helping me to keep sane, listening to me whingeing and just being there for me.

A very big thank you to Allie and Ronnie for the biggest support in all life situations, distraction when needed (for instance introducing me to the allied WW2 comedy 'Allo 'Allo and silly songs), organisation and being best friends. Allie thanks to your patience with Word, this thesis looks like it does.

Thanks to countless people from the ANU Scuba Club and the ANU Volleyball Club who made my stay in Australia special, introduced me to the fantastic oceans around here and gave me time for recreation of the soul and challenges for my body.

A special thank you to Hector, for his endless support, encouragement, fantastic food and always being there for me in the last year, which made the time unique. Also, for his offer to make voodoo charms.

Finally, I would like to thank my family. My mum, for her love and for always believing in me and encouraging me to go my own way, my big sister Sandra, for helping me whenever I needed her and my dad, who never saw me become Dr Kruemel.

Zum Schluss moechte ich mich bei meiner Familie bedanken. Bei meiner Mutter, fuer ihre Liebe, dass sie immer an mich geglaubt hat und mich ermunterte, meinen Weg zu gehen. Bei meiner Schwester, die mir immer geholfen hat, wenn ich sich brauchte und bei meinem Vater, der leider nicht erleben konnte, dass ich Dr Kruemel wurde.

Abstract

About 95 % of nutrient protein is absorbed in the mammalian intestine as amino acids and tri- and dipeptides. Once absorbed by the intestine amino acids are distributed by the circulation throughout the body. In the kidney an ultrafiltrate of the blood plasma is generated from which all amino acids are reabsorbed in the proximal tubule. System B^0 is the main amino acid transport system in these two tissues for broad neutral amino acids.

Four transporters B^0AT1 (SLC6A19), B^0AT2 (SLC6A15), B^0AT3 (SLC6A18) and ASTC2 (SCL1A5) have properties of this system when studied in isolation. B^0AT1 and B^0AT2 co-transport one Na^+-ion and one amino acid substrate. The low-affinity B^0AT1 transporter accepts most neutral amino acids, while the high-affinity transporter B^0AT2 prefers branch-chained amino acids and proline. B^0AT3 prefers alanine and glycine, but has also been reported to transport a variety of neutral amino acids. ASCT2 is a Na^+-dependent antiporter, preferring neutral amino acids except those with an aromatic side-chain. However, in two studies it has been reported that amino acid transport of ASCT2 was inhibited also by phenylalanine. Analysis of ASCT2 function *in vivo* and *in vitro*, has led to the proposal that it represents the molecular correlate of system B^0 in kidney and intestine. Mutations in B^0AT1, however, cause Hartnup disorder, a defect of neutral amino acid transport in kidney and intestine. Thus it is important to reconcile differences and to clarify the contribution of these amino acid transporters to system B^0-like transport in kidney and intestine.

Therefore, the overall aim for this thesis was to investigate the distribution and contribution of B^0AT1 (SLC6A19), B^0AT2 (SLC6A15), and ASTC2 (SCL1A5) to neutral amino acid transport in the kidney.

Immunofluorescence studies revealed localisation of B^0AT1 in the apical membrane of early (S1-S2) segments of the proximal tubule, while B^0AT2 was localised to the apical membrane of the later (S2-S3) segments. This is consistent with physiological data reporting low-affinity transport in early segments and high-affinity transport in later segments of the proximal tubule. ASCT2 was localised in the apical membrane of S2 segments and in the basolateral membrane of the distal tubule.

Transport studies with renal brush border membrane vesicles revealed a dominant transport activity that is consistent with the properties of B^0AT1. This transport activity was lacking in B^0AT1-deficient mice. B^0AT2 activity was excluded by competition studies with selective substrates. ASCT2 activity was excluded due to the lack of additional amino acid transport in brush border membrane vesicles preloaded with ASCT2 amino acid substrates. Therefore, it is concluded that B^0AT2 and ASCT2 do not contribute significantly to neutral amino acid transport in the kidney. B^0AT1 is the main transport activity for neutral amino acid transport in the kidney.

Abbreviations

°C	Degree Celsius
µg	Microgram
µM	Micromolar
A_{260}	Optical density (absorbance) at 260 nm
AA^+	cationic amino acid(s)
AA^0	neutral amino acid(s)
AF	Alexa Fluor®
Aib	Aminoisobutyric acid
AP	Alkaline phosphatase
ATP	adenosine triphosphate
BCH	2-Aminobicyclo [2,2,1]heptane-2-carbocylic-acid
bp	Base pairs
BSA	Bovine serum albumin
ca	circa
CHO	Chinese hamster ovary cells
Ci	Curie
cm	Centimetre
C-terminus	Carboxy-terminus
ddH_2O	Double-distilled water
DEPC	Diethyl pyrocarbonate
DNA	Desoxyribonucleic acid
EDTA	Ethylenediamine tetra-acetic acid
EtBr	Ethidium bromide
FCS	Foetal calf serum
G	gauge
g	Gram
g	Gravity
GABA	γ–aminobutyric acid
GST	Glutathione S-transferase
h	Hour
HEK	Human embryonal kidney cells
IPTG	Isopropyl-β-D-1-thiogalactopyranoside
kb	Kilobase
kDa	Kilodalton
kV	Kilovolt
L	Litre
LB	Luria-Bertani broth
m	Meter

m^2	Square meter
MCS	Multiple cloning site
MeAib	N-Methyl-α-aminoisobutyric acid
mg	Milligram
min	Minute
mL	Millilitre
mm	Millimetre
mM	Millimolar
mmol	Millimol
mV	Millivolt
NaOH	Sodium hydroxide
ng	Nanogram
NGS	Normal goat serum
Nip	Nipecotic acid
nL	Nanolitre
nm	Nanometre
N-terminus	Amino-terminus
OD	Optical density
OR^{2-}	Oocyte Ringer without calcium
OR^{2+}	Oocyte Ringer with calcium
PBS	Phosphate buffered saline
pmol	Picomol
RE	Restriction enzyme
RIPA	Radioimmunoprecipitation assay
RNA	Ribonucleic acid
rpm	Rounds per minute
RT	Room temperature
SDS	Sodium dodecyl sulphate
SDS-PAGE	Sodium dodecyl sulphate polyacrylamide gel electrophoresis
SOB	Super optimal broth
TAE	Tris-actetate/EDTA
U	Unit
UV	Ultra violet
V	Volt
v	Volume
vs	versus
w	Weight
wt	Wild type
Ω	Ohm

Table of Contents

Chapter 1

General Introduction

1.1 Introduction

In all animals, amino acids play a fundamental role in several biological processes, such as biosynthesis of proteins, cell growth and neurotransmission, just to mention a few. Special membrane proteins mediating amino acid transport into and out of the cell are necessary, as the hydrophobic nature of the membrane restricts the movement of amino acids across it. Hence those membrane proteins are essential for life.

1.2 Short history of the discovery of amino acid transport systems and their nomenclature

In mammalia, absorption and reabsorption of nutrients for nutrient homeostasis of the organism primarily takes place at two sites: in the small intestine and in the renal proximal tubule. Proteins are a major part of the human diet. They are taken up as part of our nutrition and are then partially hydrolysed by enzymes secreted by the stomach and intestine to form oligopeptides. These are digested further by brush border peptidase into amino acids, tri- and dipeptides. All three compounds are taken up by enterocytes of the small intestine.

In the enterocytes, peptides are hydrolysed and the resulting amino acids are released together with those absorbed directly, into the blood. Through the bloodstream, the amino acids are transported to every tissue in the body. Protein digestion and absorption is an efficient process. Less than 4 % of ingested nitrogen leaves the body in faeces. Also, only minimal amounts of amino acids are wasted in urine due to efficient reabsorption of amino acids from the primary urine. As a result less than 5 % of all ingested amino acids are discarded (Matthews, 1991).

Processes of nutrient into cells or across epithelial cells have been the subject of intensive research over several decades (reviewed in (Kilberg, 1982; Palacin *et al.*, 1998; Broer, 2008). Over the years, several mechanisms were discussed for those processes. However, it is now established that absorption of nutrients is mostly an active process occuring against a concentration gradient. It involves several specific transporters that meditate transport of amino acids, peptides, sugars, lipids and other nutrients for the body.

Already by the beginning of the twentieth century basic studies of amino acid transport into animal cells were conducted. In 1913, it was shown that amino acids can be accumulated against a concentration gradient in tissues (Van Slyke, 1913). Later, in the 1960s, more detailed information on transport processes in non-epithelial cells was elucidated by the work of the Halvor Christensen Laboratory (Oxender and Christensen, 1963). Their work showed that amino acid transporters are more likely to accept groups of similar amino acids than just single amino acids as substrates (reviewed in (Christensen, 1984; Christensen, 1990). Further investigations established a variety of transport activities using intact tissue, primary cell cultures, cell lines and preparations of cell membranes, such as brush border membrane vesicles or proteoliposomes.

In this period, before the onset of molecular cloning, some important concepts were discovered. For instance, it was shown that amino acids can be taken up against a concentration gradient into epithelial cells and that this transport often required a Na^+-gradient across apical membranes (Crane, 1965). Additionally, based on work in the 1960s, amino acid transport activities were identified and were classified as systems with abbreviations indicating their substrate specificity, which was usually broad and overlapping. This system is still in use today to describe amino acid transport activities in cells and tissues. Accordingly, the amino acid transport activity preferring leucine and other large hydrophobic neutral amino acids has been referred to as system L (Le Cam and Freychet, 1977). System A indicates a transporter preferring alanine and other small and polar neutral amino acids (Le Cam and Freychet, 1977) and system ASC denotes an alanine, serine and cysteine preferring transporter (Christensen *et al.*, 1967) .

A different nomenclature was used for systems transporting cationic amino acids and anionic amino acids. x denotes a transporter for anionic amino acids, while y denotes a cationic amino acid transporter. In this nomenclature, z refers to neutral amino acids. Upper case acronyms are used for Na^+- dependent transporters while lower case acronyms are used for Na^+- independent transporters, with the exception of system L and system T, which are in fact Na^+- independent (reviewed in (Verrey *et al.*, 2005).

However, many of the classic systems introduced by the Christensen's group did not match with the transport activities in epithelial cells, resulting in the definition of further systems (Broer, 2002). The new systems were referred to as the neutral system (B^0 for kidney or neutral brush border (NBB) for intestine nomenclature) mediating transport of neutral amino acids, the basic system ($b^{0,+}$), transporting cationic amino acids and cystine, the imino(glycine) system mediating uptake of proline, hydroxyproline and glycine and the acidic system ($X^-_{A,G}$) transporting aspartate and glutamate.

In 1990 the identification of the first mammalian amino acid transporter cDNA, encoding a GABA transporter in the human brain (Guastella *et al.*, 1990), started a cascade of efforts to identify amino acid transporter cDNAs. The cloning of the first gene for an α–amino acid transport protein, which mediated transport of cationic amino acids (Kim *et al.*, 1991; Wang *et al.*, 1991) was another breakthrough in this field. Subsequently, with the development of new molecular biological techniques together with the oocyte expression systems and homology screening, the door to the identification of genes for plasma membrane amino acid transporters was opened. It subsequently was shown that the cloned amino acid transporters matched the physiologically identified systems. Initial genomic analysis of amino acid transporter gene sequences demonstrated that these could be grouped into twelve solute carrier families (Hediger *et al.*, 2004). However, some cloned transporters could not be assigned to a classic system. The human Genome Organisation (HUGO) Nomenclature Committee Database provides a list of transporter families of the solute carrier gene series. Currently it includes 48 families.

Due to changes and inconsistency in the nomenclature, cDNA annotation is confusing at times. To facilitate this overview, Table 1 summarises the major amino acid transporter systems of mammalian epithelial cells together with their mediators, substrate specificity, mechanisms and mediating ions.

Table 1.1: Major epithelial amino acid transport systems, their substrate specificities and mechanisms.

Classic System	cDNA	SLC number	Amino Acid Substrates	Analogues	Mech-anism	Coupling Ions
A	SNAT1	SLC38A1	G, A, S, C, Q, N, H, M	MeAIB	S	Na^+
	SNAT2	SLC38A2	G, P, A, S, C, Q, N, H, M	MeAIB	S	Na^+
	SNAT4	SLC38A4	G, A, S, C, Q, N, M, AA^+	MeAIB	S	Na^+
ASC	ASCT1	SLC1A4	A, S, C, T	Cysteic acid	A	Na^+
	ASCT2	SLC1A5	A, S, C, T, Q	Cysteic acid	A	Na^+
asc	asc1/4F2hc*	SLC7A10	G, A, S, C, T	D-AA^0	A	-
B^0	B^0AT1	SLC6A19	AA^0	BCH	S	Na^+
	B^0AT2	SLC6A15	P, L, V, I, M	BCH	S	Na^+
$B^{0,+}$	$ATB^{0,+}$	SLC6A14	AA^0, AA^+, β- A	BCH	S	Na^+, Cl^-
$b^{0,+}$	rBAT/$b0^+AT^+$	SLC7A9	R, K, O, Cystine		A	-
β	TauT	SLC6A6	Tau, β– A		S	Na^+, Cl^-
Gly	B^0AT3/XT2	SLC6A18	G, AA^0		S	Na^+, Cl^-
	GlyT2	SLC6A9	G		S	Na^+, Cl^-
IMINO	IMINO/SIT1	SLC6A20	P, HO-P	MeAIB	S	Na^+, Cl^-
L	LAT1/4F2hc*	SLC7A5	H,M, L, I, V, F, Y, W	BCH	A	-
	LAT2/4F2hc*	SLC7A8	AA^0 except P	BCH	A	-
	LAT3	SLC43A1	L, I, M, F	BCH	U	-
	LAT4	SLC43A2	L, I, M, F	BCH	U	-
N	SNAT3	SCL38A3	Q, N, H		S	Na^+ (S), H^+(A)
	SNAT5	SLC38A5	Q, N, H, S, G		S	Na^+ (S), H^+(A)
PAT	PAT1	SLC36A1	P, G, A, GABA, β-A	MeAIB	S	H^+
	PAT2	SLC36A2	P, G, A		S	H^+
Phe	?	?	F, M			-
T	TAT1	SLC16A1	F, Y, W		U	-
X^-_{AG}	EAAT1	SLC1A3	E, D		S	Na^+ (S), H^+(A)
	EAAT2	SLC1A2	E, D	D-Asp	S	Na^+ (S), H^+(A)
	EAAT3	SLC1A1	E,D	D-Asp	S	Na^+ (S), H^+(A)
x^-_c	xCT/4F2hc*	SLC7A11	E, C^-		A	-
y^+	CAT1	SLC7A1	R, K, O, H		U	-
y^+L	y^+LAT1	SLC7A7	K, R, Q, H, M, L		A	Na^+ (S AA^0)
	y^+LAT2	SCL7A8	K, R, Q, H, M, L, A, C		A	Na^+ (S AA^0)

The genes coding for a transport activity are shown. Systems are classified in the solute carrier (SLC) series according to www.bioparadigms.org/slc/menu.asp and the HUGO Nomenclature Committee database (www.genenames.org/). The amino acid substrates are given in one-letter codes with neutral amino acids (AA^0), cationic amino acids (AA^+), ornithine (O) and hydroxyproline (HO-P). The transport mechanisms are: antiport (A), symport (S) und uniport (U). *Heterodimeric transporter: for achieving transport activity association with SLC3A2 is essential. Information presented in this table was taken from ((Broer, 2008)), with additional information referring to literature by (Palacin *et al.*, 1998) and (Singer *et al.*, 2009).

1.3 Organisation and anatomy of the kidney and the intestine

As mentioned before, the two major sites for reabsorption and absorption of nutrients are the kidney and the small intestine. Here, transporters assist in amino acid absorption across epithelial cell layers into the bloodstream. It is known that transporter function and activity changes along the intestine and along the kidney nephron. (Scriver and Tenenhouse, 1985)

Therefore, it is essential to investigate the distribution of those transporters in their organs, for instance by immunofluorescence to gain information about their function. This anatomy section will mostly refer to the human kidney and intestine since it is wildly described although it is generally transferrable to other mammals. In particular, to mice, which form the subject of the investigations described in this thesis.

1.3.1 The kidney

The kidney has three essential functions for the body. Firstly, it is the body's blood filter, removing metabolic waste products and toxins, such as creatinine and urea from the blood and disposing them via the urine. Secondly, it regulates electrolyte balance thus contributing to whole body homeostasis. Thirdly, it produces or activates hormones that regulate blood pressure, calcium metabolism and production of red blood cells (Evans *et al.*, 1995).

The anatomy of the kidney is shaped according to its functions. The kidneys are paired, bean shaped organs which are located behind the peritoneum on each side of the vertebral column, usually extending from the 12^{th} thoracic to the third lumbar vertebra. The size of the kidney is dependent on the body weight usually forming less than 0.5 % of the total body weight. An average human kidney is 12 cm in length while a mouse kidney is less than 1 cm.

The macroscopic structure of the kidney is shown in Figure 1.1. Each kidney is covered by a fibrous capsule. The capsule contains an opening, the hilus, accommodating the entry point for the renal artery and nerves and the exit point for the renal vein and the ureter. The hilus opens up into a space referred to as the renal sinus. The renal pelvis, a urine filled space, with its extensions, the major and minor calyces, are part of this renal sinus as well as blood vessels and nerves. The kidney itself can be divided into two layers, the cortex and the medulla. The cortex is the more granular outer region and consists of glomeruli - tiny clews of capillaries and a large number of tubules formed from epithelial structures. The medulla is the inner region and lacks glomeruli. It possesses an arrangement of tubules and blood vessels. The medulla can be subdivided into conical renal pyramids. Usually 8 to 18 of those pyramids are found in one kidney. The base of each pyramid faces the cortex while the tip of each pyramid ends into the renal pelvis. The urine flows through perforations from the pyramids into the minor calyces of the renal sinus (Boron and Boulpaep, 2005).

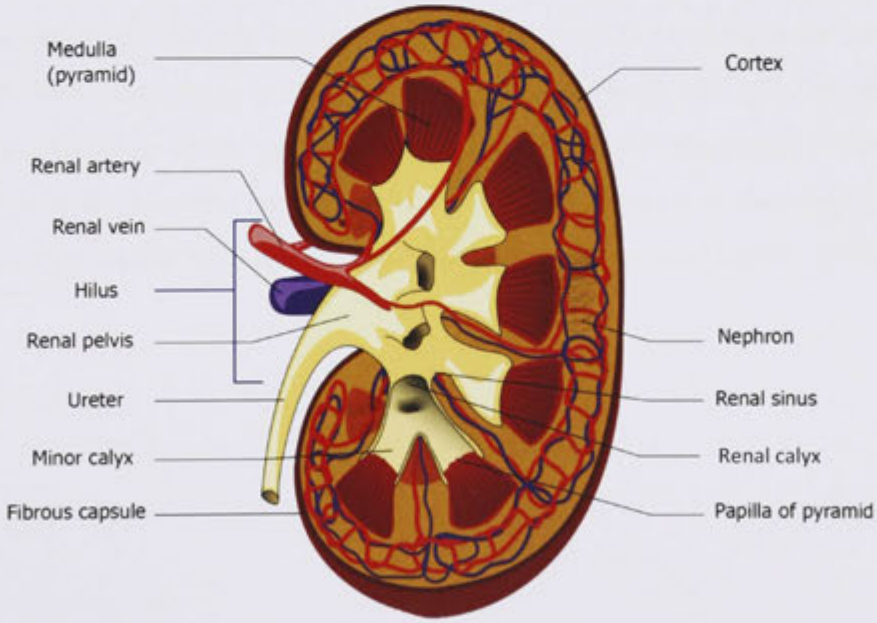

Figure 1.1: Macroscopic structure of the kidney.

Depicted are the different layers of the kidney, the capsule, the cortex, the medulla and the renal pelvis with sub-structures. Also shown is the renal pelvis making the exit and entrance to the kidney.

(Figure adapted from Boron and Boulpaep, 2005)

The functional unit of the kidney is the nephron (Figure 1.2). Each kidney contains up to 1,200,000 nephrons located mainly in the cortex and the medulla. Each nephron consists of a cluster of blood vessels, the previous described glomerulus and a tubule, an epithelial structure of many different subdivisions. The two parts are connected with each other via the Bowman's capsule or the glomerular capsule. It contains the Bowman's space which is the continuation of the tubule and regulates the pressure of the glomerulus (Mbassa *et al.*, 1988). In the Bowman capsule and the Bowman space the filtrate enters the tubule system from the vascular system.

The remaining part of the nephron consists of subdivisions of the tubule. The subdivisions are: the proximal tubulus (subdivided into the proximal convoluted tubule (PCT) and the proximal straight tubule (PST)), the thin descending and ascending loop of Henle, the thick ascending loop of Henle, the distal convoluted tubule, the connecting tubule and the initial collecting tubule. Each nephron individually possesses these subdivisions, while the following can be shared by two or more nephrons: the cortical collecting tubule, the outer medullary collecting duct and the inner medullary collection duct, which leads into the duct of Bellini. There are two types of nephrons: superficial nephrons, where most of the nephron is located in the cortex of the kidney and only short loops extend into the inner medulla and juxtaglomerular nephrons, with long loops that extend far into the medulla (Smith, 1951; Kriz and Bankir, 1988; Seldin, 2000).

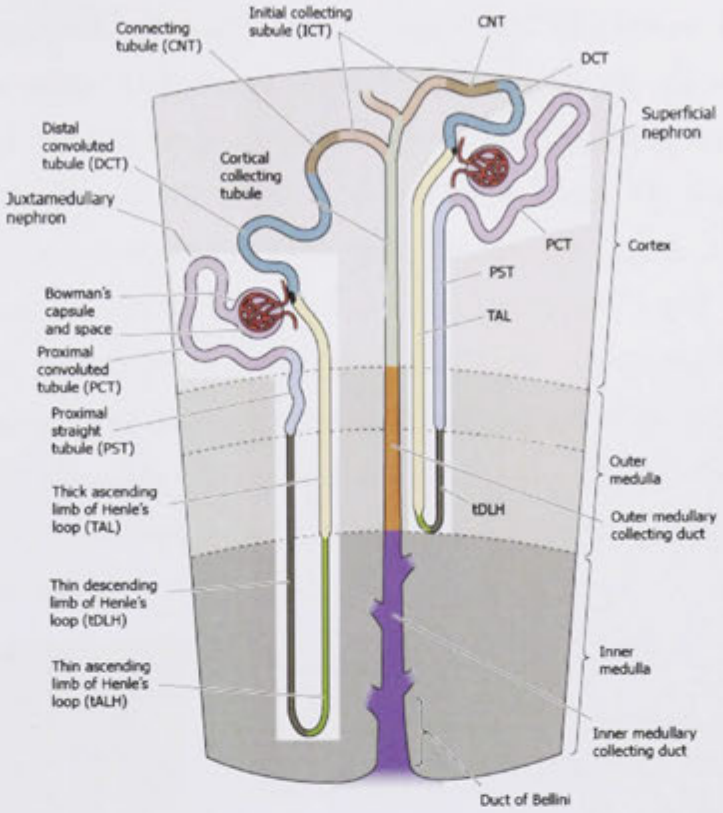

Figure 1.2: Structure of the nephron.

The two different types of nephrons are shown with their subdivisions glomerulus, proximal and distal tubulus connected by the loop of Henle and the different parts of the collecting duct.

(Figure adapted from Boron and Boulpaep, 2005)

The proximal tubulus can be further subdivided into different parts as shown in Figure 1.3. An understanding of the structure of this subdivision is necessary to understand the immunolocalisation experiments and the role of amino acid transporter distribution in Chapter 3. In low magnification the proximal tubulus consists of the proximal convoluted tubulus (PCT) and the straight proximal tubulus (PST). However, closer examination reveals a more detailed division into segments referred to as S1, S2 and S3. The S1 segment starts at the glomerulus and contains the first portion of the PCT. The cells are easy to distinguish from those of the other two segments since the glomerulus is easy to identify in kidney sections. The S2 segment starts after the S1 segment in the second half of the PCT and continues into the first half of the PST while the S3 segment covers the second half of the PST.

To distinguish between the S2 and the S3 segment, the cell morphology must be compared. From the S1 to the S3 segment, the epithelial cells become progressively thinner. This correlates with the decrease of reabsorption rates along the tubule. Furthermore, the brush border membrane of the different segments is gradually less developed and the basolateral membrane possesses a smaller cell membrane area (Smith, 1951; Kriz and Bankir, 1988; Seldin, 2000; Boron and Boulpaep, 2005). It is well known that the distribution of the transporters in these three segments is characteristic for each substrate. Transporters in the earlier segments of the proximal tubule have high capacity and usually broader specificity but lower affinity for their substrates, while transporters in the later segments of the proximal tubule possess lower capacity but higher affinity with an usual narrower substrate specificity (Scriver and Tenenhouse, 1985).

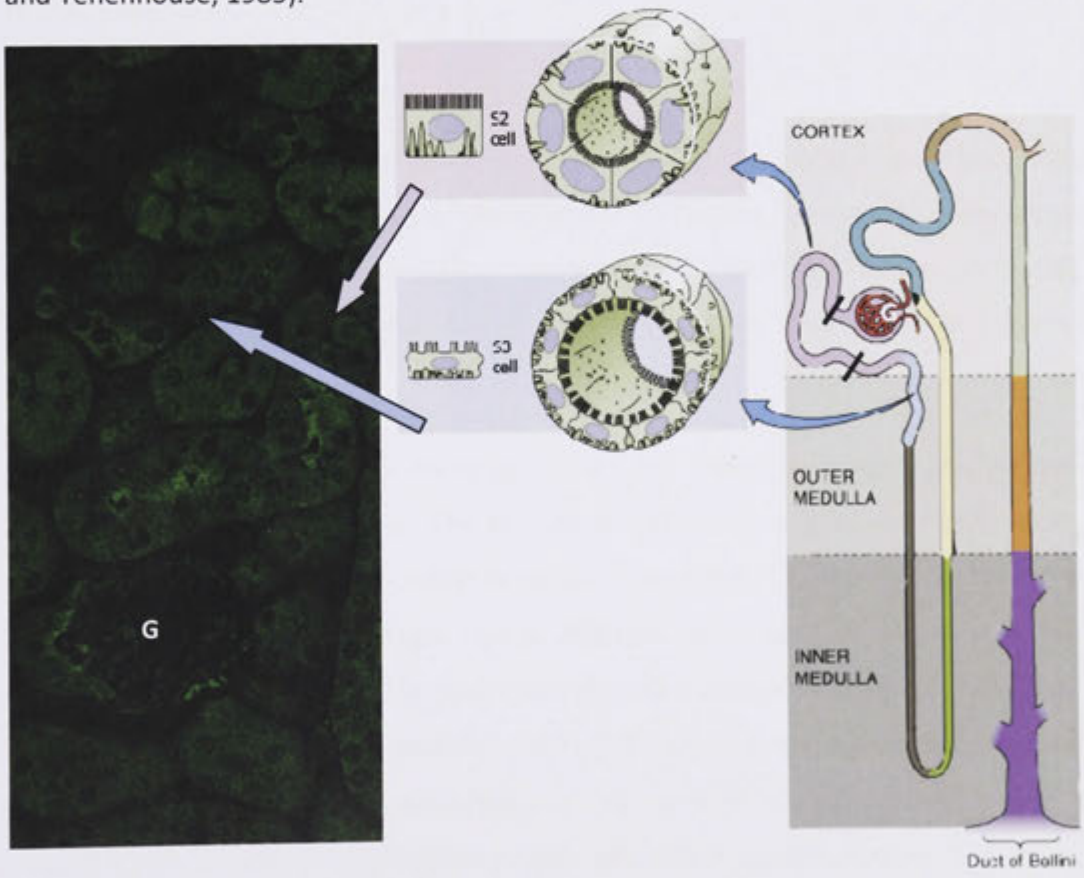

Figure 1.3: Nephron with the structure of tubule cells S2 and S3.

Depicted is a nephron and the subdivision of the proximal tubule into the segments S1 to S3 (the black lines mark the division of the nephron into the different segments) with the corresponding cell structure for S2 and S3 as described in the text above. G indicates a glomerulus, the adjacent cell to the lef is a S1 cell.

(Figure adapted from Boron and Boulpaep, 2005)

1.3.2 The Intestine

The major functions of the intestine are to absorb nutrients from digested food while discarding waste out of the body. The intestine is a convoluted tube extending through the abdominal cavity from the pyloric sphincter to the anus. It is proceeded by the stomach, the oesophagus and the mouth. In humans it consists of two segments, the small and the large intestine. The intestine averages about 8 m in human and about 25cm in mice but it differs according to size, gender and age of the person or mouse.

The wall of the intestine is composed of the mucosa, submucosa, muscularis and serosa (Figure 1.4). However, they possess structural differences in the two segments of the intestine.

1.3.2.1 The small intestine

Within the twisted loops of the small intestine, digestion is completed and absorption of the majority of nutrients occurs. The diameter of the small intestine is only about half that of the large intestine, reaching an average of 3.5 cm in human and an average of 2-3 mm in mice. It can be divided into three regions: the duodenum, the jejunum and the ileum.

The microscopic anatomy and histology of the small intestine is highly adapted for nutrient absorption (Figure 1.4). The mucosa is composed of a layer of epithelium, lamina propria and lamina muscularis mucosae. The epithelial layer itself consists of a simple epithelium, which contains several different cell types. The absorptive cells digest and absorb nutrients while goblet cells secrete mucus lubricating the passage of food. The epithelial layer also contains deep crevices, which are lined with glandular epithelium. Cells secreting intestinal juice are referred to as intestinal glands or crypts of Lieberkühn. The glands also contain paneth cells, which secret lysozyme. The lamina propria contains connective tissue and a mucosa associated lymphoid tissue while the muscularis mucosae consists of smooth muscles.

The submucosa of the duodenum contains special Brunner's glands, which secrete an alkaline mucus supporting the neutralisation of gastric acid. Generally the submucosa contains nerves, blood vessels and elastic fibre with collagen which maintains the shape of the intestine even if the intestine stretches. The muscularis of the small intestine consists of two layers of smooth muscles. The inner, thicker layer contains circular fibres while the outer, thinner layer contains longitudinal fibres. The serosa surrounds most of the small intestine except a portion of the duodenum. It is made up from loose connective tissue and is coated by the mucosa to prevent damage.

The special structural modifications of the small intestine are revealed in the anatomy of the wall, which contains circular folds or so called plicae circularis, villi and microvilli. The circular folds are deep folds of the mucosa and submucosa. They are permanent and cause a spiral movement of the food pulp rather than a movement in a straight line, allowing more time for full nutrient absorption.

The villi are finger-like projections of the mucosa. This structure amplifies the absorptive structure enormously to a total of 400 to 500 m^2. The villi are large in the duodenum and become smaller through the intestinal system. Each villus has a cover of epithelial cells and a core of lamina propria. Within the lamina propria there are blood capillaries and lymph capillaries, the so called lacteal. Absorption of nutrients takes place through the epithelial cells into both blood and lymph capillaries.

The last feature, the microvilli are a projection of the apical membrane of the absortive cells of the mucosa. They form the fuzzy layer of the brush border, which increases the absorption area further and extend into the lumen of the small intestine. The brush border membrane has two major roles. Firstly, it contains several enzymes assisting with the digestion and secondly it possesses embedded transporters important for absorption of the digested nutrients (Boron and Boulpaep, 2005; Marieb and Hoehn, 2008; Tortora and Derrickson, 2009).

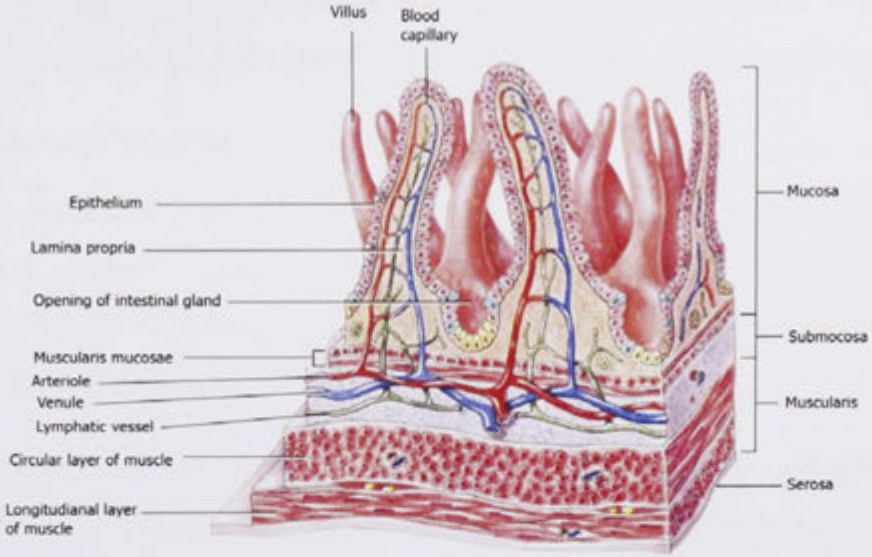

A

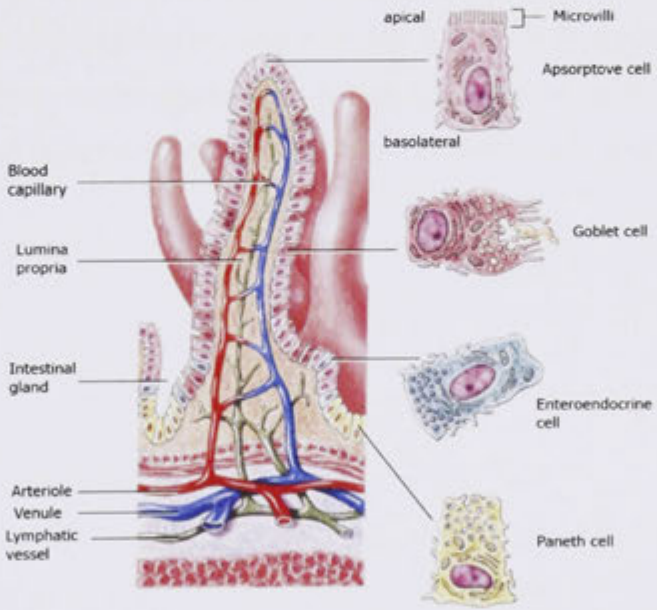

B

Figure 1.4: Histology of the small intestine.

The Figure shows the four layers of the intestine, named mucosa, submucosa, muscularis and serosa together with the structure of the villi.

A: Gross anatomical structure of the small intestine.

B: Enlarged villus structure showing the localisation of the different epithelial cells.

(Figure adapted from (Tortora and Derrickson, 2009)

The small intestine eventually opens into the large intestine, which will be only briefly mentioned here, since it is not a site of amino acid absorption, the focus of this study.

1.3.2.2 The large intestine

The function of the large intestine is to reabsorb some nutrients, such as short chain fatty acids or electrolyte and to remove the remaining water from the digested food and compress and discard the resulting faeces. It can be divided into four regions: cecum, colon, rectum and anal canal.

The wall of the large intestine differs from the small intestine in several points. For instance, the large intestine does not contain any circular folds, villi or microvilli and no cells secreting digestive enzymes since most nutrients are absorbed before reaching the large intestine. Furthermore, the mucosa is thicker and the large intestine has deeper crypts containing a higher number of goblet cells. They produce a higher dose of mucus allowing an easier passage of the digested food through the large intestine into the anal canal before it is discarded (Tortora and Derrickson, 2009).

1.4 Neutral amino acid transport in kidney and intestine epithelial cells

The absorption or transport of amino acids in epithelial cells of the intestine is an evolutionary old process and exists in most organisms, while absorption or transport of amino acids in the epithelial cells of the renal proximal tubule cells is an evolutionary late invention found in higher vertebrates. It has been shown that transport mechanisms are not conserved within mammalian families and can be easily adapted to physiological demands in evolution via mutations (Broer, 2002; Veljkovic *et al.*, 2004). To understand the different transport mechanisms, it is essential to investigate the physiology and the cells they are localised in.

Epithelial cells possess tight junctions that form a selective barrier between the individual cells of the epithelium. These junctions prevent random diffusion, for instance, backflux of amino acids across the epithelial cell layer and they also form a boundary between the apical and basolateral regions of the cell membrane. In epithelial cells, transporters exist in two different membrane locations: the apical and the basolateral membrane.

Both plasma membranes are different in almost every aspect, for instance in morphology, protein-, lipid-, carbohydrate-composition and transport properties. The transporters on the apical and basolateral membrane cooperate in the absorption of nutrients, albeit the apical transporters are more investigated than basolateral transporters due to their accessibility for studies. Vesicles derived from the basolateral membrane (BLMV) were introduced by Hopfer *et al.* (Hopfer *et al.*, 1976) and had limited use.

Transport functions across the apical membrane in the kidney are well studied. It has been shown that accumulation of most neutral amino acids in kidney brush border membrane vesicles (BBMV) requires a Na^+-electrochemical gradient (Evers *et al.*, 1976; Fass *et al.*, 1977). Proline and glycine are the exception, which transport is proton driven in some species.

Furthermore, the combined evidence from different experimental approaches (Young and Edwards, 1966; Young and Freedman, 1971; Silbernagl *et al.*, 1975) led to an acceptance that a low affinity Na^+-dependent neutral amino acid transporter (system B^0) is present in the proximal tubule of the kidney (Doyle and McGivan, 1992a; Doyle and McGivan, 1992b).

Additionally, heterogeneity of neutral amino acid transport has been reported in the kidney (Kragh-Hansen and Sheikh, 1984). For instance, a low affinity uptake of serine was observed in the PCT and a high affinity transport system was observed in the PST. Similar observations were made for phenylalanine (Kragh-Hansen *et al.*, 1984) and branched chain amino acid transport (Jorgensen *et al.*, 1990), suggesting that a variant of the system B^0 is expressed in the PST. Also, a system with similar characteristics to system ASC was reported to be present in the kidney apical membrane after solubilisation and reconstitution into liposomes of membrane transporters from rat kidney BBMV (Oppedisano *et al.*, 2004).

Only a limited number of studies were conducted with BLMV. A high affinity transport system was found in the basolateral membrane of the kidney with properties similar to system L. It preferred branched chain amino acids and aromatic amino acids, and was also inhibited by 2-Aminobicyclo[2,2,1]heptane-2-carbocylic-acid (BCH), all of which is consistent with a system L transporter. The transporter mechanism was that of an entirely Na^+-independent, electroneutral uniporter (Lash and Jones, 1984). This transport activity has not been identified at the molecular level so far.

In BLMV derived from rat small intestine, a Na^+-independent transporter of broad specificity was identified by Mircheff *et al.* (Mircheff *et al.*, 1980). The transporter had properties similar to system L. The heterodimeric LAT2/4F2 transporter has been identified as part of this activity (Pineda *et al.*, 1999).

LAT2 requires the glycoprotein heavy chain (hc) 4F2hc (SLC3A2, also known as CD98), to be present in the basolateral membrane of kidney and intestine. It is required for trafficking of the transporter to the membrane (Nakamura *et al.*, 1999; Pineda *et al.*, 1999; Rossier *et al.*, 1999; Rajan *et al.*, 2000). It transports neutral amino acids except proline with an antiport mechanism.

Transporters for neutral amino acids in the intestine have been studied in detail, especially that of alanine (Curran *et al.*, 1967). Similar to the kidney apical membrane, transport of neutral amino acids in the intestine is Na^+-dependent and no accumulation occurrs in the absence of Na^+-ions (Cohen and Huang, 1964; Schultz *et al.*, 1967).

Most groups have proposed one transporter for neutral amino acid transport in the intestinal epithelium (Newey and Smyth, 1964; Preston *et al.*, 1974) with only Sepulveda and Smith (Sepulveda and Smith, 1978) proposing two transport systems for neutral amino acids in rabbit epithelium. BBMV studies confirmed a Na^+-dependent transporter for most neutral amino acids. This system was named system B or NBB, to indicate the similarity to the kidney transporter (Satoh *et al.*, 1989; Maenz and Patience, 1992). Additionally, a system ASC-like activity was detected in the rabbit ileum (Maenz *et al.*, 1992; Munck and Munck, 1999).

Neutral amino acid transporter activity was detected in the intestinal basolateral membrane and showed properties similar in general to those found in the kidney (Mircheff *et al.*, 1980; Wilde and Kilberg, 1991). It has been reported that glutamine uptake across the intestinal basolateral membrane was Na^+-dependent and had properties of system A (Taylor *et al.*, 1989; al-Mahroos *et al.*, 1990; Wilde and Kilberg, 1991).

This glutamine uptake was inhibited by other small amino acids and by the amino acid analogue MeAiB. It was hypothesised that the system A transporter SNAT2, which is expressed in the intestine (Hatanaka *et al.*, 2000; Sugawara *et al.*, 2000), provides this function. Interestingly, SNAT2 is also expressed in the renal medulla (Reimer *et al.*, 2000) and smaller amounts are also found in the renal cortex, but have not been localised further.

Figure 1.5 gives a general overview over the described transporter system in the kidney and the small intestine.

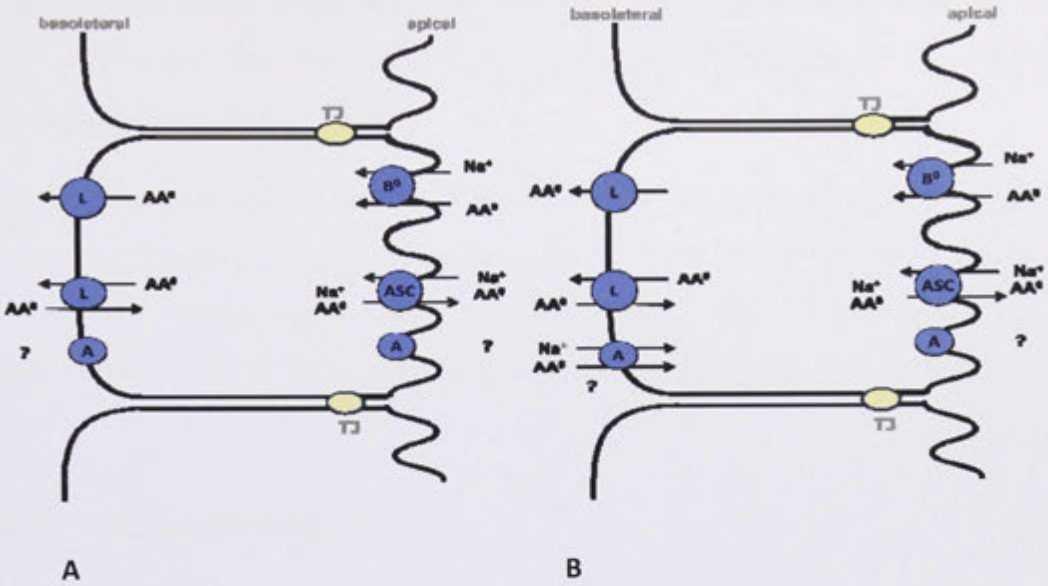

Figure 1.5: Scheme of apical and basolateral transporter activities for neutral amino acid absorption.

Neutral amino acid transporter activities involve in neutral amino acid absorption in kidney (**A**) and intestine (**B**). Letters inside the circles refer to the amino acid transport systems as defined in Table 1.1. TJ: tight junctions; AA^0: neutral amino acids; Na^+: sodium-ion.

1.4.1 Solute carrier families

As described above, transporters in mammalian cells are categorised on the basis of their sequence similarity into solute carrier families (SLC). To date 48 of these families with a total of 368 members have been identified (Hediger *et al.*, 2004); http://www.bioparadigms.org/slc).

Over the years, different candidates have been suggested as being involved in the B^0-like transport activity in the kidney and intestine. To date, the transporters involved in neutral amino acid transport belong, amongst others, to solute carrier family 1 and solute carrier family 6. Three members of these families will be investigated in this study.

1.4.2 Solute carrier family 6

Members of the solute carrier family 6 (SLC6), which is larger than solute carrier family 1 and hence mentioned here first, transport amino acids, neurotransmitters, taurine and creatine (Chen *et al.*, 2004). The SLC6 belongs to a larger superfamily of transporters with members found in all animals and some bacteria, which maintain sodium gradients, but is not found in plants, fungi and yeast (Saier, 2000). The SLC6 family currently possesses 20 confirmed members and two pseudo genes. The members can be further classified into four subfamilies (Figure 1.6) referred to as the monoamine transporter branch, the GABA transporter branch, the amino transporter branch and the amino acid transporter branch (II), previously known as the 'orphan transporter branch'. Since the first members of this family to be discovered were transporters for GABA, noradrenaline, dopamine and serotonin, the family is referred to as the neurotransmitter transporter family.

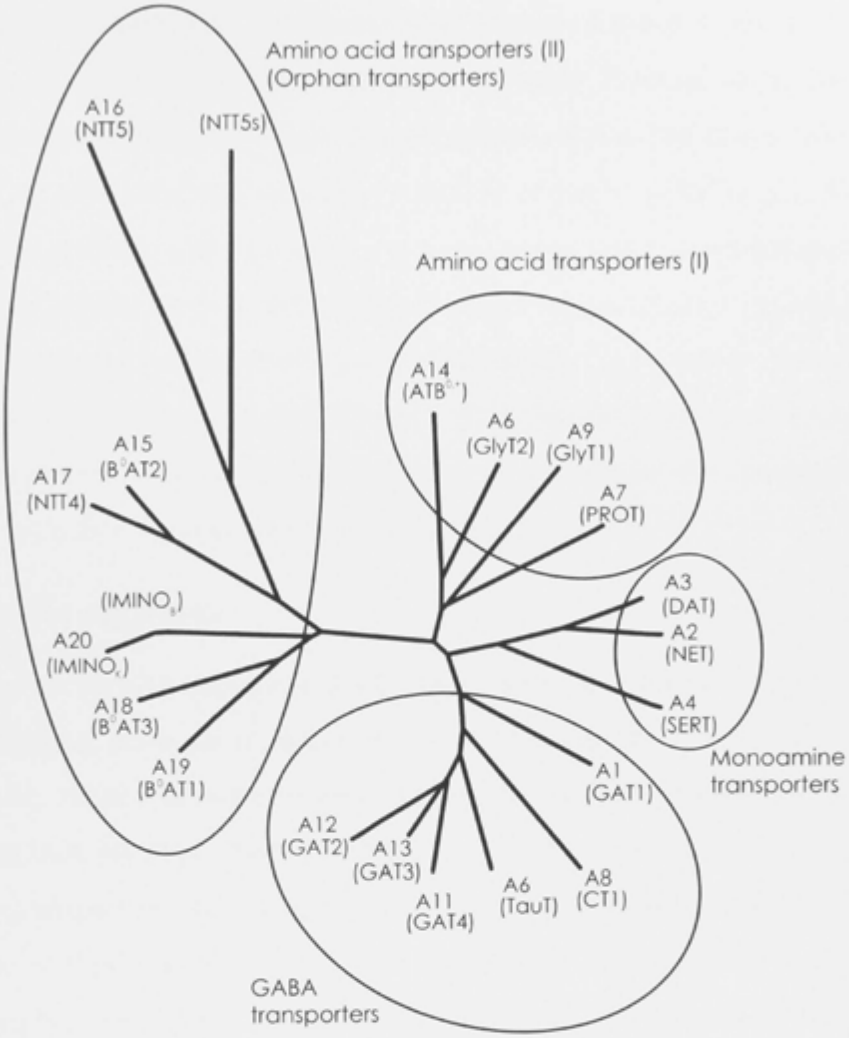

Figure 1.6: Tree of the mouse SLC6 family.

The tree shows all 20 members of the mouse SLC6 family (A1- A20) with their respective names and aliases. Note that the mouse SLC6A10, -a creatine transporter- does not have a correlate in the human genome. Also, in mouse the transporters members A16 and A20 seem to have two genes for this locus.

(Figure is adapted from (Broer, 2006))

Initially it appeared that the members of the SLC6 family were Na^+- and Cl^--dependent. It was also thought that the transport stoichiometry was the same for all family members, namely 2 Na^+ : 1 Cl^- : 1 substrate as shown for instance for the GABA transporter (Loo *et al.*, 2000). However, this notion could not be sustained when different transport mechanisms were elucidated (Broer, 2002). In fact, the number of co-transported Na^+-ions varies from one to three.

Furthermore, the serotonin transporter SERT also carries out K^+-antiport (Rudnick, 1998). The SLC6 members share the same predicted topology comprising twelve transmembrane helices and a length of approximately 500 to 700 amino acids (Chen *et al.*, 2004). In 2005, the high-resolution structure of the bacterial $LeuT_{AA}$ transporter from *Aquifex aeolicus* was elucidated, the sequence of which is homologous to SLC6 transporters (Yamashita *et al.*, 2005). This allowed the generation of homology models for SLC6 transporters and confirmation of substrate and ion-binding sites of different mammalian SLC6 transporters (O'Mara *et al.*, 2006). The SLC6 members investigated in this thesis are B^0AT1 and B^0AT2. B^0AT3 will also be discussed in the context of its renal function. The other members are reviewed in (Broer, 2006).

1.4.2.1 B^0AT1 (SLC6A19)

The neutral amino acid transporter B^0AT1 (also previously known as XT2s1 or XTRP2s1) is the molecular correlate of system B^0. It was initially cloned from mouse kidney (Broer *et al.*, 2004) and was characterised using flux studies and electrophysiological techniques (Bohmer *et al.*, 2005; Camargo *et al.*, 2005). It was named according to the mediated transport of a broad (B) variety of neutral (0) amino acids with a preference for large, aliphatic amino acids, such as leucine. The order of preference is methinone=leucine=isoleucine=valine>glutamine=asparagine=phenylalanine=cysteine =alanine>serine=glycine=tyrosine=threonine=histidine=proline>tryptophan>lysine. The substrate $K_{0.5}$ values range from 1 mM (leucine) to 11 mM (glycine). Functional characterisation showed the transporter to be Na^+-dependent but Cl^--independent. Only one Na^+-ion is co-transported with the substrate. The substrate leucine forms part of the Na^+-binding site in both the bacterial homologue LeuT and in B^0AT1, explaining that an increase of the Na^+-concentration decreases the K_m of the substrate and vice versa (Bohmer *et al.*, 2005). This finding is consistent with a random binding order, alternatively it has been suggested that the amino acid binds first to the transporter (Camargo *et al.*, 2005). The role of a putative second Na^+-binding site remains unclear (O'Mara *et al.*, 2006).

In situ hybridisation and immunofluorescence analysis localised B^0AT1 in the kidney proximal tubule (Broer *et al.*, 2004; Romeo *et al.*, 2006) and all parts of the small intestine but not the colon (Terada *et al.*, 2005; Romeo *et al.*, 2006). It was shown that its expression increases from the duodenum to the ileum in the apical membranes with a more distinct signal toward the villi tips. These results are consistent with the expression of B^0AT1 in differentiated enterocytes (Broer *et al.*, 2004). Furthermore, the transporter has also been detected in the spleen and lung. No splice variants of the transporter have been reported so far.

The mouse and especially the human SCL6A19 protein showed very little activity in heterologous expressions systems. Therefore, it was a major breakthrough discovering that expression of B^0AT1 protein in brush border membranes requires co-expression of collectrin (Danilczyk and Penninger, 2006; Malakauskas *et al.*, 2007). Accordingly, collectrin-deficient mice showed an increased amount of neutral amino acids in the urine in combination with a significantly decreased amount of B^0AT1 and IMINO (SLC6A20) in kidney BBMV. Collectrin (also known as TMEM27) is a type I membrane protein with a molecular weight of 27 kDa and was first localised in the collecting duct, which gave its name (Zhang *et al.*, 2001).

Experiments co-expressing B^0AT1 and collectrin in *Xenopus* oocytes showed a five to ten-fold increase in transport activity (Danilczyk and Penninger, 2006). Thus, it is now established that B^0AT1 requires heterodimerisation with collectrin to be expressed at the cell surface. Since collectrin is only expressed in the kidney some other auxiliary protein was required to express B^0AT1 in the intestinal cell surface. Subsequently, the peptidase angiotensin-converting enzyme 2 (ACE2), a homologue of collectrin, was reported as the B^0AT1 partner co-expressed in the intestine (Danilczyk *et al.*, 2006; Kowalczuk *et al.*, 2008; Singer *et al.*, 2009). ACE2 is a carboxy peptidase with several reported functions. For instance, it cleaves the blood pressure regulating peptide angiotensin (II) and it is involved in peptide digestion in the intestine.

In 2001, Nozaki *et al.* mapped the Hartnup disorder gene to chromosome 5 (Nozaki *et al.*, 2001). Subsequently, Kleta *et al.* and Seow *at al.* identified the SLC6A19 gene, which expresses B^0AT1, as the gene mutated in Hartnup disorder (Kleta *et al.*, 2004; Seow *et al.*, 2004). Hartnup disorder (OMIM234500) is an autosomal recessive disorder of neutral amino acid transport in the small intestine and the kidney, which occurs with at frequency of about 1:20,000 (Levy, 2001). It was named in 1956 after the first described patient, Eddy Hartnup (Baron *et al.*, 1956). Patients show a high excretion of neutral amino acids in the urine (aminoaciduria), which is the key diagnostic feature of this disease (Baron *et al.*, 1956; Levy, 2001) but it is also associated with a number of additional symptoms, such as pellagra-like skin rash and temporary cerebellar ataxia (Baron *et al.*, 1956). Additionally, smaller body height and weight (Scriver *et al.*, 1987) have been reported. It has been shown in more recent studies that sometimes the skin rash or diarrhoea in infancy are the only symptoms for Hartnup disorder. To date, 21 mutations have been identified in the B^0AT1 gene causing Hartnup disorder (Azmanov *et al.*, 2008) and reviewed in (Broer, 2009). These data have been collected from 20 families.

1.4.2.2 B^0AT2 (SLC6A15)

The neutral amino acid transporter B^0AT2 (also known as SBAT1, v7-3, NTT7-3) also has properties similar to system B^0. It was named B^0AT2 for its similarities in structure and transport mechanism to B^0AT1. B^0AT2 has been analysed in two studies (Takanaga *et al.*, 2005; Broer *et al.*, 2006). It mainly transports branched chain amino acids and proline. Leucine, isoleucine, valine, proline and methionine are transported with high affinity, with half saturation constants ($K_{0.5}$) ranging from 40 to 200 µM, while alanine, glutamine and phenylalanine were recognised with low affinity (Broer *et al.*, 2006). B^0AT2 is Na^+-but not Cl^--dependent and its transport is electrogenic. The transport mechanism is comparable to that of B^0AT1, co-transporting one Na^+-ion with one substrate (Broer *et al.*, 2006).

Initially, B^0AT2 was described as a brain specific transporter but further reverse transcription-polychain reaction (RT-PCR) studies suggested additional localisation in mouse but not human kidney (Farmer *et al.*, 2000; Takanaga *et al.*, 2005; Broer *et al.*, 2006). The localisation of B^0AT2 has been studied extensively in brain tissue (Inoue *et al.*, 1996), but its localisation in the kidney has still to be investigated. Splice variants of B^0AT2 have also been identified (Sakata *et al.*, 1999). Recent studies on B^0AT2-deficient mice identified respectively a 15 and 40 % reduction of proline and leucine transport into cortical synaptosoms in comparison to wild type control mice (Drgonova *et al.*, 2007) with mild physiologic effects. However, this study did not consider possible changes in kidney amino acid transport.

1.4.2.3 B^0AT3 (SLC6A18)

The function of the transporter B^0AT3 (also known as XT2, and previously as XTRP2 or ROSIT) could not be characterised for a long time. In the beginning it was only shown that different, shorter splice variants were generated - six in mice, for instance (Nash *et al.*, 1998). Despite testing a variety of substrates (Wasserman *et al.*, 1994), only data generated from experiments using B^0AT3-deficient mice produced the first meaningful results. The mice showed elevated levels of glycine in their urine, however other amino acids appeared to be elevated as well (Quan *et al.*, 2004).

It was only recently shown that B^0AT3, when co-expressed with ACE2 in *Xenopus laevis* oocytes, is a Na^+-and Cl^--dependent neutral amino acid transporter. It transports alanine=methionine>valine=isoleucine>glycine=serine=leucine.

Concentration dependence experiments with isoleucine and glycine revealed a $K_{0.5}$ for B^0AT3 for those substrates of 0.21 mM and 0.53 mM respectively (Singer *et al.*, 2009). In contrast, another recent study by Vanslambrouck *et al.* showed that B^0AT3 preferentially transports alanine and glycine in mice but also showed some transport activity for most neutral amino acids excluding proline. Alanine has a higher affinity for the transporter (0.9 ± 0.4 mM) compared to glycine (2.3 ± 0.4 mM).

Additionally, it was also shown that B^0AT3 interacts with collectrin, similar to B^0AT1 (Vanslambrouck *et al.*, 2010). B^0AT3 has been localised in both studies mainly in the kidney, more accurately in the brush border membranes of the late proximal tubule (S2, S3). Due to its mechanism it was categorised as a B^0-like transporter.

1.4.3 Solute carrier family 1

The solute carrier family 1 (SLC1) family consists of seven members divided into two subfamilies: five high-affinity glutamate transporters and two neutral amino acid transporters (Figure 1.7). Similar to the SLC6 family, proteins related to the SLC1 family have been identified in some bacteria, which maintain Na^+-gradients, but not in plants, fungi and yeast (Saier, 2000).

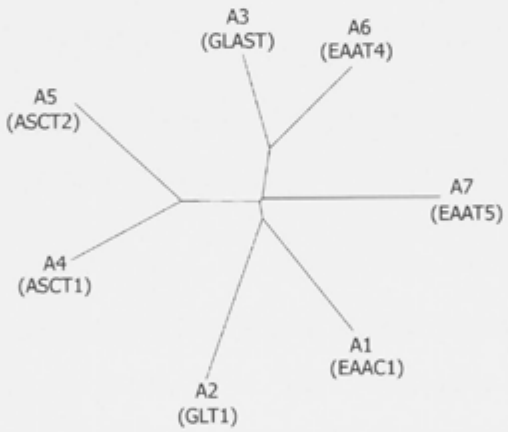

Figure 1.7: Tree of the SLC1 family.

The tree shows the SLC1 members (A1-A7) together with their common names.
(Figure adapted from Kanai, 2004)

The identification of the high-affinity glutamate transporters started in 1992, when three isoforms of transporters were independently identified. The first three members identified were EAAC1 (Kanai and Hediger, 1992), GLT1 (Danbolt *et al.*, 1992) and GLAST (Storck *et al.*, 1992). After their discovery, it was possible to identify by sequence homology two additional glutamate transporters, named EAAT4 (Fairman *et al.*, 1995) and EAAT5 (Arriza *et al.*, 1997) and two Na^+-dependent neutral amino acid transporters, referred to as ASCT1 (Arriza *et al.*, 1993) and ASCT2 (Utsunomiya-Tate *et al.*, 1996).

The glutamate transporters share 44 to 55 % amino acid sequence identity with each other. The two neutral ASC transporters are 57 % identical, while the ASC transporters are 40 to 44 % identical to the glutamate transporters (Kekuda *et al.*, 1996; Utsunomiya-Tate *et al.*, 1996; Kanai and Hediger, 2004).

The structure of the proteins belonging to the SLC1 family was first predicted to be a protein with either eight transmembrane helices with a unique, highly conserved long hydrophobic stretch near the C-terminus and a large extracellular glycosylated loop between the transmembrane domains three and four (Grunewald *et al.*, 1998; Grunewald and Kanner, 2000) or six to ten transmembrane helices (Masson *et al.*, 1999). However, the high-resolution structure of the bacterial homologue from *Pyrococcus horikoshii* revealed eight transmembrane helices and three independent binding sites for substrates, each surrounded by two helical hairpins which assist in glutamate transport through the plasma membrane (Yernool *et al.*, 2004) .

Only the neutral amino acid transporters will be further considered in this thesis. The other members were reviewed in Kanai, 2004.

1.4.3.1 ASCT1 (SLC1A4)

The amino acid transporter ASCT1 (also known as SATT) was the first transporter that showed ASC-like properties (Arriza *et al.*, 1993; Shafqat *et al.*, 1993) and was first cloned from mouse brain. Typically for system ASC, it transports, as its name indicates, L-alanine, L-serine, L-cysteine and L-threonine in a stereospecific manner. This transport was reported to be pH insensitive and occurred only in exchange with intracellular amino acids associated with one or two Na^+-ions in both directions in an electroneutral manner (Zerangue and Kavanaugh, 1996). It was shown that under some circumstances binding and transport of substrate induces inward currents. However, this was due to a substrate-gated anion conductance and not caused by the co-transport of ions (Broer *et al.*, 2000). It is expressed in a wide variety of tissues. ASCT1 will not be investigated in this project but is listed here for completeness.

1.4.3.2 ASCT2 (SLC1A5)

The amino acid transporter ASCT2 (also known as AAAT and hATB^0) is the molecular correlate of the intestinal system ASC (Kekuda *et al.*, 1996; Utsunomiya-Tate *et al.*, 1996) and was first cloned from mouse testis. ASCT2 mediates transport of small neutral amino acids such as L-alanine, L-serine, L-cysteine, L-threonine and L-glutamine with high affinity and K_m values of about 20 µM, while L-methionine, L-leucine, L-glycine and L-valine are transported with lower affinity and K_m values of 300 to 500 µM (Utsunomiya-Tate *et al.*, 1996). However, in a two studies it was observed, that ASCT2 transport activity was inhibited by phenylalanine (Kekuda *et al.*, 1996; Pollard *et al.*, 2002). Since phenylalanine is a substrate for B^0 activity, it was hypothesised that ASCT2 is or is part of the B^0 activity observed in the kidney and intestine (Kekuda *et al.*, 1996; Avissar *et al.*, 2001).

ASCT2 has been reported Na^+-dependent but not electrogenic. This apparent contradiction is explained by its antiport transport mechanism, involving an exchange of substrates and a Na^+/Na^+-ion exchange (Broer *et al.*, 2000). No fixed ratio for Na^+-ion and substrate exchange has been reported (Koser and Christensen, 1971) since the antiport nature of the ASCT2 transporter does not allow a precise prediction for Na^+-ion transport as with amino acid co-transporters. Due to the antiport mechanism, ASCT2 cannot contribute to net efflux of neutral amino acids across the apical membrane.

Northern blot hybridisations showed that ASCT2 is expressed in a wide range of tissues, mainly in kidney, large intestine, lung, skeletal muscle, testis and adipose tissue (Utsunomiya-Tate *et al.*, 1996). More recent studies with immunofluorescence and reconstitution experiments suggest localisation of the ASCT2 transporter in the apical membrane of the kidney and intestine, more specifically in the proximal tubule and the jejunum and colon of the intestine, while the duodenum and ileum show low expression (Avissar *et al.*, 2001; Oppedisano *et al.*, 2004). In contrast, studies by Green *et al.* (2004) suggested expression of ASCT2 in the basolateral membrane within the kidney proximal tubule (Green *et al.*, 2004).

The functional characterisation of ASCT2 in the small intestine revealed another ability of the transporter: it can interact with anionic amino acids at low pH. It has been shown that L-glutamate uptake via ASCT2 increases at lower pH, where it is transported with a K_m value of 1.6 mM (Utsunomiya-Tate *et al.*, 1996).

As a result, ASCT2 might contribute more to glutamate transport than to neutral amino acid transport (Pontoglio *et al.*, 1996) in the acidic microclimate of the small intestine but this has still to be confirmed. It has also been reported that splice variants for ASCT2 exist due to imprecise recognition of the first start codon (Tailor *et al.*, 2001).

1.5 Methods of investigation of amino acid transporters

The study of transporter proteins is important for our understanding of cell physiology. Because of the overlapping substrate specificity of transport proteins, the analysis of individual transporters in their natural, cellular environment can be difficult. Heterologous expression systems have been developed to overcome this problem and they are routinely used to characterise transport proteins. The most commonly used expression system for mammalian transport proteins is the *Xenopus laevis* oocyte expression system. BBMV, reconstituted transporters and cultured cell lines are also used to investigate the role of transporters.

1.5.1 The *Xenopus leavis* expression system

The oocytes of the South African clawed frog *Xenopus laevis* have been used as an expression system to study the function of membrane proteins since it was demonstrated that oocytes could express the β-globin gene following cRNA injection (Gurdon *et al.*, 1971).

The oocytes' ability to express large quantities of exogenous protein and their relatively large diameter of up to 1.3 mm are the advantages of this system. Furthermore, the oocytes contain enough energy and nutrition for protein synthesis and cell growth with little dependence on the environment. Due to these circumstances, the oocytes possess only a few endogenous transport proteins. Thus there is little interference with the transporters to be investigated.

If the desired membrane protein is successfully trafficked into the plasma membrane of the oocyte, functional studies using radioactive uptake and electrophysiology can be performed. This system has previously been used to analyse and characterise transporters, for instance B^0AT1 (Broer *et al.*, 2004), B^0AT2 (Broer *et al.*, 2006) and ASCT2 (Broer *et al.*, 2000).

1.5.2 Brush border membrane vesicles

Another system to characterise the function of epithelial amino acid transporters are BBMV. This system has been used since the 1970s (Murer *et al.*, 1976). Apical and basolateral plasma membranes are different in almost every aspect, including morphology, protein-, lipid-, carbohydrate-composition and transport properties. These differences are exploited in the procedure to achieve separation of both membranes. The different protein to lipid ratios and the different carbohydrate contents result in different physical properties of the two membranes, their density and surface charge. These properties allow the separation of the apical and basolateral membrane by precipitation and centrifugation (Murer and Gmaj, 1986). During preparatory precipitation and centrifugation steps, an enrichment of brush border membranes takes place, which form vesicles. *Ex vivo* transport studies using radioactive uptake can then be performed.

These transport studies are described more detailed in (Murer and Kinne, 1980; Murer *et al.*, 1983). In general, the BBMV are suspended in a buffer of neutral pH, containing Mannitol HEPES and Tris. At time point zero, at which no internal Na^+-ions or substrates are present in the vesicles, the vesicles are added to the uptake buffer containing sodium and the radiolabelled substrate. The substrate and Na^+-ions then bind quickly to the transporter and transport into the vesicles occurs, stimulated by the inwardly directed Na^+-gradient. This transport increases the internal Na^+-ion and substrate concentrations in a short period of time, causing the Na^+-gradient to dissipate.

The process can vary in time, for instance amino acid transport is maximal after 15 seconds (sec) (Chesney et al., 1986), while glucose uptake is maximal after 1 minute (min) (Murer et al., 1976). The dissipation of the Na^+-gradient during transport causes an overshoot of amino acid uptake. After the initial overshoot is reached, the concentration of Na^+-ions and substrates in the vesicles equilibrates with the uptake buffer possibly due to the transporters involved and leakage from the vesicles.

As a comparison and control, the substrate transport is also investigated in an uptake buffer based on potassium-salt instead of sodium-salt. With an inwardly directed K^+-gradient no 'overshoot' should occur, rather the concentration of substrate within the vesicles should increase gradually. At the time point at which an equilibrium between the substrate and ion concentrations within the vesicles in the sodium and potassium buffers is reached, the concentrations within the vesicles should also be at equilibrium with the concentrations remaining in the two buffers.

It is known that the equilibrium time point with BBMV varies with different transporters (Hopfer et al., 1973; Ganapathy and Leibach, 1982; Chesney et al., 1986). Also, the equilibrium time point of the two different uptake buffers, sodium and potassium, is sometimes not very congruent (Ganapathy and Leibach, 1982) but achieves a tolerable variance within an acceptable timeframe. Figure 1.8 shows a typical Na^+-dependent amino acid transport into BBMV.

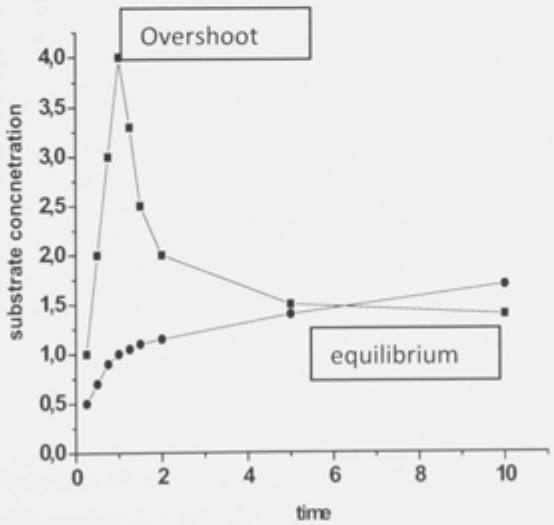

Figure 1.8: Generic example of Na^+-dependent amino acid transport measured into BBMV in Na^+- and K^+-based buffer.

Na^+-based buffer, depicted with squared, shows an overshoot after one min. While K^+-based buffer, depicted with circles, does not show an overshoot.

Additionally, the potassium selective ionophore valinomycin is frequently used to investigate Na^+-dependent transport. When vesicles are preloaded with potassium, the addition of valinomycin will render the membrane permeable to potassium.

Dilution of the vesicles into K^+-free buffer (a sodium buffer) will generate a K^+-gradient, which in turn will generate a potassium diffusion potential. Substrate and ion transport measured in this sodium buffer will display a greater overshoot than transport in a sodium buffer without preloading with valinomycin and potassium. This method has frequently been used to identify rheogenic transport processes (Ganapathy and Leibach, 1982). A typical graph of Na^+-dependent renal brush border membrane vesicle transport in the presence and absence of valinomycin is depicted in Figure 1.9.

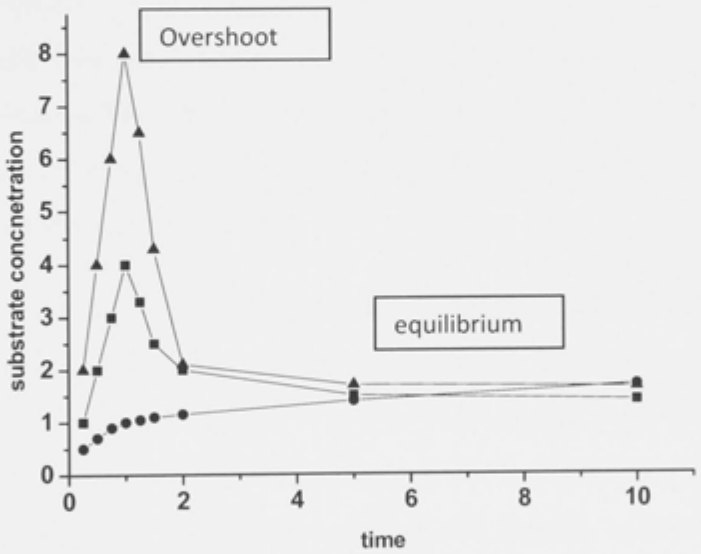

Figure 1.9: Generic example of Na^+-dependent amino acid transport measured with or without valinomycin preloaded BBMV.

Amino acid transport with valinomycin preloaded BBMV, depicted with triangles shows a much higher over shoot than amino acid transport without valinomycin preloaded BBMV in Na^+-based buffer, depicted with squares. The control of amino acid uptake in unpreloaded BBMV in K^+-based buffer shows no overshoot.

A major limitation in this system is that the interpretation of the data is often difficult since a mixture of transporters is expressed in the brush border membrane and often inhibitors are not available for certain transporters. Furthermore, as described earlier, the broad substrate specificities of the transporters are often overlapping, limiting the ability to determine the contribution of each transporter. Nevertheless, brush border membrane vesicles are frequently used for transporter investigations (Fass *et al.*, 1977).

1.5.3 Epithelial cell cultures

When the physiologist Sydney Ringer developed a salt solution containing the chlorides of sodium, potassium, calcium and magnesium which was suitable for maintaining the beating of an isolated animal heart outside of the body (Ringer, 1880), this breakthrough laid the foundations for establishing cell cultures. However, it became only a routine laboratory technique in the 1950s (Kanazawa *et al.*, 1953) due to the relatively slow cell growth rate in comparison to bacteria, making cell cultures vulnerable to bacterial contaminations.

More recently, epithelial cell cultures (primary cultures and immortalised cell lines) have come to play an important role in the characterisation of epithelial amino acid transporter function. The advantages of this system are that the cells are relatively easy to maintain, they are structurally simple and are identically. The major limitation is the dedifferentiation of the cultured cells which generally occurs (Verrey *et al.*, 2005). The opossum kidney (OK) cell line to date is the most conserved proximal tubule cell line and has been used to characterise the function of several amino acid transporters, for instance LAT2/4F2 (Fernandez *et al.*, 2003).

Furthermore, cell lines can be transfected or infected with transport proteins, even though their transfection rate can vary highly (Peel, 2004). Once transfected, the cells are able to express those proteins with their own machinery and subsequently the expressed transport proteins can be investigated.

1.6 Aims of this thesis:

Which neutral amino acid transporter is the main B^0 transporter in the kidney and intestine has been the subject of controversial discussion over the past few years (Avissar *et al.*, 2001; Sundaram *et al.*, 2007; Broer, 2009). The main intention of this PhD project was to investigate the role of the three neutral amino acid transporters B^0AT1, B^0AT2 and ASCT2 in neutral amino acid transport in the kidney using different approaches.

First, the localisation of B^0AT1, B^0AT2 and ASCT2 was determined in mouse kidney and intestine tissue by immunofluorescence using B^0AT1, B^0AT2 and ASCT2-specific antibodies. The exact localisation of B^0AT2 in the kidney was previously unknown, while the localisation of B^0AT1 needed to be confirmed. The localisation of ASCT2 needed to be investigated since it was reported to be in different location.

Second, the three neutral amino acid transporters were characterised after expression in *Xenopus laevis* oocytes to determine substrate specificity. This information was compared to transport data gained using BBMV of mouse kidney with the aim of identifying the contribution of each transporter.

Third, a B^0AT1-deficient mouse was characterised using immunofluorescence approaches and BBMV experiments. The BBMV results from wild type mice were compared with those obtained from B^0AT1-deficient mice, to confirm the roles identified for B^0AT1, B^0AT2 and ASCT2.

Chapter 2

Materials and Methods

2.1 Materials

2.1.1 Enzymes, chemicals and molecular biology kits

Restriction endonucleases and DNA modifying enzymes were purchased from New England Biolabs (NEB, Ipswich, USA), Roche Molecular Biochemicals (Basel, Switzerland), Promega (Madison, USA) and TaKaRa Technology (Shiga, Japan). Molecular biology grade chemicals, reagents and antibiotics were purchased from Sigma-Aldrich (St. Louis, USA), Invitrogen (Carlsbad, USA), AMRESCO (Solon, USA)) and MERCK KGaA (Darmstadt, Germany). Plasmid DNA isolation miniprep and midiprep kits and Endofree Plasmid Maxi Kit were purchased from either Invitrogen (Carlsbad, USA) or QIAGEN (Hilden, Germany). Gel extraction and PCR purification kits were obtained from Invitrogen (Carlsbad, USA) or Millipore (Millipore, Billerica, USA). RNA extraction Kit was purchased from Macherey-Nagel (Dueren, Germany). Radiolabelled [3,4,5-^{3}H]L-Leucine (115.4 Ci/mmol) was purchased from MP Biomedicals, Inc. (Irvine, USA), L-[G-^{3}H] Glutamine (59.0 Ci/mmol).

2.1.2 Markers

The 1kb DNA Ladder, GeneRuler 100 bp DNA Ladder and Supercoiled DNA Ladder were purchased from NEB, Fermentas (Burlington, USA) and Invitrogen.

For protein gels, SeeBlue Plus2 Prestained Standard was obtained from Invitrogen.

2.1.3 Disposable materials

Petri Dishes were supplied by Bacto Laboratories (Liverpool, Australia). 96-well microtiter plates, 0.2 mL microfuge tubes, 15 mL tubes and pipette tips were purchased from Sarstedt (Nuermbrecht, Germany), 1.5 mL and 2 mL tubes were obtained from Eppendorf (Hamburg, Germany). 50 mL Falcon tubes were purchased from BD Biosciences (San Jose, USA). All cell culture work equipment was obtained from Nalge/Nunc (Roskilde, Denmark).

2.1.4 Antibiotics

The antibiotics ampicillin and kanamycin (ICN Biomedicals, Aurora, USA) were added to bacterial growth media at final concentrations of 100 µg/mL and 50 µg/mL, respectively, for propagation of *Escherichia coli* cultures harbouring plasmid DNA with their respective resistance genes. All of these antibiotics were filter sterilised (0.22 µm). Ampicillin was stored as 50 mg/mL stock solution and Kanamycin was stored as 20 mg/mL stock solution.

Gentamycin was added to OR^{2+} at a final concentration of 10 mg/L and prepared as the other antibiotics. Gentamycin was stored as a 50 mg/mL stock solution.

2.1.5 Bacterial strains and plasmids

The *Escherichia coli* strains DH5α (Invitrogen) and XL1- Blue (Stratagene Inc., La Jolla, USA) were used as host bacteria for plasmid transformation. Following transformation, the *E. coli* strains were cultured in LB media using antibiotic resistance selection according to the contained plasmid. The genotypes of the *E. coli* strains used in this study are presented in Table 2.1.

Table 2.1: Description of Bacterial Strains used in this thesis

Bacterial Strain	Genotype	Source
E. coli DH5α	- F- ϕ80lacZΔM15 Δ(lacZYA-argF) U169 recA1 endA1 hsdR17 (rk-, mk+) phoA supE44 λ- thi-1 gyrA96 relA1	Invitrogen
E. coli XL1-Blue	- recA1 endA1 gyrA96 thi-1 hsdR17 supE44 relA1 lac [F´ proAB laclqZ Δ M15 Tn10 (Tetr)	Stratagene

For short-term storage, plates with E. coli colonies were stored at 4 °C, usually up to 1 month, after which they were autoclaved and discarded. For long-term storage a flask containing LB broth plus the appropriate antibiotic was inoculated from a single colony and vigorously shaken at 200 rpm overnight at 37 °C. The next day, a 600 µL aliquot of culture was mixed with 400 µL 50 % glycerol and stored at -80 °C.

The expression vectors and plasmids used in this study are detailed in Table 2.2 and in the appendix B respectively. The pGHJ vector was used for the expression of mRNA in *Xenopus laevis* oocytes. The multiple cloning site (MCS) in this plasmid is flanked by the 5' and 3' untranslated regions of the *Xenopus* β-globin gene, which facilitates the translation of injected cRNA that is produced by *in vitro* transcription (Liman *et al.*, 1992)

The pGEX-2T vector was used for the expression of glutathione-S-transferase (GST) fusion proteins in *E.coli.*, which is not part of this thesis but mentioned for completeness. This vector contains the *tac* promoter, which can be induced by IPTG.

The pcDNA 3.1 (+) vector was used for expression of genes in mammalian cells such as human embryonic kidney cells (HEK) and Chinese hamster ovary cells (CHO). It has a human cytomegalovirus immediate-early (CMV) promoter for high-level expression in a wide range of mammalian cells. The multiple cloning site is in forward (+) orientation to facilitate the cloning and it contains a neomycin resistance gene for selection of stable cell lines.

Table 2.2: Description of expression vectors used in this thesis

Name	Features	Source
pGem-He-Juel (pGHJ)	- MCS flanked by the 5' and 3' untranslated regions of the *Xenopus* β-globin gene - β-lactamase gene for ampicillin resistance - T7 Promoter upstream of the 5' β-globin un-translated region - SP6 Promoter downstream of the MCS	Modified from pGEM (Liman *et al.*, 1992)
pGEX-2T	- MCS downstream of GST gene - *tac* promoter upstream of GST gene - β-lactamase gene for ampicillin resistance - *lacI*^{q} gene for the control of the *tac* promoter	GST Gene Fusion System (Amersham Biosciences)
pcDNA 3.1 (+)	- CMV promoter for high- level expression in a wide range of mammalian cells - *T7* promotor downstream of the CMV promotor - Neomycin resistance for selection of stable cell lines, additional ampicillin resistance	Invitrogen

The plasmids generated or used in this study are presented in the Appendix B in detail.

2.1.6 Antibodies

Antibodies used in this study and their used dilutions are presented in Appendix C.

Primary and secondary antibodies were either produced at Pineda Antibody-Service (Berlin, Germany) or purchased from Vector Laboratories (Burlingame, USA), Pharmingen (San Diego, USA) or Invitrogen.

2.2 Methods- Molecular Biology: preparative DNA techniques

2.2.1 Preparation of plasmid DNA

Plasmids were isolated from a 5 mL overnight culture of *E. coli* grown in LB broth with the appropriate antibiotic using the PureLink Quick Plasmid Miniprep Kit (Invitrogen, Carlsbad, USA) or the QIAprep Spin Miniprep kit (QIAGEN, Hilden, Germany). The manufacturer's protocols were followed. Plasmid DNA quality and concentration was determined with a NanoDrop Spectrophotometer (NanoDrop Technologies, Wilmington, USA) as described in Section 2.3.3.

In order to obtain larger amounts of plasmid DNA (up to 200 μg/Midi-prep or 750 μg/Maxi-prep) the Qiafilter Midi and Maxi Kit (QIAGEN) was used following manufacturer's instructions.

For the preparation of large quantities of plasmid DNA for mammalian cell transfection the endonuclease free Maxi-prep kit (QIAGEN) was used, following the manufacturer's instructions.

All of these kits utilise the alkaline lysis method of plasmid DNA extraction.

The DNA was used for cloning, expression, *in vitro* transcription, restriction digests, PCR applications and sequencing reactions. The DNA was separated on agarose gels (1.3.1), examined under the UV transilluminator and photographed using the GelDoc Imaging system described in Section 2.3.2.

2.2.2 DNA extraction from agarose gels

Following agarose gel electrophoresis (Section 2.3.1) and ethidium bromide (EtBr) staining, the DNA band requiring purification was excised from the agarose gel using a clean scalpel and placed in a clean microfuge tube. This procedure was done by dividing the sample in an analytical and a quantitative fraction loaded into two adjacent lanes of the gel. Only the lane containing the analytical fraction was cut out and stained with EtBr. The position of the band was marked and the corresponding area of the unstained sample fraction was cut out without exposing to EtBr and UV light to avoid damage or mutation of the DNA. The excised DNA band was isolated from the agarose gel using either QIAquick Gel Extraction Kit (QIAGEN) or PureLink Quick gel Extraction Kit (Invitrogen) following manufacturer's instructions.

DNA quality and concentration was determined with the NanoDrop Spectrophotometer as described in section 1.3.3.

2.3 Molecular Biology: analytical DNA techniques

2.3.1 Agarose gel electrophoresis

Horizontal submerged TAE-agarose gels were run according to protocols described by Sambrook (Sambrook, 2001). Agarose (0.8 to 2 %) was dissolved in 1x TAE buffer. One fifth volume of loading buffer (Fermentas) was added to samples before loading onto the gel. The DNA was separated at 5 to 15 V/cm 45 to 180 min. A 1kb DNA Ladder, a 100bp DNA Ladder or a Supercoiled DNA Standard was routinely run on the agarose gels to determine the size and estimate the concentration of the unknown DNA on these gels. The 3 kb band in the 1 kb GeneRuler Fermentas DNA Ladder contained 70 ng DNA when run at 500 µg/mL, whereas the NEB DNA Ladder contained 125 ng DNA when run at 500 µg/mL and 7 to 8 µL was loaded.

1x TAE buffer	40 mM	Tris-HCl	
	20 mM	Sodium acetate	
	1 mM	EDTA	pH7.8

2.3.2 Visualisation and imaging of nucleic acids

Following agarose electrophoresis, nucleic acids were stained in approximately 0.5 µg/mL EtBr in ddH_2O for 15 to 20 min and destained for 5-10 min in ddH_2O. The DNA was visualised by illumination on a UV transilluminator (340 nm) and photographed using the GelDoc Imaging system (Bio-Rad Laboratories, USA).

2.3.3 Quantification of nucleic acids

To quantify the amount of plasmid DNA, genomic DNA, RNA or protein the NanoDrop Spectrophotometer (NanoDrop Technologies, Wilmington, USA) was used. Absorbance at 260 nm was used to measure the concentration of DNA and RNA as described by Sambrook (Sambrook, 2001). It was assumed that an OD of 1.0 corresponds to 50 µg/mL of double-stranded DNA. The presence of proteins and other contaminations was estimated by measuring the $A_{260/280\ nm}$ ratio. A ratio of between 1.8 and 2.0 indicates a DNA preparation largely free from contaminating proteins. RNA was quantified using the same procedure, where an OD of 1.0 corresponds to 40 µg/mL of RNA. The presence of proteins and other contaminants was estimated by measuring the $A_{260/280\ nm}$ ratio, where a ratio of between 1.8 and 2.0 was taken to indicate a clean preparation.

2.3.4 Oligonucleatides/Primers

All oligonucleotides of this study were custom-synthesised by Sigma-Proligo (Newcastle, Australia) and are listed in Appendix C.

2.3.5 Polymerase chain amplification (PCR)

PCR was used to analyse expression levels of genes after reverse transcription of mRNA to cDNA and to amplify fragments for cloning and screening purposes. The amplification of DNA fragments by PCR was performed in a Corbett Research GC1-96 thermal cycler (CR Corbett Research Life Science) as described below.

The *Pfu*II Ultra polymerase (Stratagene) was used in experiments where high fidelity amplification was required for cloning purposes, and the manufacturers' instructions were followed. A 10 mM mixture of the deoxyribonucleotide triphosphates (dNTPs) dATP, dTTP, dGTP and dCTP (Invitrogen) was made up and stored at -20 °C in aliquots. Template DNA concentration as well as the annealing temperature varied in individual sets of reactions. Generally, a PCR reaction was carried out in 0.2 mL thin- walled tubes, containing 1/10 volume 10x PCR buffer , 10x dNTPs stock solution in a dilution of 1/10, 0.5-0.6 µM primer, 1-4 U enzyme and 20-100 ng template DNA. The final volume was made up to either 20 µL, 50 µL (for normal PCR) or 100 µL (for RT-PCR) with sterile ddH_2O.

Reactions were performed under the following general conditions:

Denaturation step	95 °C	2 min
Cycling program	[28-35 cycles]	
Denaturation	95 °C	30 sec
Annealing	56-67 °C	30 sec
Extension	72 °C	30-200 sec
Final extension	72 °C	10 min

Amplification of PCR products was monitored by gel electrophoresis (1.3.1).

In some instances a gradient PCR was carried out to determine the optimal annealing temperature for a given set of primers.

2.3.6 Restriction endonuclease digestion of DNA

Plasmids and genomic DNA fragments were digested by incubation with 10 to 20 U of restriction enzyme (RE) per 0.5 to 1.0 µg DNA in the recommended restriction enzyme buffers supplied by the manufacturer. Restriction digests were carried out for 1 to 3 h, depending on the concentration of DNA to be digested at the recommended temperature. Restriction digests of DNA with multiple enzymes were carried out simultaneously if the restriction enzyme buffers were compatible. When different reaction buffers were required, the DNA was digested first with one restriction endonuclease and the buffer was adjusted accordingly to accommodate the sec restriction endonuclease. After restriction digests the DNA was either purified as described in Section 2.3.7 or extracted from agarose gel using a gel extraction kit before using in cloning or transformation experiments.

2.3.7 Purification of DNA fragments

DNA, restriction endonuclease digestions or PCR reactions were purified and concentrated with Microcon® centrifugal filter devices (Millipore), or a PureLink PCR purification kit (Invitrogen), following manufacturers' specifications. Both products are able to separate larger DNA fragments from proteins, salts and small (<300 bp) DNA fragments.

2.3.8 Cloning

2.3.8.1 Dephosphorylation of linearised plasmid DNA

Antarctic Phosphatase (NEB) treatment was used to remove 5'-phosphate groups from the cloning vector after restriction digestion and before ligation in cases where a single restriction enzyme site was used for cloning. The phosphatase treatment prevented preferential self-ligation of the vector backbone.

2.3.8.2 Ligation

To ligate fragments, 1 µL of T4 DNA Ligase of the T4 Quick Ligation Kit (NEB) was added to a 20 µL final reaction volume containing 1x Quick Ligase buffer and vector: insert at a ratio of 1:3 or 1:5. Ligation reactions were carried out for 1 to 25 min at 25 °C. In addition to the experiment, several control ligations were performed to test the efficiency of the ligation reaction and the quality of the vector. These usually included parallel ligations in the absence of insert DNA to determine the background clones arising from self-ligation and inefficiently dephosphorylated vector.

Before transformation of the ligated products, the DNA was usually concentrated using tRNA precipitation. 1 µL of tRNA (5 µg/µL) was added to the ligation reaction as well as 0.5 volumes of 7.5 M ammonium acetate and 2.5 volumes of 100 % ice-cold ethanol. After 10 min incubation at room temperature (RT), the solution was centrifuged for 20 min at 10,000 g. The pellet was washed with 250 µL 70 % ethanol and centrifuged again for 10 min at 10,000 g. After air drying the pellet, it was dissolved in 5 µL of sterile H_2O and 2.5 µL was used for a transformation reaction (1.3.8.3).

2.3.8.3 Competent bacteria and transformation

High efficiency transformation (ca. 10^5 to 10^7 transformants/µg of circular DNA) of *E. coli* strains was achieved by electroporation using a Bio-Rad Gene Pulser electroporator with a Bio-Rad Pulse Controller II (Bio-Rad Laboratories, Hercules, USA). Precipitated DNA (2.5 µL) was mixed with a 40 µL aliquot electrocompetent DH5α *E. coli* cells (Sambrook, 2001) and left on ice for 1 min.

The mixture of cells and DNA was transferred into a cold Bio-Rad electroporator cuvette and subjected to an electrical pulse field (the Gene Pulser was set to 25 µF and 2.5 kV, and the Pulse Controller was set at 200 Ω, using a cuvette of 0.2 cm gap width). After the pulse, 750 µL SOC media was immediately added to the cells. The mixture was transferred to a 15 mL tube and incubated at 37 °C for 1.5 h with moderate shaking to allow expression of the antibiotic resistance gene and recovery of transformed *E. coli* cells. Aliquots of the transformation mix were spread on agar plates with appropriate antibiotics in accordance to the resistance gene present on the plasmid. The agar plates were subsequently incubated at 37 °C overnight. Clearly visible colonies were analysed further (1.3.9).

SOC medium	20 mM	Glucose
	10 mM	NaCl
	10 mM	$MgCl_2$
	10 mM	$MgSO_4$
	2.5 mM	KCl
	2 %	Tryptone
	0.5 %	Yeast extract

2.3.9 Rapid screening of transformed colonies

To screen bacterial transformants for those that had taken up a recombinant vector, a colony cracking method was employed. Single bacterial colonies were resuspended in 40 µL EDTA. Afterwards 40 µL of a freshly made 2x cracking buffer for lysing the bacteria was added. The mixture was incubated for 5 min at RT before 10 µL marker mix was added. The mixture was incubated on ice for 5 min before it was centrifuged for 3 min at 10,000 g. 20 µL of the supernatant was subsequently run on an agarose gel adjacent to a supercoiled DNA Ladder. Those plasmids containing the insert of interest could be discriminated by their size.

2x cracking buffer:	0.2 g/mL	Sucrose
	0.5 % w/v	SDS
	0.2 M	NaOH
Marker mix:	0.5 M	KCl
	8 % v/v	Bromophenol blue
	1 %	Triton X-100

2.3.10 Sequencing of constructs and construct analysis

Correct constructs were confirmed by DNA sequencing. Usually a sequencing reaction contained of 2 µL Big Dye Terminator (BDT) v3.1, 3 µL of 5x BDT sequencing buffer (Applied Biosystems), 3.2 pmol of the appropriate primer, 300 ng of double stranded (ds) template DNA and sterile ddH_2O to a final reaction volume of 20 µL. Depending on the gene, a T7-, SP6- or self-designed primers were used. Sequencing reactions were run in a PCR machine described in Section 2.3.5 under the following general conditions:

Denaturation step	94 °C	5 min
Cycling program	[30 cycles]	
Denaturation	96 °C	10 sec
Annealing	50 °C	10 sec
Extension	60 °C	240 sec
Holding samples	20 °C	

For purification of the reaction, 2 µL of 3 M sodium actetate (pH 5.2) and 50 µL of 100 % ethanol was added and incubated at RT for 15 min. After centrifugation for 20 min at 10,000 g the sample pellet was washed twice with 250 µL 70 % ethanol with a centrifugation of 5 min at 10,000 g after each step. The air dried sample was then sent to sequencing.

Sequencing was performed at the Biomolecular Resource Facility (BRF), John Curtin School of Medical Research (JCSMR), (Australian National University [ANU], Canberra, Australia), using ABI 3730 DNA Analyser (Applied Biosystems, Foster City, USA).

Sequences were viewed using the Chromas software program (McCarthy, 1998) and searches for homologue DNA sequences were carried out using the BLAST program through the National Center for Biotechnology Information (NCBI) (http://www.ncbi.nlm.nih.gov/BLAST, (Altschul *et al.*, 1997)

2.4 Protein techniques

2.4.1 Expression and purification of protein for antibody production

The antibodies against B^0AT1, B^0AT2 and ASCT2 used in this thesis were designed in the Broer laboratory prior to the commencement of this thesis and are mentioned here for completeness.

The GST Gene Fusion System (Amersham Biosciences) was used to produce amino- and carboxy-terminal peptides of B^0AT1 and B^0AT2 (v7-3) fused to *E. coli* GST protein. These fusion proteins were used for the production of B^0AT1 and B^0AT2 specific antibodies.

Primers used for generating those proteins are as followed:

Name	RE-site	Sequence
mB0AT1-Nterminus-sense	GGATCC *BamH*I	CCCATGGTGAGGCTTGTG
mB0AT1-Nterminus-antisense	GAATTC *EcoR*I	ACTGGGCCTTCTTCTCCCA
mB0AT1-Cterminus-sense	GGATCC *BamH*I	CCCAAGTTCATCAGAAATTGT
mB0AT1-Cterminus-antisense	GAATTC *EcoR*I	AGTTCTTAAGGTCCCCA
mV7-3Nterm1-sense	GCGAATTCAT *EcoR*I	ATGCCTAAGAATAGCCAAAGTG
mV7-3Nterm1-antisense	GCGAATTC *EcoR*I	TTGCAGCTTACTGTTCCAGGC
mV7-3Cterm1-sense	GCGAATT *EcoR*I	CGTCGCTGCAACCTCATAGAT
mV7-3Cterm1-antisense	GCGAATCC *EcoR*I	CCAGTCAGACTCTGGCATATC

The pGEX-2T expression vector (Section 1.5) was used to produce recombinant GST fusion proteins using standard cloning techniques as outlined in sections 2.3.5 to 2.3.10. Subsequently the protocol of the Bornstein Laboratory at the University of Washington for the preparation of bacterial expressed recombinant GST- fusion proteins was followed (http://depts.washington.edu/bornlab/Born-Protocol.html; Seattle, USA).

Freeze dried protein samples were sent to Pineda antibody service for production of specific antibodies.

The mASCT2 antibody was produced by Pineda antibody service against the peptide sequence:

N-REPSGDSSATC—COOH

2.4.2 GST-depletion of polyclonal antisera

GST-fusion protein was used to generate an antibody against B^0AT1 and B^0AT2. Therefore the obtained serum samples contain antibodies that recognise the target protein and GST. To remove the antibodies that recognise GST, immobilised GST columns (Pierce, Rockford, USA) were used following the manufacturers' manual. Unbound antibodies were retained while the bound anti-GST antibodies were discarded.

2.4.3 Bradford assay

Protein concentrations were determined using the Sigma Bradford reagent with BSA dilutions as standard (Bradford, 1976).

For the production of a standard curve, BSA stock solutions with 50 mg/mL, 75 mg/mL. 100 mg/mL, 200 mg/mL, 300 mg/mL, 400 mg/mL and 500 mg/mL were made up and kept at -20 °C. BSA standard was thawed on ice and experimental protein samples were diluted as required (generally, 1:10, 1:100 and 1:1,000) and kept on ice. 30 µL of BSA standards or diluted protein samples were transferred to a microtiter plate in duplicates or triplicates.

Bradford reagent (270 µL) was added to each well and reactions were mixed carefully before incubation for 10 to 15 min at RT. Absorbance at 595 nm was measured using a Bio-Tech µQuad Microplate Spectrophotometer (Biotech Instruments, USA). The protein concentration of the samples were calculated by the program KC4 version 3.4 using the generated BSA standard curve as reference.

2.4.4 Western Blot

2.4.4.1 Sample preparation

After concentration estimation with the Bradford assay (2.4.3) the samples were prepared following the NuPAGE Technical Guide (all NuPAGE reagents were obtained from Invitrogen). Samples (generally containing between 1 and 2 µg/µL protein) were diluted with water to a final volume of usually 20 µL, 4x NuPAGE LDS Sample Buffer and 10x NuPAGE Reducing Agent. The mixture was heated for 10 min at 70 °C, briefly centrifuged and loaded on to the SDS-PAGE gel.

2.4.4.2 SDS-PAGE

NuPAGE Novex 4 to 12 % Bis-Tris 1 mm precast gels were assembled in the XCell *Surelock* Mini-Cell (Invitrogen) following the manufacturers' instructions. To this end, the upper chamber was filled with 200 mL 1x NuPAGE MES Running Buffer containing 500 µL NuPAGE Antioxidant. The lower chamber was filled with 700 mL of 1x NuPAGE MES Running buffer. Samples were loaded together with a pre-stained protein Ladder (Invitrogen) as an indicator for protein transfer from the gel to the membrane. The samples were run on gels at 200 V for 40 to 60 min depending on the size of the protein.

2.4.4.3 Western Immunoblot

Western blotting was performed to detect specific protein in samples run on polyacrylamide gels. Proteins were transferred onto a Hybond nitrocellulose membrane using either the Invotrogen iBlot system or the BioRad System (2 h at 100 V) following manufacturers' instruction. Non-specific binding was blocked by incubating the membrane in PBST containing 5 % skim milk powder overnight at 4 °C.

The membranes were washed three times with PBST for 15 min on an orbital shaker. The membranes where incubated for 2 h at RT with the appropriate dilution of primary antibody in PBST with 1.6 % skim milk powder. Following three washes (15 min each) with PBST, the membranes were incubated on an orbital shaker for 1 h at RT in secondary antibody (Horseradish-peroxidise labelled donkey anti-rabbit IgG, Amersham Biosciences, UK) made up with 1.6 % skim milk powder in PBST. Membranes were washed three times for 15 min in PBST. To detect the proteins on the membranes, the Enhanced Chemiluminescence (ECL) Western Blot Analysis System (Amersham Biosciences) was used. A mixture of the two detection reagents was applied to the washed membrane and exposed for 1 min. After removing the detection reagents, the chemiluminescence was detected with Hyperfilm ECL (Amersham Biosciences) in a dark room. The films were processed using a Kodak Processor. The exposure times varied depending on the intensity of the signal, usually ranging from 10 sec to 15 min.

2.5 Immunofluorescence

2.5.1 Sample preparation

Fixation of human tissue was performed following the protocol described preciously by Broer *et al.* (Broer *et al.*, 2008). All human tissue samples were prepared by our collaborator in Sydney using their ethical approval from the University of Sydney.

Fixation of mouse tissues was performed following the protocol described previously by Kowalczuk *et al.* (Kowalczuk *et al.*, 2008). Intact kidney or intestine of C57BL6 mice was placed into ice-cold 0.9 % NaCl to remove the kidney capsule or rinsed with ice-cold 0.9 % NaCl to remove all remaining faeces. The tissue specimens were placed in freshly made Formalin (at least 20 times the volume of the tissue) and incubated depending on the tissue size for 2 to 24 h. The fixation was initiated at RT and after the first hour the fixative was exchanged. At the end of the fixation period, tissue was transferred into ethanol and was processed for paraffin embedding at the Microscopy and Cytometry Resource Facility (MCRF) at the JCSMR.

Formalin (10 % neutral buffered):	100 mL	Formalin (40 % formaldehyde)
	4 g	NaH2PO4, H2O
	6.5 g	Na2HPO4
	1 L	ddH2O total volume

2.5.2 Immunofluorescence

Immunofluorescence was used to localise amino acid transporters in mouse tissue. The procedure described by Kowalczuk et al., 2008 was generally followed. However, several modifications for enhanced quality were acquired. These are presented in detail in Chapter 3.

2.5.3 Confocal microscopy

Confocal microscopy was carried out to examine localisation of amino acid transporters, transfection efficiency in mammalian cells and expression and trafficking of amino acid transporters in oocytes.

A BioRad Radiance 2000 (BioRad Laboratories) or a Leica TCS SP5 (Leica Microsystems, Wetzlar, Germany) at the JCSMR was used to detect fluorescence. Generally, in the bright field microscope the vitelline layer of oocytes, the membranes of mammalian cells or mouse tissue was focused using a low objective lens, such as 10x objective lens. Image capture was then done at higher magnification. The images were viewed using the Laser Sharp 2000 program (BioRad Laboratories) or the LAS-AF program (Leica Microsystems).

2.6 Xenopus oocyte expression

2.6.1 *In vitro* transcription

In vitro transcription was used to produce cRNA from plasmid DNA for functional studies in oocytes. Plasmid DNA was linearised to terminate transcription at the end of the cDNA. Plasmid DNA (5 µg) was linearised in an overnight digestion with a suitable restriction enzyme (Section 2.3.6), and then examined by agarose gel electrophoresis

(Section 2.3.1) for quality and completeness of the digestion reaction. Subsequently, the DNA was purified by extracting enzymes and proteins from the aqueous solution using an equal volume of phenol/chloroform (1:1) equilibrated in 1 M Tris-HCl, pH 8.0.

The samples were mixed by vortexing, incubated for 1 min on ice and the phases were separated by centrifugation at 16,000 g for 5 min at RT. The upper, aqueous layer (approximately 100 µL) was transferred to a new tube. The DNA was then precipitated for 2 to 3 h at -20 °C after adding 10 µL of 2 M NaCl and 200 µL of 100 % ice-cold ethanol. The mixture was centrifuged for 20 min at 16 000 g, the pellet was washed with 1 mL of 70 % ethanol and centrifuged again for 10 min at 16 000 g. The dried pellet was dissolved in 12 µL of DEPC-treated water. The linearised and purified DNA (2 µg) was used as template for the in vitro transcription using the mMESSAGE mMACHINE T7 promotor kit (Ambion Applied Biosciences, USA) following the manufacturers' instructions. The complementary RNA (cRNA) generated in this reaction was purified with a phenol/chloroform extraction, using an equal volume of phenol/chloroform (1:1) equilibrated in 1 M Tris-HCl, pH 8.0. The samples were completely mixed and the phases were separated by centrifugation at 16,000 g for 5 min at RT. The upper, aqueous layer was transferred to a new tube and mixed again with an equal volume of phenol/chlorophorm. Subsequent mixing and spinning yielded a new aqueous phase. All two phenol layers were reextracted with 100 µL 100 mM Tris, pH 8.0. All three aqueous layers were combined and cRNA precipitated at –70 °C for at least 3 hours (h) after adding 0.5 volume 7.5 M NH_4OAc and 2.5 volume ice-cold ethanol. The mixture was centrifuged for 35 min at 16,000g and the pellet was washed one with 1 mL 70 % ethanol and centrifuged for 20 min at 16,000g. After drying the pellet in a dessiccator, it was dissolved in 20 µl of nuclease free water. The RNA was incubated for 3 min at 65 °C to dissolve the pellet properly and the amount of RNA in the sample was measured using the NanoDrop Spectrophotometer (Section 2.3.3). The RNA was diluted to a concentration of 1 µg/ml, dispensed into 5 µl aliquots and stored at -80 °C.

2.6.2 Oocyte preparation and injection

Xenopus laevis oocytes were prepared as described previously (Broer, 2003).

Female *X. laevis* (South African Xenopus Facility; Knysna, South Africa) were anaesthetised 20 to 40 min by submersion in 0.15 % MS222 anaesthesia solution. Anaesthesia was judged complete when the frog could be turned onto its back without eliciting a response. The frog was placed (belly up) on an absorbance paper sheet placed on top of a tray of ice. A small (< 1 cm) incision was made through both the skin and muscle layers of the lower abdomen. Sections of ovary were removed with tweezers and scissors and placed into OR^{2-} buffer. The incision was closed with one absorbable suture in the muscle layer, and two non-absorbable stitches in the skin layer. The frog was left to recover under a damp paper towel, and was submerged in water once awake.

By using scissors, the removed ovary was separated into small pieces of around 50 oocytes each. These sections were then incubated in 50 mL of 1.5 mg/mL collagenase D (from *Clostridium histolyticum*) in OR^{2-} buffer for 2 to 4 h at 28 °C under slight agitation until the majority of oocytes were no longer clumped or associated with blood vessels or follicular cells. The collagenase was washed off with at least 500 mL OR^{2-} followed by at least three rinses in OR^{2+} buffer. The oocytes were stored overnight in this buffer at 18 °C.

On the following day, healthy oocytes of an appropriate developmental stage (stage V or VI; (Broer, 2003) were selected for microinjection. Oocytes were injected with 10 to 25 ng of the appropriate cRNA. Injections were performed with a Nanoliter Injector (World Precision Instruments, Sarasota, USA), using capillaries pulled on a Flaming/Brown micropipette puller (Sutter Instrument Co., Novato, USA). Oocytes were maintained for up to 5 days at 18 °C in OR^{2+} buffer containing 50 µg/L gentamycin. The oocyte medium was changed daily.

Anaesthesia solution:	1.5 g/L	3-aminobenzoic acid ethyl ester	
	1 mM	$NaHCO_3$	
OR^{2-} buffer:	82.5 mM	NaCl	
	2.5 mM	KCl	
	1 mM	$MgCl_2$	
	1 mM	Na_2HPO_4	
	5 mM	HEPES	pH 7.8
Collagenase D	1.5 mg/mL (Roche, USA) made in OR^{2-}		
OR^{2+} buffer	82.5 mM	NaCl	
	2.5 mM	KCl	
	1 mM	$CaCl_2$	
	1 mM	$MgCl_2$	
	1 mM	Na_2HPO_4	
	5 mM	HEPES	pH 7.8

2.6.3 Total membrane preparation of oocytes for Western Blotting

This method was used to enrich all membrane proteins from oocytes. 3 to 5 days after injection, 25 oocytes were homogenised in 1 mL of homogenisation buffer by trituration. The homogenate was spun in a microcentrifuge at 2,000 g for 10 min at 4 °C. The supernatant was transferred to a fresh tube and spun at 14,0000 g for 30 min at 4 °C in a Beckman Optima MAX ultracentrifuge (Beckman, Fullerton, USA). The supernatant was discarded and the pellet was dissolved in 50 µl of homogenization buffer containing 4 % SDS. The samples were then analysed on SDS-PAGE (Section 2.4.4.2) followed by Western Immunoblot (Section 2.4.4.3).

Homogenization buffer	50 mM	Tris/HCl	pH 7.6
	100 mM	NaCl	
	1 mM	EDTA	pH 8.0
	1x protease inhibitor		

2.6.4 Immunofluorescence with oocytes

Immunofluorescence with oocytes was performed to analyse the expression of the investigated amino acid transporters and the quality of the primary antibody.

Seven to ten oocytes were incubated in 4 % paraformaldehyde in PBS for 30 min with slow rotation. After aspirating the paraformaldehyde, the oocytes were washed three times for 10 min with PBS with slight rotation. Subsequently, the oocytes were incubated in 100 % methanol for 20 min at -20 °C. After incubation, the oocytes were washed three times for 10 min with PBS under slow rotation. To reduce the amount of unspecific binding of the antibody, the oocytes were incubated in 3 % BSA, 1 % NGS and 0.1 % Triton-X-100 in PBS for one hour with slight rotation. The oocytes were then incubated in the appropriate dilution of the primary antibody (made in 1 % BSA and 0.01 % Triton-X 100 in PBS pH7.4) for 2 h at RT. The oocytes were then washed three times with PBS for 10 min. Incubation with the secondary antibody (1:500 dilution made in 1 % BSA and 0.01 % Triton-X 100 in PBS) was carried out for 2 h with slow rotation in the dark to prevent bleaching of the fluorophore. Unbound antibodies were removed by washing with PBS three times for 10 min and the oocytes were viewed in a confocal microscope (Section 1.5.3).

2.6.5 Oocyte transport assays

Radioisotope uptake measurements were carried out in oocytes 3 to 5 days after RNA injection (Section 2.6.2).

Frequently used solutions:

ND 96:	96 mM	NaCl	
	2 mM	KCl	
	1.8 mM	$CaCl_2$	
	1 mM	$MgCl_2$	
	5 mM	HEPES	pH 7.4, titrated with NaOH

2.6.6 Efflux experiments

Efflux assays were performed on groups of seven to ten oocytes, and were carried out at RT. The oocytes were washed twice with 4 mL ND96 transport buffer. They were then preloaded by incubation for 10 min in 90 µL of uptake buffer containing radiolabelled and non-labelled amino acids to give a final substrate concentration of 50 to 100 µM. Subsequently the oocytes were washed three times with 4mL ND96 and the efflux experiment was commenced with the addition of 1mL ND96 buffer containing 1 mM of non-labelled amino acid substrate. Samples were taken after 0, 5, 10, 20 and 30 min. After 30 min, the assays were terminated by washing the oocytes four times in ice-cold ND96 buffer. Each oocyte was then transferred into a separate scintillation vial and lysed by the addition of 200 µL of 10 % SDS. 3 mL scintillation fluid (Packard Biosciences, USA) was added and the radioactivity counted in a Beckman LS 6500 scintillation counter (Beckman, USA).

2.6.6.1 Competition experiments

Uptake assays were performed on groups of eight to ten oocytes, and were carried out at RT. The oocytes were washed twice with 4 mL ND96 transport buffer. The competition experiment was commenced with the addition of 90 µL ND96 containing 50 µM radiolabeled substrate and a non-labelled amino acid at a final substrate concentration of 5 mM. After 10 min, the assays were terminated by washing the oocytes four times in ice-cold ND96 buffer. Each oocyte was then distributed into a separate scintillation vial and lysed by the addition of 200 µL of 10 % SDS. 3 mL scintillation fluid was added and the radioactivity counted in a Beckman LS 6500 scintillation counter.

2.7 Brush border membrane vesicles (BBMV)

2.7.1 Isolation of proximal tubular brush border membrane vesicles

For the isolation of brush-border membrane vesicles the procedure described by Biber *et al.* (Biber *et al.*, 2007) was followed. However, several modifications for enhanced quality were developed. These are presented in detail in Chapter 4.

2.7.2 Alkaline Phosphatase (AP) Assay

To identify the enrichment of brush border membrane and therefore the quality of the BBMV, the enrichment of AP activity was measured. To this end, 1 mL of AP buffer and 100 µL of phosphatase substrate solution (Sigma, one tablet dissolved in 9.6 mL AP buffer) was incubated at 37 °C for 5 min. The reaction was started by adding 20 µL of diluted vesicle sample (usually dilutions 1:10, 1:100 and 1:1000 were used) and incubated at 37 °C for 5 to 8 min. The reaction was stopped by adding 1 mL of 500 mM NaOH. The absorbance was measured at 405 nm using a Cary 50 Bio UV-Visible spectrophotometer (Varian, Australia).

AP buffer:	1 M	Diethanolamine	
	0.5 mM	$MgCl_2$	pH 9.8 adjusted with HCl

2.7.3 Uptake experiment with BBMV

Radioisotope uptake measurements were carried out immediately after BBMV preparation in order to avoid degeneration of the vesicles at 25 °C.

20 µL of vesicle solution was added to 80 µL uptake buffer containing 100 µM non-labelled and labelled amino acid substrates. The mixture was vortexed and after 15 second (sec) a 20 µL sample was removed and the uptake was stopped by adding it to 4 mL ice-cold stopping buffer. The diluted samples were filtered using a manifold filtration device (Amersham Pharmacia). Subsequently, the filters were washed three with 4 mL stop solution. The filters were then transferred into separate scintillation vials and covered with 6 mL scintillation fluid. The radioactivity was counted in a Beckman LS 6500 scintillation counter.

Sodium uptake buffer was used to measure the uptake while potassium uptake buffer was used as a control. Two to three samples were taken for every time point and blank controls were measures as duplicates of filtered uptake buffer with substrate in respective dilution.

Uptake buffers:

sodium:	100 mM	NaCl	
	100 mM	D-Mannitol	
	20 mM	HEPES/Tris	pH 7.4
potassium	100 mM	KCl	
	100 mM	D-Mannitol	
	20 mM	HEPES/Tris	pH 7.4
Stop solution:	280 mM	D-Mannitol	
	20 mM	HEPES/Tris	pH 7.4

2.7.4 Competition Experiments with BBMV

Competition experiments were conducted following the same procedure as for uptake experiments (Section 2.7.4).

For these experiments the uptake buffer also included one of the competing amino acids leucine (10mM final concentration), glutamine (30 mM final concentration), proline (30 to 50 mM final concentration), phenylalanine (30 mM final concentration) or glycine (30 mM final concentration).

2.8 Mammalian cells

2.8.1 Cell lines and culturing conditions

In this study, the mammalian cell lines HEK 293 (ATCC- The Global Biorecourse Centre, Manassas, USA) and CHO- K1 (kindly provided by the Ian Young group, JCSMR, Canberra, Australia) were used. The cells were grown at 37 °C in a 5 % CO_2 humidified atmosphere in a HERA cell 240 CO_2 incubator (Heraeus- Thermo Scientific, USA). HEK cells were cultured in RPMI media with 10 % FCS, 2 mM Glutamine and 1mL of penicillin-streptomycin solution (Sigma) and CHO cells were cultured in Dulbecco's modified eagle's media plus nutrient mixture F-12 HAM (Sigma) with 2 % FCS and 1mL penicillin-streptomycin solution. The cells were subcultured when they were confluent, by washing with PBS and dislodging them using 0.25 % trypsin EDTA (Invitrogen). The trypsin activity was neutralised with FCS-containing medium and the cells were centrifuged at 900 g for 5 min in a Beckman GS-6R centrifuge. The cells were resuspended in complete medium and subcultured into flasks, dishes or on microscope slides as required for the various experiments.

2.8.2 Transient transfection of mammalian cells

Cells were either subcultured on microscope slides (LabTek II Chamber System, Nunc) or on 56.2 cm^2 petri dishes. Upon reaching 50 to 80 % confluency they were used for transfection. For the transfection either the Lipocetamine LTX Reagent with addition of Plus reagent was used or Lipofectamine 2000 (both from Invitrogen) following the manufacturers' instructions. Briefly, for transfection on 8-well microscope slides, the transfection mixture containing 200 ng of DNA, 0.5 µL of Lipofectamine LTX reagent and 0.2 µL PLUS reagent in 40 µL Opti-MEM medium (Invitrogen) was added to each well already containing 200 µL of Opti-MEM.

After incubation of the cells for 24 h at 37 °C in a 5 % CO_2, humidified atmosphere, the media was changed back to normal growth media and the cells were incubated for another 24 h. The cells were then used for immunofluorescence (Section 2.8.4) or were lysed for Western Blot analysis (Section 2.8.3). For each transfection controls were included, containing non-transfected cells and mock transfected cells (vector only control).

2.8.3 Lysis of cells for Western Blot

Protein expression in transfected mammalian cells was examined by Western Blot. Cells were washed twice with 10 mL PBS buffer, then scraped off the flask and taken up in ice-cold PBS buffer, centrifuged for 5 min at 900 g and washed again with 10 mL PBS. After centrifugation at 900 g for 5 min ice-cold Lysis buffer (usually 3-5 mL) was added to the cells and the mixture was incubated for 15 to 20 min on ice. The cells were centrifuged at 12,000 g at 4 °C and the supernatant was used to prepare samples for Western Blotting (Section 1.4.4.1 to 1.4.4.3).

RIPA (Lysis) buffer:	50 mM	Tris-HCl	pH 7.8
	150 mM	NaCl	
	0.5 %	SDS	
	0.1 %	Sodium deoxycholate	
	1 %	Triton X-100	
	1x	complete EDTA-free protease inhibitor (Roche)	

2.8.4 Immunofluorescence microscopy of mammalian cells

Immunofluorescence microscopy was performed to analyse transfection efficiency and expression of the amino acid transporters in mammalian cells.

Transfected cells and controls were washed with PBS. The cells were then fixed with either 3.5 % paraformaldehyde in PBS for 10 min at RT or with pre-cooled 100 % methanol at -20 °C for 10 min. After washing cells twice with PBS for 10 min they were incubated with 0.1 % glycine in PBS for 5 min at RT.

Subsequently, the cells were permeabilised with 0.3 % Triton X-100 in PBS for 10 min. The cells were then incubated for 2 h at 37 °C in a humidified environment with primary antibody in various dilutions and different blocking reagents depending on the mammalian cells and antibody. To remove non-specific binding, the cells were washed twice with 0.1 % Triton X-100 in PBS for 10 min and incubated for 1 h at 37 °C in a dark, humidified environment with the secondary antibody in appropriate dilution. After washing the cells twice with 0.1 % Triton X-100 in PBS for 10 min the cells were mounted with the anti- fade reagent ProLong Gold (Invitrogen) and examined under the confocal microscope Leica TCS SP5 (Section 2.5.3).

2.9 Statistical Analysis

Statistical analysis was performed using Origin Statistical program (Origin Version7 0300, 1991-2002 Origin Lab Corporation Ma, USA). Student's t test was used to compare samples.

Additional statistical analysis, including one-way Analysis of Variance (ANOVA) and post hoc Bonferroni tests were conducted using the GraphPad InStat program (InStat Version 3.06 32bits for windows, GraphPad Sofware Inc., La Jolla, USA). A p- value < 0.05 was considered as significant and was marked with asteriks in the figures.

Chapter 3

- Distribution of the amino acid transporters

B^0AT1, B^0AT2 and ASCT2

in kidney and intestine

3.1 Introduction and aim of this study

In previous studies, the tissue biodistribution of B^0AT1 and ASCT2 has been analysed (Avissar *et al.*, 2001; Broer *et al.*, 2004; Green *et al.*, 2004). It has been determined that B^0AT1 is localised in the early segments of the proximal tubule and in the apical membrane of the whole intestine except the colon.

ASCT2 has either been detected apically in the early segment of the proximal tubule and in all segments of the intestine or controversially was shown to be in the basolateral membrane of the proximal tubules (Green *et al.*, 2004). The study by Avissar *et al.* further suggested that ASCT2 is the main apical transporter for neutral amino acids in intestine and kidney.

To clarify the relative roles of B^0AT1 and ASCT2, the localisation of both transporters was determined with antibodies designed against an ASCT2 peptide in our own laboratory. In addition, the localisation of B^0AT2 in the kidney was determined. Because the antibodies had not been used before, their specificity needed to be characterised prior to immunofluorescence studies on mouse tissue.

3.2 Results

The immunofluorescence studies with tissue sections described in this chapter had to be optimised depending on the antibody used, particularly for the antibody against B^0AT2. This antibody showed high non-specific binding to mouse tissue. The optimised protocol is shown in detail below:

3.2.1 Immunofluorescence protocol

- It is important for this protocol that throughout the whole procedure the slides never dry out.
- Slides were first deparaffinised by sequential 10 min immersion in HistoClear, 100 % ethanol and 95 % ethanol in a Coplin jar.
- The slides were then washed three times for 5 min with PBS followed by three washes with distilled water each for 5 min in a Coplin jar.
- The deparaffinised slides were immersed using a slide holder in 600 ml of boiling 1 mM sodium citrate buffer (pH 6.0) in a 2 L beaker. The sodium citrate buffer was kept boiling for 15 min and then removed from the hot plate.
- The submerged slides were incubated in the buffer for a further 20 min as it cooled down.
- The slides were then taken out and washed with PBS three times for 5 min in a Coplin jar.
- The tissue sections on the slides were outlined with a Pap Pen (Invitrogen).
- 150 to 200 µL of blocking solution in PBS was applied to each section until the sections were totally covered.
- The slides were then incubated in a humidified incubation chamber at 37 °C for 1.5 to 2.5 h.
- After incubation, the blocking solution was removed and 150 to 200 µL of primary antibody diluted in PBS was applied immediately to the sections until completely covered.

- The slides were incubated in a humidified incubation chamber at 37 °C for 0.5 to 1.5 h.
- After incubation, the primary antibody was removed and the slides were washed three times for 5 min in PBS in a dark Coplin jar to remove any unbound antibodies.
- After washing, the PBS buffer was removed as much as possible and where necessary, the Pap Pen was applied again.
- 150 to 200 µL of the secondary antibody diluted in PBS was applied to the sections immediately.
- The slides were incubated in a humidified incubation chamber in the dark at 37 °C for 0.5 h.
- After incubation, the secondary antibody was removed and the slides were washed three times for 5 min with PBS in a Coplin jar in the dark.
- The PBS buffer was removed completely from the slides, which were then mounted with ProLong Gold antifade reagent (Invitrogen) to preserve the fluorescence of the section. The antifade reagent was allowed to set over night.
- Digital images were obtained using the x40 or x60 oil objective with a LAS-AF system installed on a Leica TSC SP5 confocal microscope using the lasers according to the fluorochrome used.
- Control sections were stained with secondary antibody only.
- Images were, if necessary, processed using Adobe Photoshop CS3 Extended Version 10.0.1 (Adobe Systems, San Jose, CA, USA) to enhance contrast. Images of controls and treated sections were processed using the same settings.

3.2.2 Characterisation of the B^0AT1 antibody

The neutral amino acid transporter gene for B^0AT1 had been predicted to have a molecular mass of 71 kDa. The antibody against mouse B^0AT1 was raised against a GST-fusion protein of the N-terminus.

To elucidate whether the B^0AT1 antibody was suitable for immunofluorescence studies on tissues, Western Blot analysis of B^0AT1 injected oocytes was conducted first. Oocytes were injected with mouse B^0AT1 cDNA and after 3 to 5 days, proteins were prepared for Western Blot analysis. Non-injected oocytes were used as a control. B^0AT1 was detected as a 65 kDa band in the injected oocytes, but no band was visible in the control oocytes.

Western blot analysis conducted with the pre-immune serum from the antibody production revealed a faint protein band at 95 kDa (Figure 3.1), which was only detected with the final serum after a long exposure time.

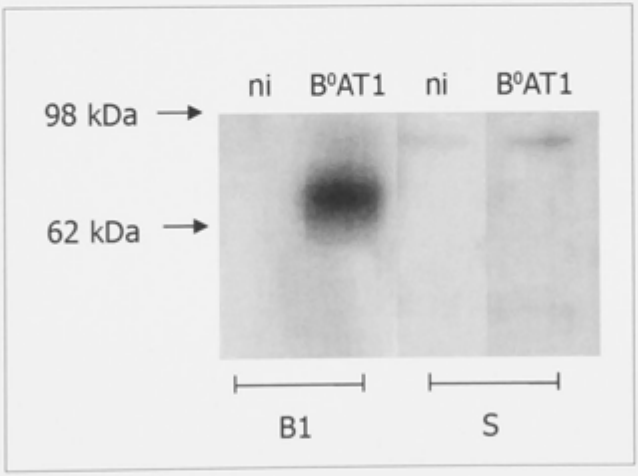

Figure 3.1: Evaluation of the mouse B^0AT1 antibody in oocytes.

B^0AT1 cRNA injected oocytes (B^0AT1) and non-injected oocytes (ni) were lysed, the lysates were then separated by SDS-PAGE and transferred onto a nitrocellulose membrane. The membrane was incubated either with rabbit anti-mB^0AT1 (B1) or pre-immune serum isolated from the same rabbit (S) during antibody production. The bands were visualised using a chemiluminescent Western Blot detection kit. B^0AT1 was detected in the injected oocytes only. Another faint protein band was only detected in the pre-immune serum control as well.

To test whether the antibody was suitable for immunostaining, oocytes were injected with human and mouse B^0AT1 cRNA. Non-injected oocytes were used as a control. Four days after injection, the oocytes were fixed with 4 % paraformaldehyde and subsequently detected with either chicken anti-human B^0AT1 antibody stained by goat anti-chicken secondary antibody conjugated to Alexa Fluor® (AF) 488, a green fluorophore, or rabbit anti-mB^0AT1 antibody detected by donkey anti-rabbit secondary antibody conjugated to AF 488.

Staining was then observed using a confocal microscope. In the membrane, fluorescence was detected in oocytes injected with human and mouse B^0AT1, while no or only negligible fluorescence was observed in non-injected oocytes (Figure 3.2). This indicates that both B^0AT1 antibodies are suitable for immunofluorescence studies.

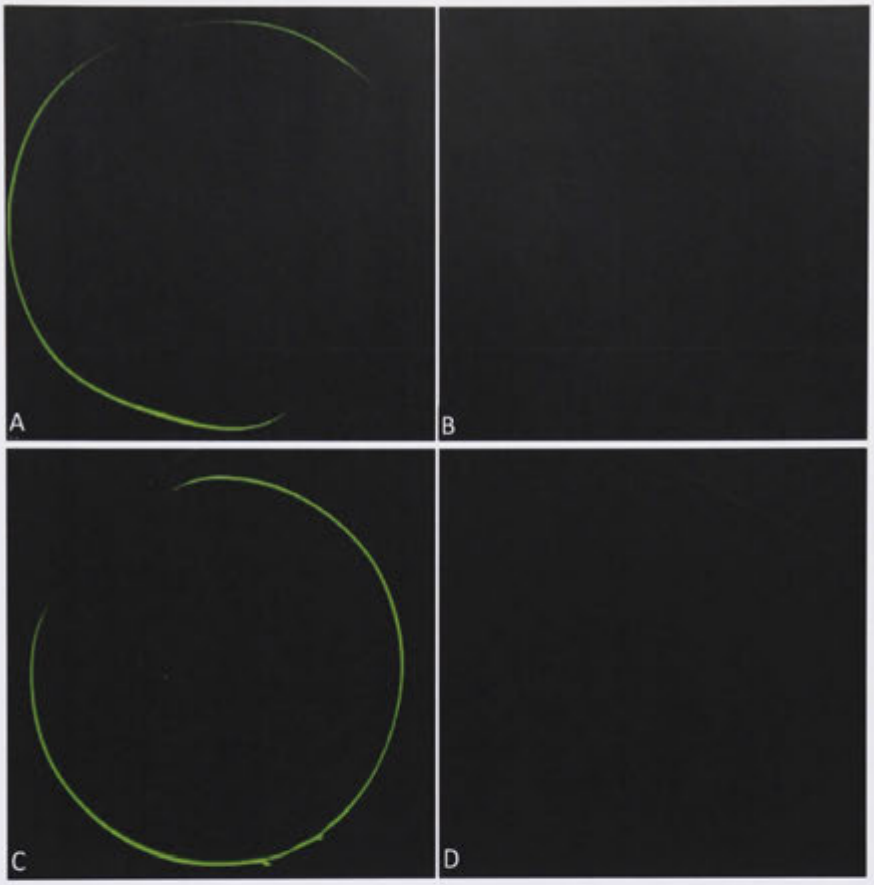

Figure 3.2: Evaluation of human and mouse B^0AT1 in oocytes.

Both human (**A**) and mouse (**C**) B^0AT1 cRNA injected oocytes showed bright green fluorescence of the oocyte membrane. Non-injected oocytes (**B**, **D**) used as negative control show no (**B**) or very faint (**D**) fluorescence. Original magnification, x10.

3.2.3 Characterisation of the B^0AT2 antibody

The neutral amino acid transporter gene for B^0AT2 had been predicted to form a protein with a molecular weight of 81 kDa. Two antibodies were generated against mouse B^0AT2 protein, one against a GST-fusion protein of the C-terminus, the other against a GST-fusion protein of the N-terminus of the protein.

To investigate if these antibodies were suitable for immunofluorescence studies on tissues, Western Blots analysis were conducted. Oocytes were injected with mouse B^0AT2 cRNA and after 3 to 5 days prepared for Western Blot analysis. Non-injected oocytes were used as controls. B^0AT2 was detected as a band with the molecular weight of 81 kDa in the injected oocytes, but not in the controls.

An additional protein with a higher molecular weight than 82 kDa was detected as a weaker band. This protein was present in both the control and injected oocytes. Western Blot analysis conducted with the pre-immune serum from the antibody production showed the same unknown protein band (Figure 3.3).

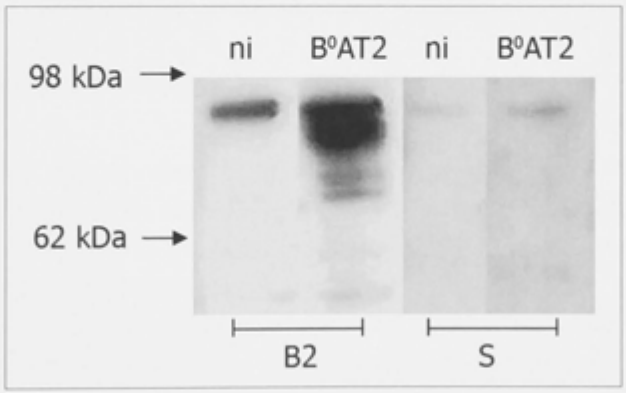

Figure 3.3: Evaluation of mouse B^0AT2 N-terminal antibody in oocytes.

B^0AT2 cRNA injected oocytes (B^0AT2) and the non-injected oocytes (ni) were lysed, the lysates were then separated by SDS-PAGE and transferred onto a nitrocellulose membrane. The membrane was incubated either with B^0AT2 (B2) or pre-immune serum isolated from the same rabbit (S). The bands were visualised using a chemiluminescent Western Blot detection kit. B^0AT2 was detected in the injected oocytes only. Another unknown protein was detected, which was present in non-injected oocytes and albeit weaker in the pre-immune serum control as well.

In addition, B^0AT2 transfected HEK-293 (HEK) cells were also examined using Western Blot analysis. Non-transfected HEK cells were used as control. The B^0AT2 protein was detected as a strong band at 81 kDa in the B^0AT2 transfected HEK cells, but was also present at lower intensity in the non-transfected HEK cells (Figure 3.4).

As the HEK cell line is derived from kidney tissue, it appears possible that HEK cells express B^0AT2 endogenously, which will be investigated further below.

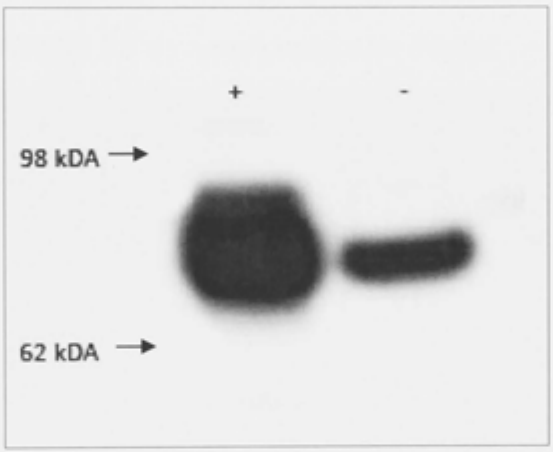

Figure 3.4: Western Blot analysis of mouse B^0AT2 in HEK cells.

B^0AT2 transfected HEK cells, are denoted as '+' and the non transfected HEK cells are denoted as '–'. The protein lysates were separated by SDS-PAGE and transferred onto nitrocellulose membrane. The membrane was incubated with the B^0AT2 N-terminal antibody. The bands were visualised using a chemiluminescent Western Blot detection kit. The 98 kDa and the 62 kDa markers are indicated by black arrows. B^0AT2 was detected as an 81 kDa protein enriched in transfected cells, but was also present in non-transfected HEK cells.

To test whether the antibody was useful for immunofluorescence microscopy, oocytes were injected with mouse B^0AT2 cRNA. Non-injected oocytes were used as a control. After 4 days, the oocytes were fixed with 4 % paraformaldehyde and subsequently stained with rabbit anti-B^0AT2 C-terminal antibodies. The primary antibodies were detected by donkey anti-rabbit secondary antibody conjugated to AF 488. Flourescence was then observed using a confocal microscope. The membranes of both the injected and non-injected oocytes showed a bright fluorescence staining with the antibody. However, weak immunofluorescence was also detected in the non-injected oocytes (Figure 3.5). The fluorescence was fainter in the non-injected oocytes than the injected oocytes, but the results were not convincing enough to determine that the B^0AT2 antibody was suitable for immunofluorescence studies.

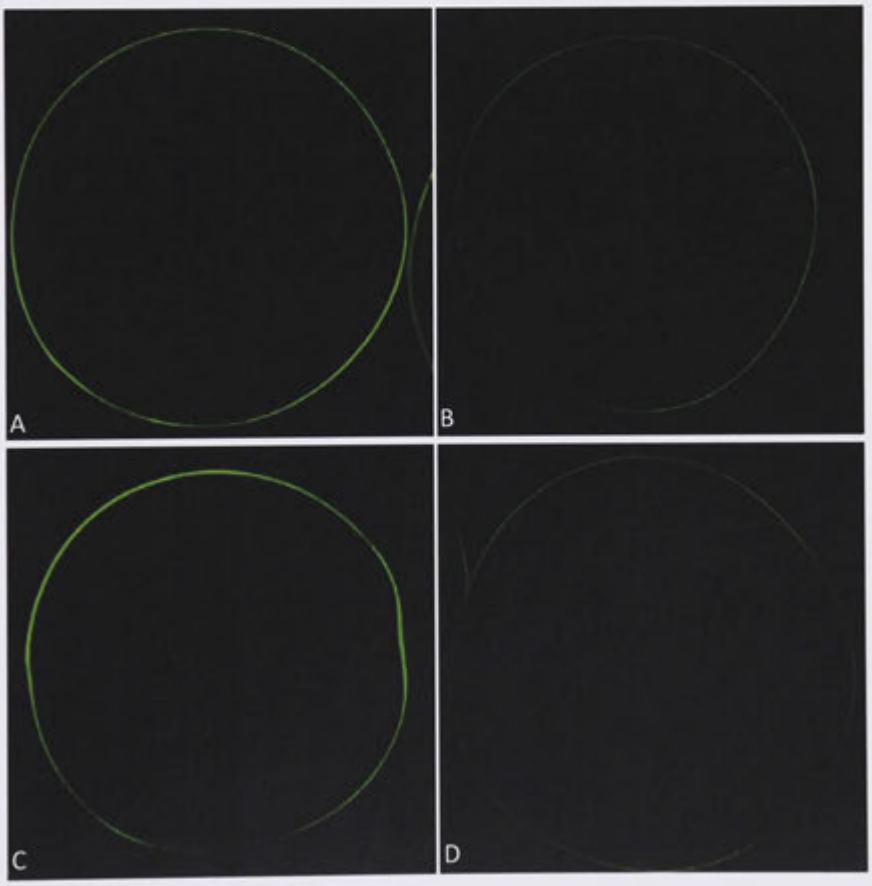

Figure 3.5: Evaluation of mouse B^0AT2 antibody in oocytes.

B^0AT2 cRNA injected oocytes stained with C-terminus (**A**, **B**) and N-terminus (**C**, **D**) antibodies showed bright green fluorescence of the oocyte membrane. Non-injected oocytes (**B, D**) were used as negative controls and showed weak fluorescence in both experiments. Original magnification, x10.

Further preliminary immunofluorescence studies to determine which antibody was most suitable for this project showed slightly better results for the N-terminus specific antibody (data not shown) than the C-terminus specific antibody. For this reason, the N-terminus specific antibody was chosen for all subsequent experiments.

To investigate the B^0AT2 antibody further, HEK cells were transfected with B^0AT2 cDNA. After 48 h the cells were fixed with 3.5 % paraformaldehyde and subsequently stained with rabbit anti-B^0AT2 antibody detected by donkey anti-rabbit secondary antibody conjugated to AF 488. B^0AT2 staining was detected in the cytosol of B^0AT2 transfected cells, but also weakly in non-transfected cells (Figure 3.6).

Similar to the Western Blot results this suggested that HEK293 cells express B^0AT2 endogenously. This experiment also could not confirm the suitability of the antibody for immunofluorescence studies.

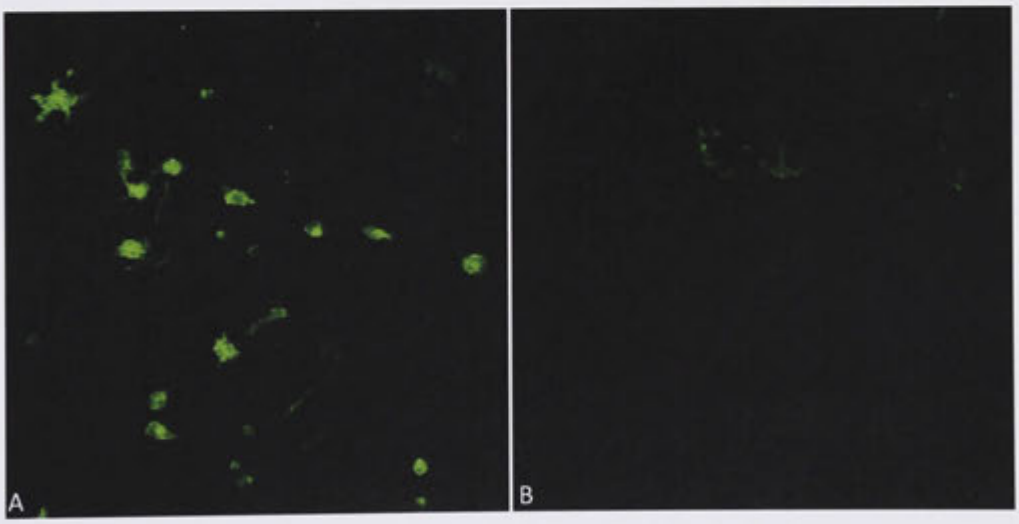

Figure 3.6: Evaluation of N-terminal B^0AT2 antibody in HEK cells.

A: Bright B^0AT2 staining was detected in the cytosol of transfected HEK cells **B:** Weaker immunofluorescence was observed in the non-transfected HEK cells. Original magnification, x10.

RT-PCR was used to test for the endogenous expression of B^0AT2 in HEK cells. RNA from HEK cells was obtained and reverse transcribed into cDNA. The cDNA was then examined by PCR using various primer pairs. Actin was used as a positive control and two primer pairs spanning the C-and N-terminus were used to test for B^0AT2 existence. Figure 3.7 shows the result of this RT-PCR reaction. RNA and water were used as templates in the controls. The actin primers produced a faint product in the RNA only control, implying a slight contamination of the RNA with genomic DNA. In the water only control no product was amplified, indicating the absence of DNA and RNA contaminations. The positive actin control showed a bright actin-specific product of 100 bp. Only the primers for the C-terminus region of the B^0AT2 cDNA generated a visible product. This indicates that HEK cells express B^0AT2 endogenously explaining the results of the Western Blot analysis and the immunofluorescence microscopy.

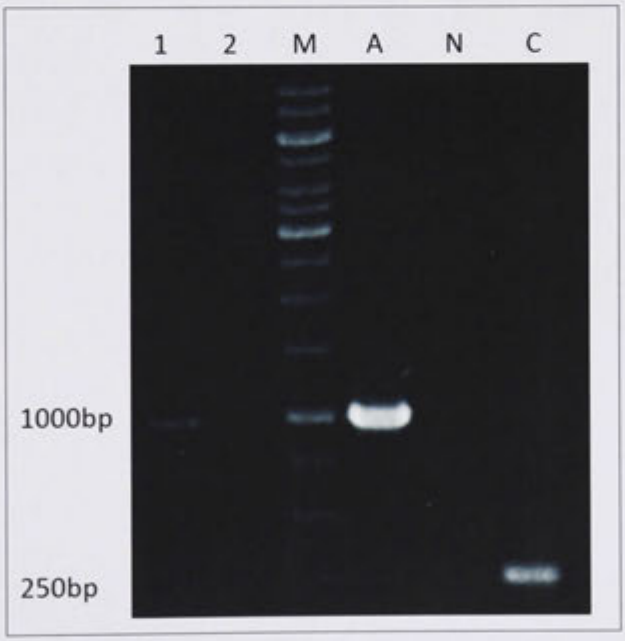

Figure 3.7: RT-PCR of HEK cells with actin, B^0AT2 N- and C- terminal specific primers.

Total RNA was isolated from HEK cells and reverse transcribed into cDNA. The 250 bp and the 1 kb band of the 1kb marker, denoted as M, are accentuated. RNA was used as a template in the negative control and tested with actin primers, denoted as 1. It generated a faint product of actin, indicating slight genomic DNA contamination. When water was used as a template, denoted as 2, no specific fragment was generated. The positive actin control, denoted as A, amplified a 1kb actin-specific fragment. With the primer pairs of the N- and C-terminus of B^0AT2, denoted as N and C only the C-terminus was amplified as 250bp specific fragment.

Further RT-PCR experiments showed that Chinese hamster ovary cells (CHO) did not express B^0AT2 endogenously (data not shown). These cells were used for B^0AT2 transfection, and were fixed with 3.5 % paraformaldehyde 48 h after transfection. Subsequently the cells were treated with rabbit anti-B^0AT2 antibody and the protein was detected by donkey anti-rabbit secondary antibody conjugated to AF 488. B^0AT2 fluorescence was detected in the cytosol of B^0AT2 transfected CHO cells. No fluorescence was observed in non-transfected cells and only faint background fluorescence was detected in mock-transfected cells (cells transfected with pcDNA3.1+ vector only) (Figure 3.8). This indicates that the B^0AT2 antibody was suitable for immunofluorescence studies with tissue sections.

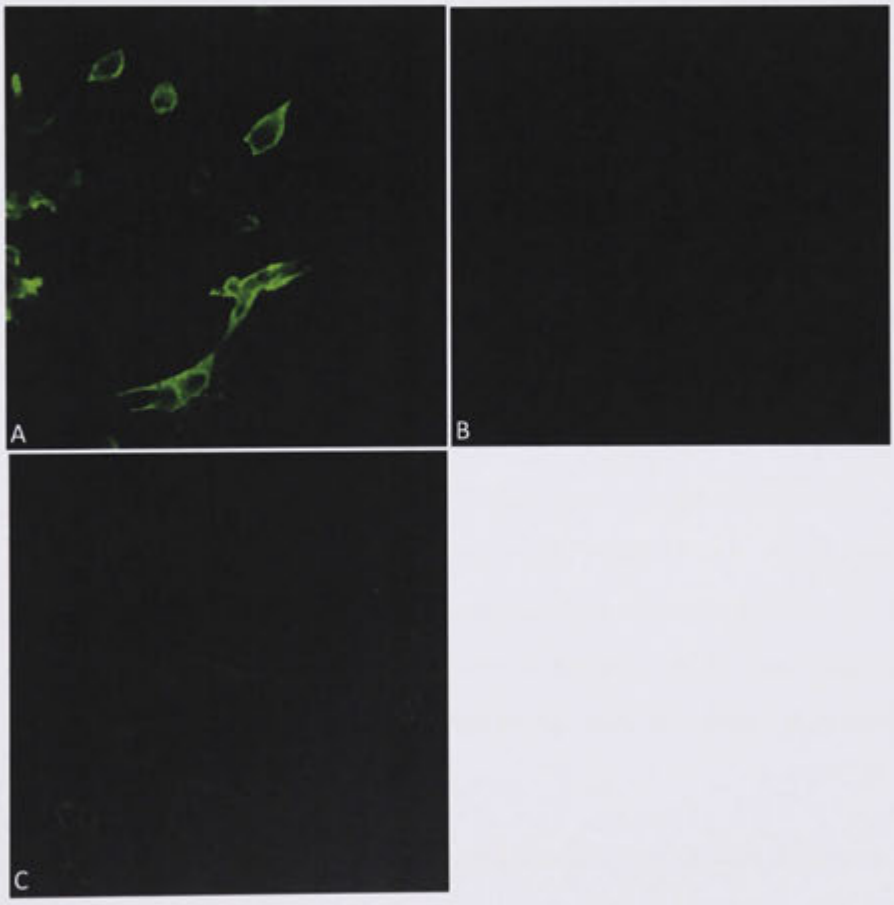

Figure 3.8: Evaluation of mouse N-terminal B^0AT2 antibody in CHO cells.

A: Bright green B^0AT2 staining was detected in the cytosol of the transfected CHO cells **B:** No fluorescence was revealed in the non-transfected CHO cells. **C:** Only a faint fluorescence was detected in the mock-transfected CHO cells. Original magnification, x10

3.2.4 Characterisation of the ASCT2 antibody

The neutral amino acid transporter gene for ASCT2 has been predicted to form a protein of 58 kDa. Two ASCT2-specific antibodies were investigated. One antibody, kindly provided by the Avissar laboratory, was raised against the human ASCT2 C-terminus (characterised in Avissa *et al.*, 2001), while the second was designed in our laboratory against the mouse ASCT2 peptide epitope N-REPSGDSSATC—COOH. The specificity of the antibody designed in our laboratory was already analysed in the honours thesis of Tobias Heckel (Heckel, 2002). He showed that the detection of ASCT2-like immunoreactivity is reduced in Western Blots when the antibody is incubated with the immunogenic peptide, indicating that the antibody is specific for ASCT2.

The two primer sequences are 82 % identical. The amino acid sequence of human ASCT2 is highly homologous to those of rat and mouse ASCT2 (Broer A. *et al.*, 1999; Liao, K. and Lane, M.D., 1995). For instance, the amino acid sequence of mouse ASCT2 is 83 % identical to rat ASCT2 sequence. Furthermore, the human amino acid sequence of ASCT2 possesses 42 % similarity to the mouse amino acid sequence and 56 % similarity to the rat amino acid sequence of ASCT2. The first step was to test which of the antibodies was more appropriate to detect ASCT2 in tissue of different species.

Human, mouse and rat tissue samples were first analysed using Western Blot analysis. Protein samples were prepared identically, separated by SDS-PAGE and after transfer onto a nitrocellulose membrane, ASCT2 was detected by immunoblotting. The Avissar laboratory antibody detected a 47 kDa protein in human and mouse tissue, but no protein in rat tissue. Longer exposure time revealed a weak protein band at 58 kDa and 63 kDa in all tissues (data not shown).

Detection with our own ASCT2 antibody revealed a band at 53 kDa in human tissue. This protein was not detected in rat tissue, but was observed with longer exposure time in mouse tissue (data not shown). Furthermore, a protein of around 100 kDa was detected in mouse and rat tissue, consistent with the size of an ASCT2 dimer. With longer exposure time a protein band became visible in the 77 to 80 kDa range in all tissues (Figure 3.9). To resolve these discrepancies, further tests were performed.

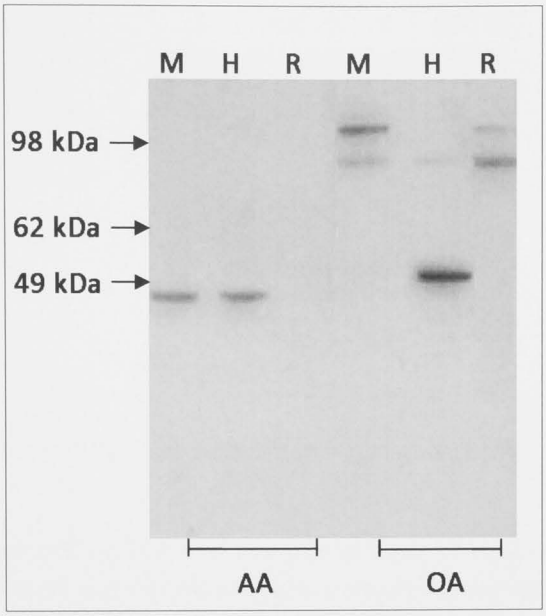

Figure 3.9: Detection of ASCT2- like immunoreactivity in different tissues by anti-human and anti-mouse antibody.

The tissue samples from mouse (M), human (H) and rat (R) were prepared identically, subsequently separated by SDS-PAGE and transferred onto a nitrocellulose membrane. The membrane was either incubated with anti-human ASCT2 antibody received from the Avissar laboratory, denoted with AA or with anti-mouse ASCT2 antibody generated in our own laboratory, denoted as OA. The bands were visualised using a chemiluminescent Western detection kit. The marker sizes are indicated by black arrows. ASCT2-like activity was detected as a distinct 47 kDa band with the AA antibody in human and mouse but not in rat tissue. ASCT2-like immunoreactivity detection with OA revealed a 53 kDa protein in human tissue, but not in mouse and rat, but recognised bands at 85 kDa and 105 kDa in rat and mouse tissue.

Oocytes were injected with ASCT2 cRNA and non-injected oocytes were used as a control. After 3 to 4 days the oocytes were prepared for Western Blot analysis. Again, both ASCT2 antibodies were investigated. Surprisingly, ASCT2-like immunoreactivity was detected as a 47 kDa protein in both non-injected and injected oocytes with the antibody received from the Avissar laboratory. Similarly, our own antibody detected two proteins around 80 kDa and 100 kDa in both injected and non-injected oocytes (Figure 3.10). These results were inconclusive with respect to antibody specificity.

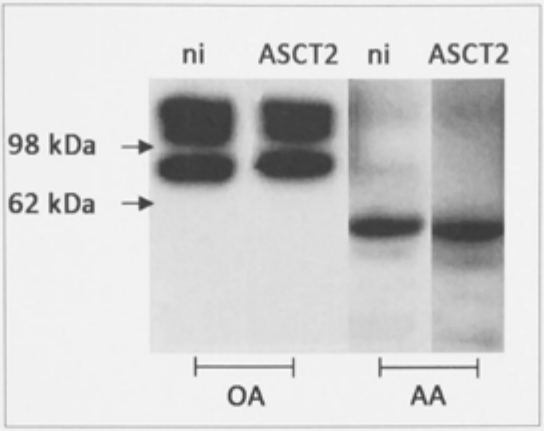

Figure 3.10: Detection of ASCT2-like activity in oocytes by anti-human and anti-mouse antibody.

ASCT2 cRNA injected oocytes (ASCT2) and non-injected oocytes (ni) were lysed, the proteins were separated by SDS-PAGE and transferred onto a nitrocellulose membrane. The membrane was either incubated with anti-human ASCT2 antibody received from the Avissar laboratory, denoted with AA or with the anti-mouse ASCT2 antibody designed in the Broer laboratory, denoted as OA. The bands were visualised using a chemiluminescent Western Blot detection kit. The Avissar antibody detected a protein of 47 kDa in both injected and non-injected oocytes. With our own antibody two immunoreactive bands were detected at about 80 kDa and 100 kDa.

Additional Western Blot analysis with transfected CHO cells was undertaken to investigate, which antibody against ASCT2 would be suitable for further experiments. CHO cells were transfected with either ASCT2 cDNA or mock (the pcDNA3.1+ vector only control). Non-transfected cells were used as a second control. The cells were lysed 48 h after transfection, and the proteins were separated by SDS-PAGE. The Avissar antibody detected a 58 kDa protein after prolonged exposure in all three cell types. The transfected CHO cells did show an increase of the detected protein in comparison to non- or mock-transfected cells. With the antibody designed by our own laboratory a number of bands at 41, 47, 54, 62, 79, 98 and 178 kDa were detected in ASCT2-transfected cells, but not in mock-transfected or non-transfected cells. Immunoreactivity was particularly strong at 98 kDa. These proteins appear as a result of ASCT2 transfection and therefore are likely to represent different isoforms or degradation products of ASCT2 as reported previously (Tailor *et al.*, 2001). A protein of around 54 kDa was weakly detected in both mock- and ASCT2-transfected cells (Figure 3.11).

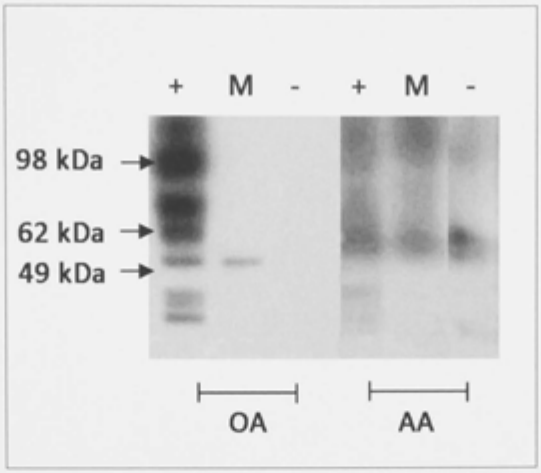

Figure 3.11: Evaluation of anti human- and anti mouse-ASCT2 antibody in CHO cells.

ASCT2 cDNA transfected CHO cells are denoted as '+', mock-transfected CHO cells are denoted as 'M' and non-transfected CHO cells are denoted as '–' . Protein lysates were separated by SDS- PAGE and transferred onto nitrocellulose membrane. The membrane was incubated with anti-human ASCT2 antibody received from the Avissar laboratory, denoted with AA and with an anti-mouse ASCT2 antibody designed in our own laboratory, denoted as OA. The bands were visualised using a chemiluminescent Western Blot detection kit. The 98 kDa, the 62 kDa and the 49 kDa size of the marker are indicated by black arrows. ASCT2-like immunoreactivity was detected as a weak band at 58 kDa protein with the Avissar antibody in all three cell types. The antibody designed in our own Laboratory detected several bands in ASCT2 cDNA transfected cells at 41, 47, 62, 79, 98 and 178 kDa, a weak band of 54kDa was detected in mock-transfected cells and no immunoreactivity was detected in non-transfected cells.

In summary, the Avissar antibody failed to detect ASCT2-like immunoreactivity in two different expression systems. These results were confirmed by immunofluorescence studies of CHO cells. Cells were fixed with 3.5 % paraformaldehyde 48 h after transfection, incubated with rabbit anti-human ASCT2 antibody (Avissar laboratory), which was subsequently detected by donkey anti-rabbit secondary antibody conjugated to AF 488. Immunofluorescence was detected in the cytosol of ASCT2 cDNA transfected CHO cells but fluorescence of similar intensity was detected in non-transfected cells as well. Mock-transfected cells showed less fluorescence in comparison to ASCT2 transfected and non-transfected cells. However, the fluorescence observed with the secondary antibody only was as bright as in ASCT2 cDNA transfected cells (Figure 3.12).

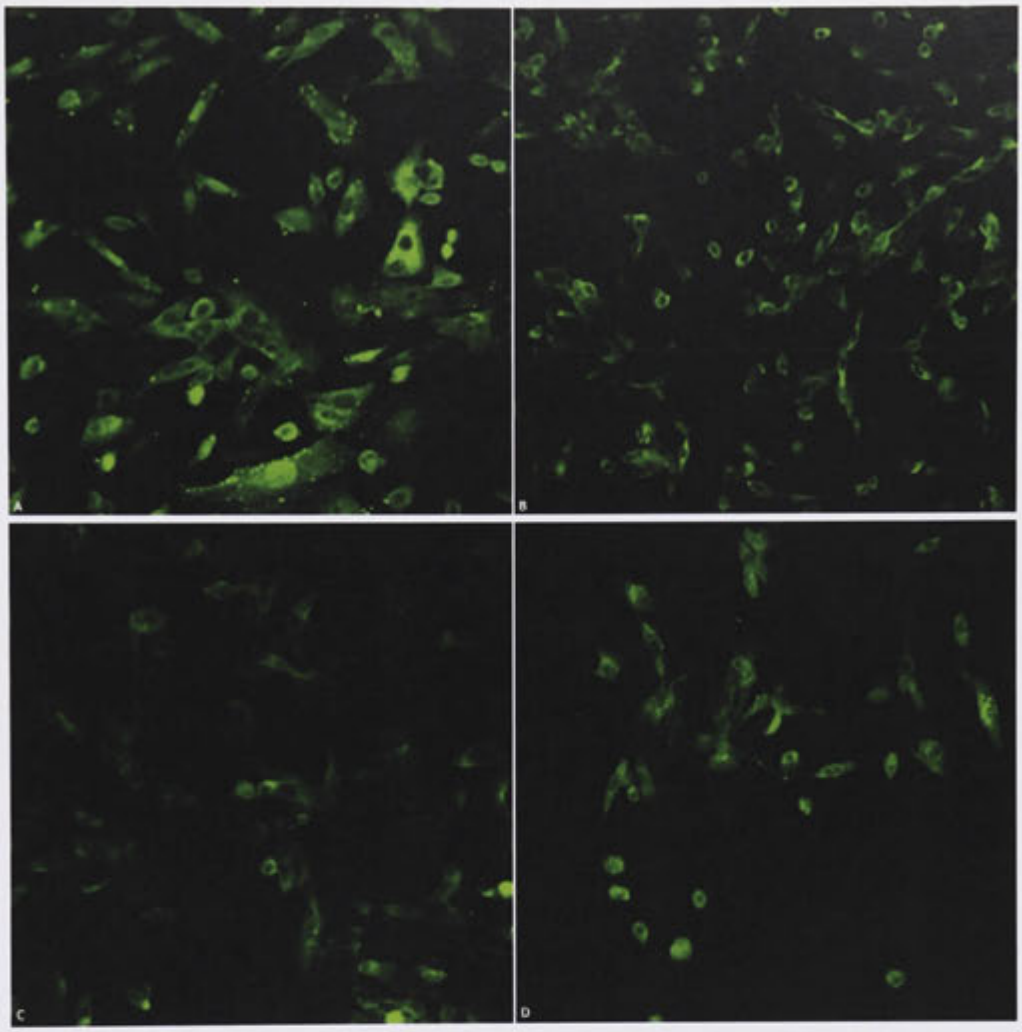

Figure 3.12: Evaluation of anti-human ASCT2 antibody for immunofluorescence in paraformaldehyde fixed CHO cell.

Immunofluorescence studies were conducted with paraformaldehyde fixed ASCT2 transfected (A), non-transfected (B) and mock-transfected CHO cell (C).

A: Bright green immunofluorescence was detected in the cytosol of ASCT2 transfected CHO cells. **B:** Similar levels of fluorescence were also observed in the non-transfected CHO cells. **C:** The mock-transfected CHO cells showed a fainter fluorescence than A and B. **D:** Staining with the secondary antibody only as a control resulted in similar fluorescence intensity as A and B. Original magnification, x10.

The absence of a significant difference in fluorescence between transfected, non-transfected cells and cells treated with secondary antibody only, suggested that the antibody was not suitable for immunofluorescence studies on paraformaldehyde-fixed tissue. Therefore, the fixation method of the cells was changed from paraformaldehyde to a less aggressive fixative, the organic solvent acetone.

CHO cells were transfected with ASCT2 cDNA as described above and fixed after 48 h with acetone. The cells were then stained with both, rabbit anti-human ASCT2 (Avissar) and rabbit anti-mouse ASCT2 (Broer) antibodies and the protein was detected by donkey anti-rabbit secondary antibody conjugated to AF 488 as described above. With the antibody from the Avissar laboratory a faint fluorescence was detected in the cytosol and in the plasma membrane of the transfected CHO cells. Mock-transfected CHO cells showed only slight background staining (Figure 3.13). No staining was observed in non-transfected CHO cells (data not shown).

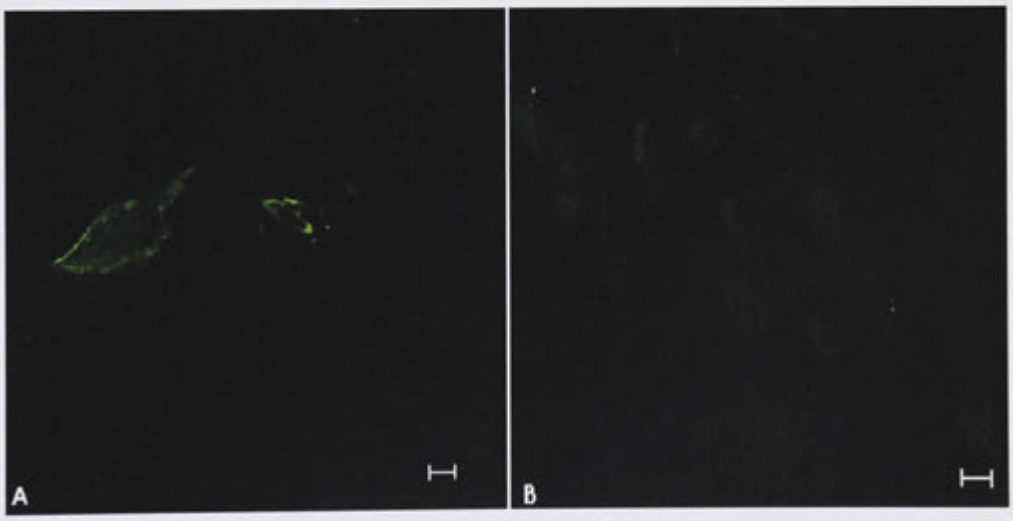

Figure 3.13: Evaluation of anti-human ASCT2 antibody for immunofluorescence in acetone fixed CHO cell.

Immunofluorescence studies were conducted with the Avissar antibody, with acetone fixed ASCT2 transfected (A) and non-transfected (B) CHO cell.

A: Faint green ASCT2-like immunoreactivity was detected in the cytosol and the plasma membrane of the transfected CHO cells. **B:** The mock-transfected CHO cells showed slight background staining. Original magnification, x10. Scale bars represent 10 µm.

The antibody designed in our laboratory, by contrast, showed bright fluorescence in the cytosol of the transfected cells (Figure 3.14 A). In mock-transfected cells only a slight background staining was detected (Figure 3.14 B). No staining was noted in the non-transfected CHO cells (data not shown).

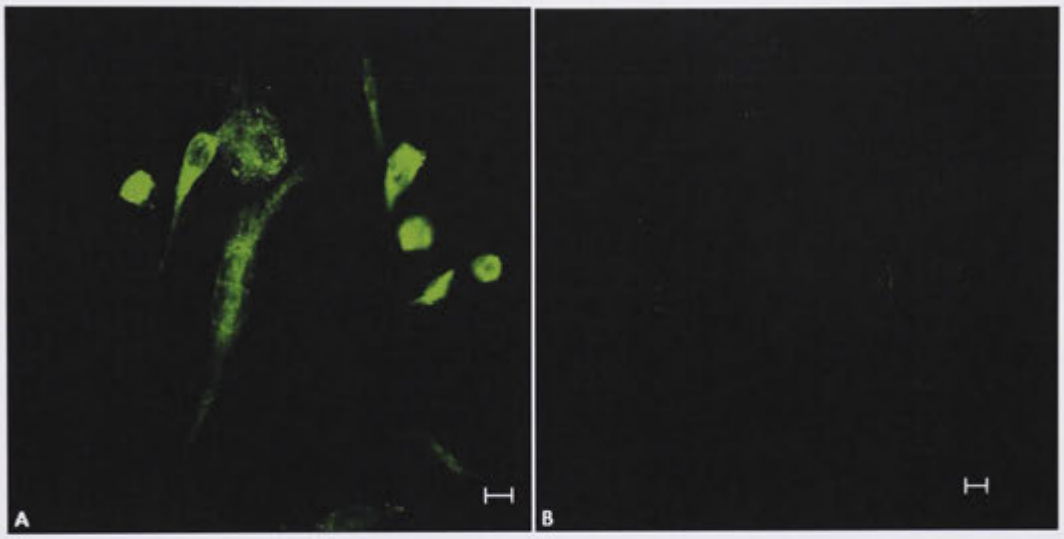

Figure 3.14: Evaluation of anti-mouse ASCT2 antibody in acetone fixed CHO cells.

Immunofluorescence studies were conducted with the Broer antibody, with acetone fixed ASCT2 transfected (A) and non-transfected (B) CHO cell

A: Strong ASCT2-like immunoreactivity was detected in the cytosol of the transfected CHO cells. **B:** The mock-transfected CHO cells showed slight background staining. Original magnification, x10. Scale bars represent 10 µm.

In summary, only the antibody designed in our laboratory detected ASCT2-like bands and immunofluorescence in transfected cells and was therefore chosen for further analysis.

3.2.5 Immunofluorescence of B^0AT1, B^0AT2 and ASCT2 in mouse kidney and intestine

3.2.5.1 Confirmation of B^0AT1 localisation in mouse kidney and intestine

C57Bl/6 adult mouse kidney and intestine specimens were pre-fixed with 10 % NBF, then embedded in paraffin, sectioned and de-paraffined. Boiling sodium citrate (1 mM) buffer at pH 6 was subsequently applied to retrieve the cross-linked antigenic sites formed during the fixation. Subsequently, the sections were incubated with rabbit anti-mB^0AT1 antibody detected by donkey anti-rabbit secondary antibody conjugated to AF 488. The kidney proximal tubules were identified by incubation with biotinylated lotus tetragonobolus lectin (LTL), which was detected by Strepavidin-Texas Red. B^0AT1 fluorescence was observed in the mouse kidney in the S1 segment and the S2 segment of the proximal tubule. The staining was only observed in the apical membrane of the cells. In the intestine, B^0AT1 was detected in the apical membrane of the villi showing a gradual decrease from the top of the villi towards the crypt cells of the intestine (Figure 3.15). B^0AT1 was observed in nearly all parts of the intestine (data not shown).

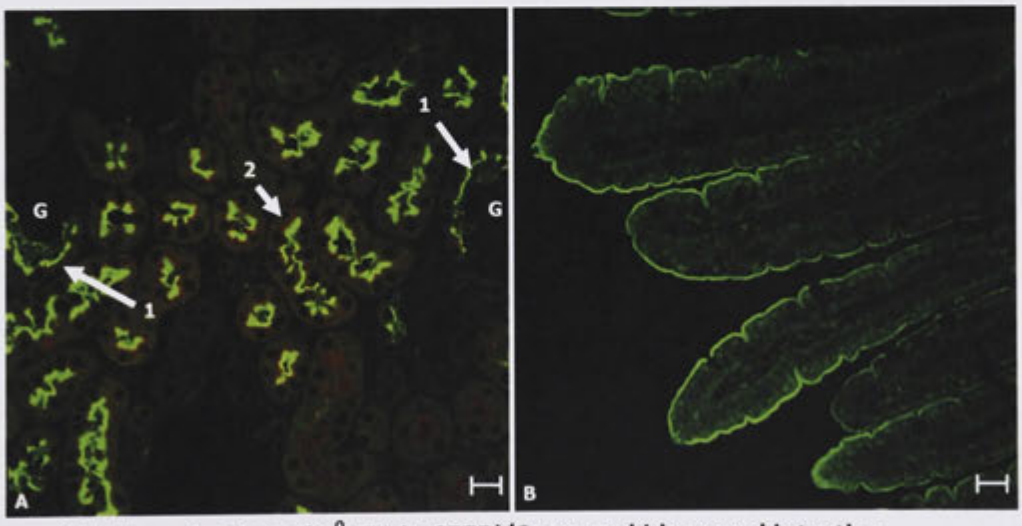

Figure 3.15: Localisation of B^0AT1 in C57Bl/6 mouse kidney and intestine.

B^0AT1 was identified using a rabbit primary antibody, detected by a donkey anti-rabbit secondary antibody conjugated to AF 488 (green). Kidney proximal tubules were visualised using biotinylated Lotus Tetragonobolus Lectin (LTL), detected with Strepavidin-Texas Red (red). G represents a glomerulus. **A**: B^0AT1 was detected on the apical membrane of the early proximal tubulus segments S1 (i.e. near the glomerulus), denoted as 1, and S2, denoted as 2. **B**: B^0AT1 staining was detected in the apical membrane of the villi. It was more strongly expressed at the tip of the villi, gradually decreasing towards the crypt cells. Original magnification, x40. Bars represent 10 µm.

3.2.5.2 Determination of B^0AT2 localisation in mouse kidney and intestine

To determine the B^0AT2 localisation, the same procedure was used as with B^0AT1, as described above. B^0AT2 immunofluorescence was observed in the apical membrane of the later segments of the proximal tubulus, namely S2 and S3. Furthermore, B^0AT2 was only noted in a very small percentage of cells. B^0AT2 was not detected in the intestine. Only a faint background staining was observed (Figure 3.16).

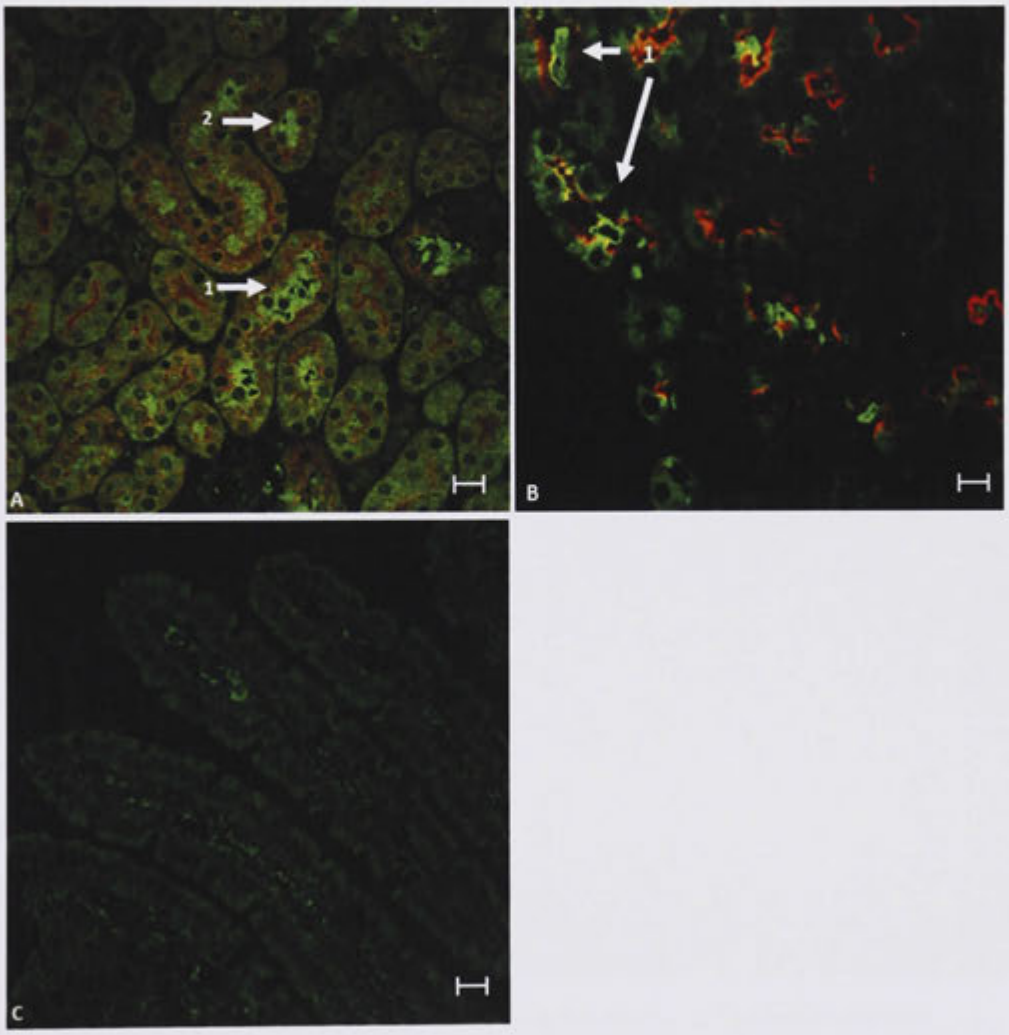

Figure 3.16: Localisation of B^0AT2 in C57Bl/6 mouse kidney and intestine.

B^0AT2 was detected using a rabbit primary antibody and a donkey anti-rabbit secondary antibody conjugated to AF 488 (green). Kidney proximal tubules were visualised with biotinylated LTL and SA-Texas Red (red) as marker. **A**: B^0AT2 was detected on the apical membrane of the later proximal tubulus segments S2, denoted with 1, and S3, denoted as 2 **B**: B^0AT2 was detected in a more distinct manner on the apical membrane of the renal S2 segment, denoted with 1. **C**: B^0AT2 staining was not detected in the intestine. Original magnification, x40. Bars represent 10 µm.

3.2.5.3 ASCT2 localisation in human kidney and intestine

The ASCT2 staining was undertaken by our collaborator Jessica Vanslambrouck in Sydney with human specimens. Kidney and intestine specimens were pre-fixed with 10 % NBF, followed by paraffin embedding and sectioning. Using the procedure explained above, the kidney sections were stained with peanut agglutinin (PNA), a distal tubule marker conjugated to AF 568 (red) and an anti-human ASCT2 antibody. The ASCT2-specific antibodies were detected by goat anti-rabbit secondary antibody conjugated to AF 488. ASCT2-like immunoreactivity was detected on the apical membrane of the proximal tubulus and also on the basolateral membrane of the distal tubulus. In these experiments of B^0AT1, and ASCT2 in the proximal tubulus revealed co-localisation of B^0AT1 and ASCT2-like immunoreactivity in the S2 segment, while only ASCT2-like immunoreactivity was expressed in the S3 segments (proximal straight tubules, data not shown). For this co-staining B^0AT1 was identified using a chicken primary anti-B^0AT1 antibody detected by goat anti-chicken secondary antibody conjugated to AF 594. ASCT2 was identified using a rabbit anti-ASCT2 primary antibody detected by goat anti-rabbit secondary antibody conjugated to AF 488 (Figure 3.17).

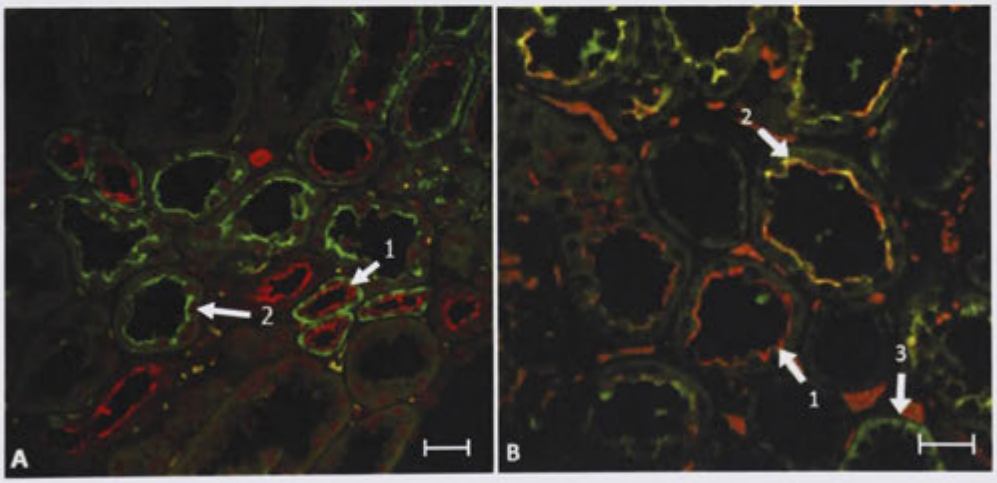

Figure 3.17: Localisation of ASCT2-like immunoreactivity in human kidney.

A: ASCT2-like immunoreactivity was identified using a rabbit primary antibody stained by a goat anti-rabbit secondary antibody conjugated to AF 488 (green). Kidney distal tubules were co-stained with PNA conjugated to AF 568 (red) as marker. ASCT2-like immunoreactivity was detected on the basolateral membrane of the distal tubules (1), but also on apical membrane of some proximal tubules (2). **B:** Co-staining with B^0AT1 stained with chicken primary antibody detected by AF 594 (red) (1), revealed co-localisation of both transporters on a proportion of the proximal tubule (S2-segment)(2) but also in the basolateral membrane of tubules were B^0AT1 was absent (3). Original magnification, x40. Bars represent 30 µm. Figure kindly provided by J. Vanslambrouck, Sydney University.

To investigate ASCT2 localisation in the intestine, ASCT2 was identified using a rabbit primary antibody detected by goat anti-rabbit secondary antibody conjugated to AF 488. ASCT2-like expression was limited to the basolateral membrane of the base of the crypt cells. These cells mainly consist of Paneth cells (Figure 3.18). However, a positive staining was also obtained in goblet cells further up the villi. This staining of mucin within the goblet cells is most likely a result of non-specific binding by the rabbit anti-ASCT2 antibody. Antibodies raised in rabbits possess a well recognised attribute to generate high levels of non-specific binding to mucin in goblet cells (Rogers *et al.*, 2006).

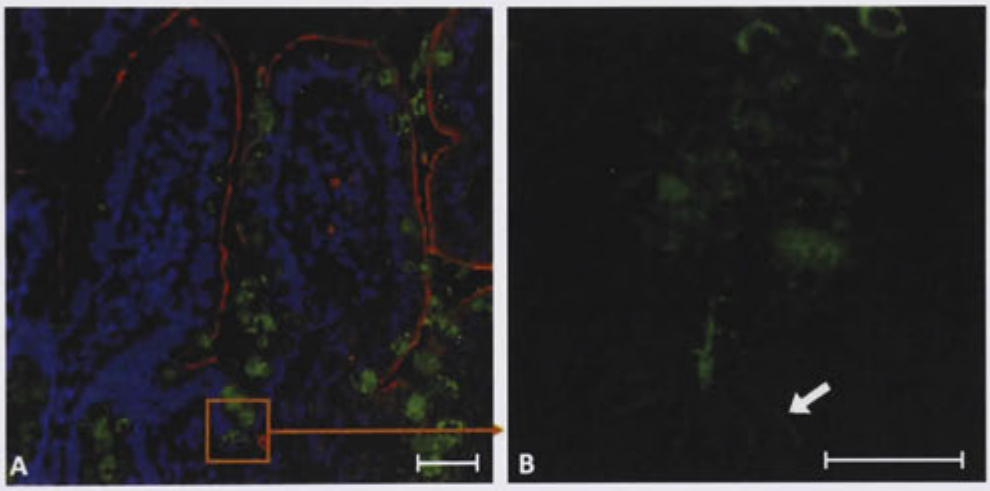

Figure 3.18: Localisation of ASCT2-like immunoreactivity in human intestine.

ASCT2-like immunoreactivity was localised using a rabbit primary antibody and detected by a goat anti rabbit secondary antibody conjugated to AF 488 (green). B^0AT1 was localised with chicken primary antibody and detected by a goat anti chicken antibody conjugated to AF 594 (red). **A-B:** B^0AT1 staining was detected in the apical membrane of enterocytes of the intestinal villi. However, ASCT2-like staining was restricted to the basolateral membrane of the crypt cells (arrow). Staining of mucin within the goblet cells by rabbit anti-ASCT2 antibody is most likely an artefact. Original magnification, x40 (A) and x100 (B). Bars represent 30 µm. Figure kindly provided by J. Vanslambrouck, Sydney University.

3.3 Discussion and future directions

3.3.1 Characterisation of the B^0AT1 antibody

The characterisation of the antibody against B^0AT1 demonstrated the suitability of the antibody for immunofluorescence studies. Western Blot analysis detected a clear signal for a protein of the size reported for B^0AT1. Staining of B^0AT1-injected oocytes revealed clear fluorescence signals confirming the suitability of the antibody for immunofluorescence.

3.3.2 Characterisation of the B^0AT2 antibody

The characterisation of the antibody against B^0AT2 confirmed the suitability of the antibody for immunofluorescence studies. Comparable to the B^0AT1 results, Western Blot analysis detected a clear signal for a protein of a size consistent with B^0AT2, alongside a weaker non-specific protein in oocytes. This protein proved to be part of the pre-immune response of the rabbit in which the antibody was raised. Other smaller proteins were also detected, which could be either detection of B^0AT2 splice variants reported previously (Sakata *et al.*, 1999) or unspecific labelling. The oocyte expression studies suggested however, that the antibody might not be as useful for immunofluorescence studies.

Due to the weak immunofluorescence observed in B^0AT2 cRNA injected oocytes, cell lines were used to express the transporter. Firstly, HEK cells were chosen as they have been shown to be easily transfected. Both Western Blot analysis and immunofluorescence studies suggested that HEK cells express B^0AT2 endogenously, which was confirmed by RT-PCR. It is well known that reverse-transcription may terminate prematurely (Kotewicz *et al.*, 1988; Lodish, 2000) and the whole cDNA might not be generated. For this reason, detection of the B^0AT2 N-terminus via RT-PCR may not have been successful.

As an alternative, CHO cells were chosen to test the antibody because B^0AT2 has not been reported to be expressed in ovaries. Immunofluorescence studies of this cell line proved the suitability of the antibody for immunofluorescence studies using mouse tissue with staining observed in the cytosol of the cells, but not on the cell surface.

It has been reported that B^0AT1 needs to form a heterodimer with collectrin in kidney or ACE2 in intestine to be trafficked into the cell membrane (Danilczyk and Penninger, 2006; Malakauskas *et al.*, 2007; Kowalczuk *et al.*, 2008). Due to the similarity of B^0AT1 and B^0AT2, co-expression of one of these auxiliary proteins might be required for surface expression in a transfection system. Thus, a further step in this investigation would be to co-transfect CHO cells with B^0AT2 and either collectrin or ACE2. This experiment could establish if B^0AT2 needs to form a heterodimer with one of the protein homologues to be trafficked into the cell membrane, although this was not observed to be a requirement in the oocyte expression system (Kowalczuk *et al.*, 2008).

3.3.3 Characterisation of the ASCT2 antibody

Two different ASCT2 antibody properties were tested in this thesis. Although the antibody received from the Avissar laboratory has been characterised recently (Avissar *et al.*, 2001), this study indicated a different result.

The molecular weight of ASCT2 has been analysed in various studies (Avissar *et al.*, 2001; Bungard and McGivan, 2004; Choudry *et al.*, 2006; Lim *et al.*, 2006; Avissar *et al.*, 2008). However, these studies have reported different molecular weights for ASCT2. (Avissar *et al.*, 2001; Bungard and McGivan, 2004; Lim *et al.*, 2006).

Avissar *et al.* characterised two custom-made polyclonal antibodies raised against either rabbit ASCT2 or human ASCT2 peptide. The antibody against rabbit-ASCT2 detected one band between 57 and 65 kDa in ASCT2 cDNA transfected cervical cancer cells retrieved from Henrietta Lacks (HeLa) cells, but several bands of 78, 88 and 94 kDa in rabbit renal tissue as well as a band between 80 and 90 kDa in different parts of the gastrointestinal tract of rabbits.

The antibody against human ASCT2 detected a 57 to 63 kDa protein in transfected HeLa cells and two proteins at 57 and 94 kDa in human C2BBe1 cells, but also additional proteins at 88 and 130 kDa. The 57 and 94 kDa proteins were demonstrated to be the ASCT2 specific proteins. Different protein glycosylation states were assumed to be the reason for some of the variations. Alternatively, different splice variants were hypothesised as a possible explanation (Avissar *et al.*, 2001).

Bundard and McGivan characterised an ASCT2 antibody raised against an ASCT2 peptide. A band of 58-60 kDa was detected in non-transfected COS cells, which increased with transfection (Bungard and McGivan, 2004). In 2006, Lim *et al.* used an amino terminal tail isoform-specific ASCT2 antibody to detect the protein. Multiple bands at 70, 85 and 120 kDa were detected in membranes prepared from rat brain, which the study explained as due to different glycosylation (Lim *et al.*, 2006). In the same year, ASCT2 was detected as a 54 kDa band in BBMV derived from rat jejunum (Choudry *et al.*, 2006). Recently, ASCT2 was detected with a molecular weight of 81 kDa in CaCo and C2 cells (Avissar *et al.*, 2008).

In Western Blot analysis, the Avissar antibody detected mostly a protein of lower molecular weight as reported previously for ASCT2, while our antibody detected either a molecular weight that corresponds to the predicted ASCT2 molecular weight or sizes that are consistent with a dimer or trimer of ASCT2. In 2001, Tailor *et al.* reported truncated forms of ASCT2. They are thought to result from imprecise recognition of the first start codon. Therefore, the smaller protein could have been the result of translation initiation at a later methionine codon (Tailor *et al.*, 2001).

The most likely explanation for the different size detected by the Avissar antibody could be the specific detection of one of those truncated ASCT2 proteins. It is also generally known, that the detection quality of antibodies declines with repeated freeze and thaw cycles, which could indicate another possibility for the different size detection. Furthermore, the differences in fluorescence intensity in with transfected cells indicated a higher quality of ASCT2 antibody designed in the Broer laboratory.

Interestingly, with different fixation methods for transfected CHO cells, different results were generated. Paraformaldehyde is a cross-linking reagent, which forms intermolecular bridges normally through the free amino groups and therefore creates a system of linked antigens. Acetone on the other hand removes lipids and dehydrates the cell, thus it precipitates the proteins at the cellular level. Cross-linking reagents preserve the structure of the cells better than organic solvents, but also may reduce the antigenicity of some cell components since cell membrane membranes are still intact and therefore requires the addition of a permeabilisation step, which allows the antibody access to the target (Oliver, 2010).

It appears likely that the same restriction of the fixative applies to tissue samples in the same way as to transfected cells. ASCT2 was found mainly within the cytosol in transfected cells and not in the plasma membrane similar to a previous study (Gegelashvili *et al.*, 2006). In 2006, Gegelashvili *et al.* observed that ASCT2 trafficking is dependent on the pH value of the surrounding media.

In 2005, Holmseth *et al.* investigated systematically the quality of antibodies generated against a peptide along the primary sequence of the membrane protein. In this report antibodies raised to synthetic peptides did not always recognise the native protein (Holmseth *et al.*, 2005), hence detection with these antibodies might not be accurate. Furthermore, it seemed the ability of a peptide antibody to recognise the parent protein is a property of the peptides and not of the immunisation protocol used. Additionally, the specificity of such an antibody is hard to predict because cross-reactivity to unrelated proteins is frequently observed.

All these results will be considered in the discussion of the localisation of the neutral amino acid transporters in Chapter 6. The ASCT2 antibody used in this chapter was raised against a synthetic peptide. Hence the results should be observed with caution. For future experiments an ASCT2 antibody against a full length GST-fusion protein might be more suitable.

Chapter 4

Contribution to epithelial amino acid transport by the transporters B^0AT1, B^0AT2 and ASCT2

4.1 Introduction and aim of this study

The substrate specificity of the three neutral amino acid transporters B^0AT1, B^0AT2 and ASCT2 has been investigated intensely in previous studies. B^0AT1 was reported to transport all neutral amino acids with low affinity (Bohmer *et al.*, 2005; Camargo *et al.*, 2005), while B^0AT2 was characterised to transport neutral, branched chain amino acids and methionine with high affinity (Takanaga *et al.*, 2005; Broer *et al.*, 2006). Both transporters operate with a Na^+-dependent symporter mechanism. ASCT2, by contrast, is a Na^+-independent antiporter. It has been identified as a transporter accepting neutral amino acids with high affinity except aromatic amino acids (Kekuda *et al.*, 1996; Kekuda *et al.*, 1997; Avissar *et al.*, 2001). Despite the individual characterisations, little is known about the different contribution to neutral amino acid transport *in vivo*. Nevertheless, controversial speculations have been made about which of these transporters is the main contributor to the uptake of neutral amino acids in the intestine and in the kidney (Kekuda *et al.*, 1996; Avissar *et al.*, 2001). To clarify the contribution of each transporter, uptake was determined using mouse kidney brush border membrane vesicles after confirming the substrate specificity of each transporter.

4.2 Results

The preparation of and transport studies with brush border membrane vesicles (BBMV) in this chapter were optimised to generate reproducible results with the vesicles. The optimised protocol is shown in detail below:

4.2.1 Preparation of brush border membrane vesicle from mouse kidney:

- It is important for this procedure that every solution and material is pre-cooled on ice before use. Furthermore, it is essential to work quickly and consistently.
- After killing the animal, both kidneys were taken out and placed into a pre-cooled glass dish with ice-cold buffer A.
- The kidneys were cut into small pieces and added into a 2 mL Eppendorf test tube containing 0.8 mL of ice-cold buffer A.
- The kidney pieces were homogenated with a Polytron mixer at the highest setting for 1 min. During the homogenisation the Eppendorf test tube was cooled on ice.
- An aliquot (approximately 100 µL) was removed and kept on ice in an Eppendorf test tube for alkaline phosphatase and Bradford tests.
- 1.12 mL of ddH_2O was added to the lysate and mixed by inverting the Eppendorf test tube five times.
- 22 µL of a 1 M $MgCl_2$ stock solution was added to the mix for a final concentration of 1 mM. The Eppendorf test tube containing the mixture was inverted five times.
- The Eppendorf test tube was incubated on ice for 15 min with occasional mixing.
- The solution was centrifuged at 1,500g for 15 min at 4 °C in a table top centrifuge.
- Afterwards, the supernatant was decanted into a new pre-cooled tube and was centrifuged again in a Sorvall RC5C Plus centrifuge at 30,000 g for 30 min at 4 °C.
- The supernatant was discarded and the remaining pellet was resuspended in a small amount of (150 µL) buffer B using a 1 mL syringe with a 25 G needle.
- After resuspension, a further 4 mL of buffer B was added to the mixture.

- The resuspended pellet was then transferred into a tight-fitting glas potter (15 mL total volume) and homogenised with 10 strokes on ice. If the vesicles needed to be preloaded for ASCT2 analysis, ATP at a final concentration of 4 mM buffered with 4 mM $MgCl_2$ and unlabelled glutamine or leucine at a final concentration of 10 mM was added before the homogenisation.
- Subsequently, the resuspended pellet was transferred into a SS-34 centrifuge tube and 50 µL of a 1M $MgCl_2$ stock solution (for a final concentration of 12 mM) was added to the homogenised solution into the potter.
- The homogenate was incubated for 15 min on ice followed by centrifugation at 1,500 g for 15 min at 4 °C in a Sorvall RC5C Plus centrifuge.
- The supernatant was decanted into a new cooled tube and centrifuged at 30.000 g for 30 min at 4 °C.
- The resulting supernatant was discarded and the pellet was resuspended in 150 µL buffer C using a 1 mL syringe with a 25 G needle.
- The suspension was filled into a chilled glass potter, which already contained 4 mL of buffer C and the whole mixture was homogenised with 10 strokes. If the vesicles needed to be preloaded for ASCT2 analysis, ATP up to a final concentration of 4 mM buffered with 4 mM $MgCl_2$ and unlabelled glutamine or leucine at a final concentration of 10 mM was added to the buffer before the homogenisation. For preloding with valinomycin K_2SO_4 buffer was used for dilution, containing valinomycin (0.1mg/ml).
- The homogenate was transferred into a new cold centrifuge tube and the vesicles were collected by centrifugation at 48,000 g for 30 min at 4 °C in a SS-34 rotor.
- The supernatant was discarded and the resulting pellet was resuspended in the desired volume of buffer C (for two kidneys the end volume was no greater than 120 µL) using a 1 mL syringe with a 25 G needle.
- The vesicles were kept on ice for immediate use.

Buffer A:	300 mM	D-Mannitol	
	5 mM	EGTA	
	12 mM	Tris- HCl	titrated with HCl to pH 7.1
Buffer B:	150 mM	D-Mannitol	
	2.5 mM	EGTA	
	6 mM	Tris- HCl	titrated with HCl to pH 7.1

Buffer C:	280 mM	D-Mannitol	
	10 mM	HEPES	
	10 mM	Tris- HCl	titrated with HCl to pH 7.3

4.2.2 Substrate specificity measured with the usage of *Xenopus leavis* expression

4.2.2.1 Substrate specificity of B^0AT1

The B^0AT1 substrate specificity has been extensively analysed in our laboratory in previous studies. Broer *et al.* used flux measurements to determine the substrate specificity of B^0AT1 (Broer *et al.*, 2004). The data from this study are reproduced here for confirmation (Figure 4.1). Additionally, Bohmer *et al.* used two electrode voltage-clamp techniques in the *Xenopus laevis* oocyte expression system to measure the leucine induced current (Bohmer *et al.*, 2005).

Uptake of [^{14}C]leucine was inhibited by all neutral amino acids. B^0AT1 was strongly inhibited (>80 %) by cysteine, methionine, alanine, isoleucine, valine, leucine, asparagine, serine, glutamine, phenylalanine and alanine. Medium inhibition (50 to 80 %) was observed with threonine, glycine, proline, histidine, tyrosine, tryptophan and the amino acid analogue 2-Aminobicyclo[2,2,1]heptane-2-carbocylic-acid (BCH). No significant inhibition was observed with addition of arginine, lysine, aspartate, glutamate and N-Methyl-α-aminoisobutyric acid (MeAiB) (Figure 4.1).

Confirmation of B^0AT1 substrate specificity was obtained by flux measurements. All neutral amino acids produce an inward current (Bohmer *et al.*, 2005).

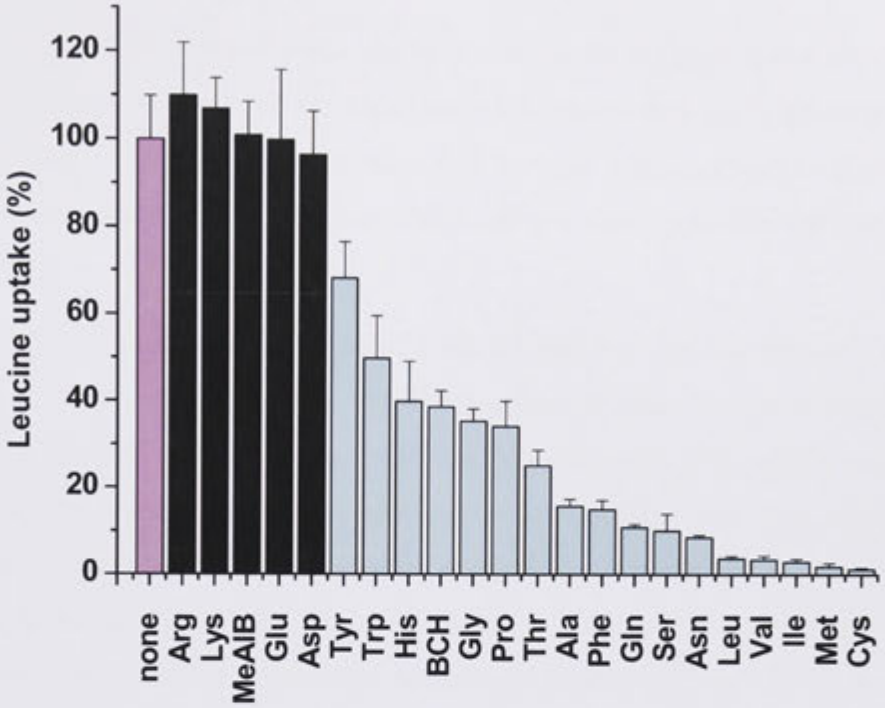

Figure 4.1: Substrate specificity of mouse B^0AT1.

Oocytes expressing mB^0AT1 cRNA were incubated for 4 days. [^{14}C]leucine uptake (100 µM) was determined in the presence or absence of 20 mM unlabelled amino acids or their analogues. Each bar represents the mean ± standard deviation of 10 oocytes. Data are compiled from three different experiments. The transport activity of non-injected oocytes was subtracted in each case as a control. The three-letter code is used for amino acids: MeAiB, N-Methyl-α-aminoisobutyric acid; BCH, 2-Aminobicyclo[2,2,1]heptane-2-carbocylic-acid. The B^0AT1 substrates have been highlighted in light blue, the uninhibited control is shown in magenta.

(Figure adapted from (Broer *et al.*, 2004).

4.2.2.2 Substrate specificity of B^0AT2

The B^0AT2 substrate specificity has also been extensively analysed in our laboratory in a previous study. Broer A. *et al.* (2006) used flux measurements and two electrode voltage-clamp recordings in B^0AT2-expressing *Xenopus laevis* oocytes to characterise the substrate specificity. The data from this study are reproduced here for comparison (Figure 4.2).

Uptake of [^{14}C]proline was strongly (>90 %) inhibited by methionine, leucine, isoleucine, valine, proline and the amino acid analogue aminoisobutyric acid (Aib). A partial (40 to 90 %) inhibition was observed with phenylalanine, serine, threonine, glutamine, asparagine, histidine, hydroxyproline (HO-Pro) and the amino acid analogues BCH and nipicotic acid (Nip). No significant inhibition was determined with glycine, tyrosine, tryptophan, cysteine, arginine, lysine, aspartate or glutamate. Additionally, a number of amino acid related compounds such as MeAib, β-alanine, GABA and betaine (Bet) also did not inhibit the uptake of [^{14}C]proline (Figure 4.2). Confirmation of B^0AT2 substrate specificity was obtained by flux measurements. The amino acids proline, leucine, methionine and alanine produced an inward current as well as the amino acid analogue Aib.

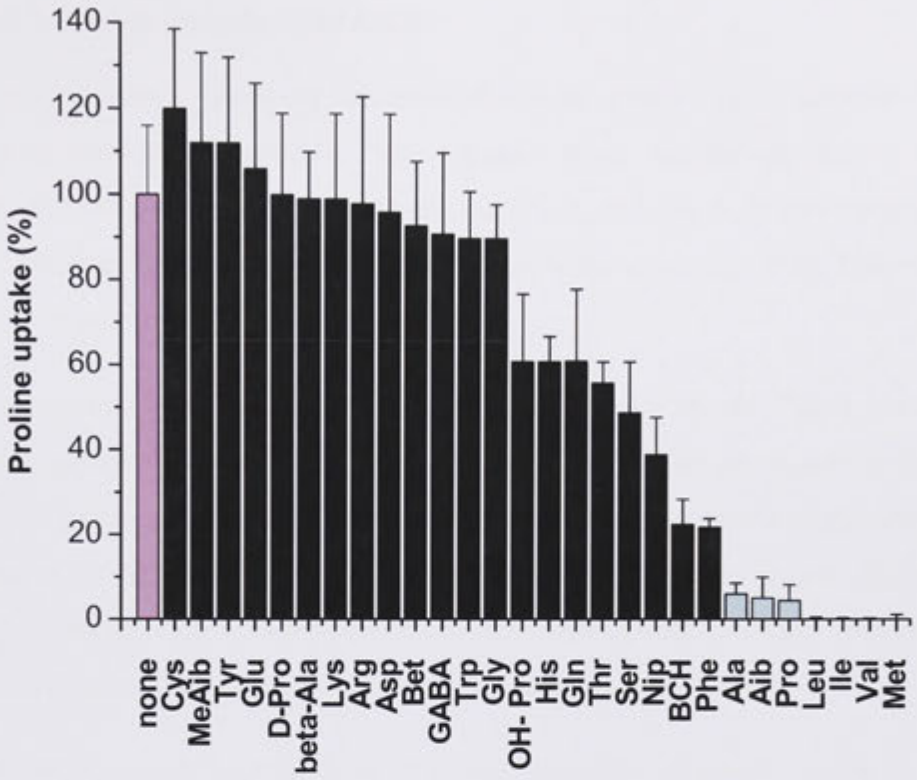

Figure 4.2: Substrate specificity of mouse B^0AT2.

Oocytes expressing mB^0AT2 cRNA were incubated for 4 to 6 days. [^{14}C]proline uptake (50 µM) was determined in the presence or absence of 5 mM unlabelled amino acids or their analogues. Each bar represents the mean ± standard deviation of 10 oocytes. Data are compiled from three different experiments. The transport activity of non-injected oocytes was subtracted in each case as a control. The B^0AT2 substrates have been highlighted in light blue, the uninhibited control is shown in magenta.

(Figure adapted from Boer A. *et al.*, 2006)

4.2.2.3 Substrate specificity of ASCT2

The ASCT2 substrate specificity has previously been analysed by Utsunomiya-Tate *et al.*, using transport studies in the *Xenopus laevis* oocyte expression system (competition and exchange experiments), but also by Kekuda *et al.* and Pollard *et al.*, using competition experiments on transfected cells (Kekuda *et al.*, 1996; Pollard *et al.*, 2002), obtaining different results.

Utsunomiya-Tate *et al.* measured in inhibition experiments 10 µM [^{14}C]alanine uptake was measured in the presence of 1 mM unlabelled amino acids or related compounds. Strong inhibition was observed for alanine, serine, threonine, cysteine, glutamine and asparagine, while weaker inhibition was detected for methionine, leucine, glycine and valine. All amino acids were transported in an L-stereospecific manner. The additional uptake experiment was consistent with the competition experiment.

In contrast, the study by Kekuda *et al.* showed inhibition of alanine uptake with the amino acids alanine, serine, cysteine, threonine, methionine, leucine, valine, tryptophan, glutamine and asparagine (Kekuda *et al.*, 1996). The study by Pollard showed inhibition of alanine uptake with the amino acids serine, glutamine and to a lesser extent leucine. Additionally, inhibition was observed with phenylalanine in neuroblastoma cells (NBL-1) cells but not in human cariocarcinoma (JAR) cells (Pollard *et al.*, 2002).

To validate these observed variations in ASCT2 transport for human ASCT2, human ASCT2 substrate specificity was analysed. Human ASCT2 was chosen since it was not been analysed previously, whereas the mouse ASCT2 is well characterised (Utsunomiya-Tate *et al.*, 1996). Oocytes were injected with human ASCT2 cRNA and non-injected oocytes were used as controls. Four to six days after injection, groups of seven to ten oocytes were used to determine the substrate specificity of human (h) ASCT2 by challenging the uptake of 50 µM [^{14}C]glutamine with a 100 fold excess of unlabelled L-amino acids as described in Chapter 2.

[^{14}C]glutamine uptake was strongly inhibited (≥90 %) by threonine, serine, glutamine, asparagine and valine. Weaker inhibition (70 to 85 %) was observed with leucine, methionine, cysteine and glycine. The inhibition by these amino acids was highly significant ($p<0.001$). All other amino acids tested showed inhibition of less than 40 % (Figure 4.3) ($p<0.01$ to not significant).

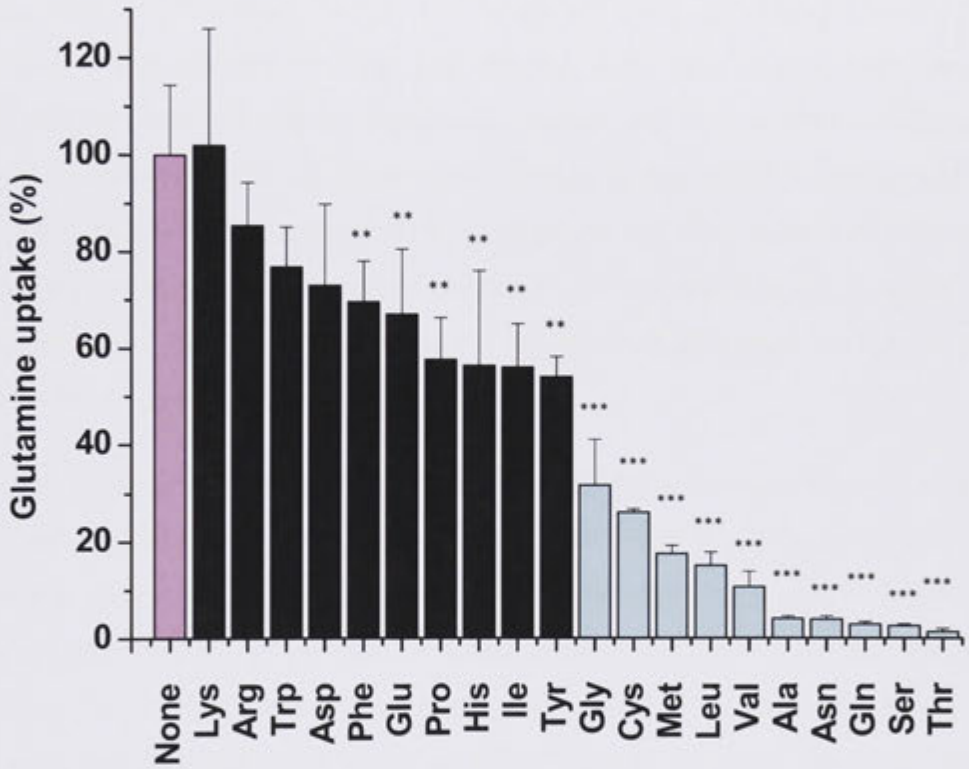

Figure 4.3: Substrate specificity of human ASCT2.

Oocytes expressing hASCT2 cRNA were incubated for 4 to 6 days. [^{14}C]glutamine uptake (50 µM) was determined in the presence or absence of 5 mM unlabelled amino acids. Each bar represents the mean ± standard deviation of seven to ten oocytes. * indicates the statistical significance with *** ($p<0.001$) and ** ($p<0.01$). Data are compiled from three different experiments. The ASCT2 substrates have been highlighted in light blue, the control is shown in magenta.

Amino acids competing with the uptake of [^{14}C]glutamine, may or may not be substrates of the transporter as mentioned above. As a result exchange experiments were conducted with [^{14}C]glutamine preloaded oocytes to demonstrate translocation via ASCT2. Oocytes were injected with hASCT2 cRNA and incubated for four to five days.

Batches of seven to ten oocytes were washed twice with ND96 buffer and subsequently pre-incubated for 10 min in 90 µL ND96 containing 50 µM [^{14}C] glutamine. The preloading reaction was stopped with three washes with ice-cold ND96. After the washing step the buffer was removed and 1 mL of ND96 containing 1 mM unlabelled amino acid was added to the oocytes. 150 µL samples were taken from the supernatant at 5, 10, 20 and 30 min. After the last time point the efflux was stopped by washing the oocytes three times with ice-cold ND96 buffer. Oocytes that were pre- incubated with [^{14}C]glutamine and subsequently incubated in substrate-free ND96 buffer were used as a control.

High glutamine efflux (60 to 90 % of the preloaded [^{14}C]glutamine) was observed with nearly all neutral, non-aromatic amino acids, namely alanine, asparagine, cysteine, glutamine, glycine, leucine, methionine, serine, threonine and valine. The efflux of these was highly significant ($p<0.001$) in comparison to the control. The only exception was isoleucine ($p>0.05$). Only very weak efflux (0 to 15 % of the preloaded radioactive glutamine) was detected with all other tested amino acids, including the ND96 control (Figure 4.4). No significance could be shown ($p>0.05$).

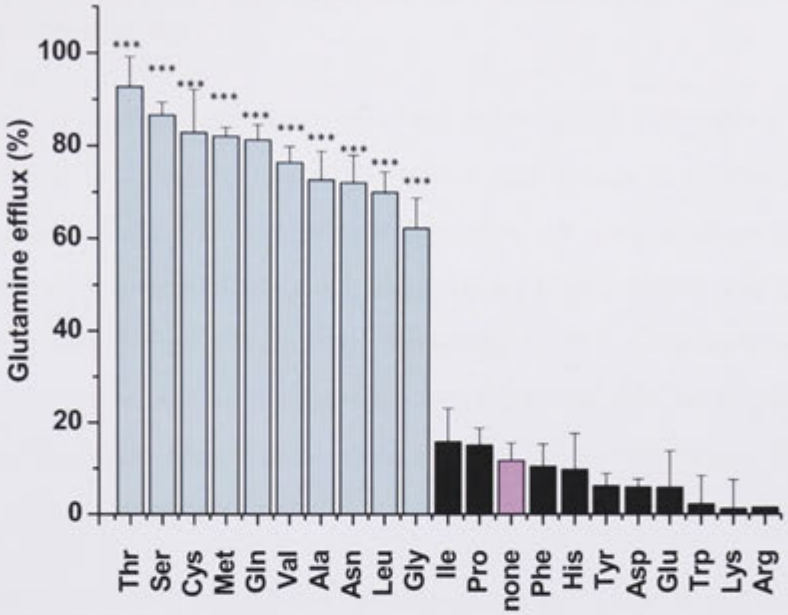

Figure 4.4: Substrate specificity of human ASCT2 determined by exchange activity.

Oocytes expressing hASCT2 cRNA were incubated for four to five days. The oocytes were preloaded for 10 min with [^{14}C]glutamine (50 µM) and subsequently efflux of the radioactively labelled glutamine was determined in the presence or absence of 1 mM unlabelled amino acids over 30 min. Each bar represents the mean transport activity of seven to ten oocytes. *** indicates the statistical significance at $p<0.001$. The experiment represents one of four repeated experiment with different batches of oocytes. The ASCT2 substrates have been highlighted in light blue. The control efflux in ND96 buffer is depicted in magenta.

4.2.3 Analysis of the amino acid transport contribution in brush border membrane vesicles

After determining the substrate specificity of the amino acid transporters B^0AT1, B^0AT2 and ASCT2, their contribution to neutral amino acid transport in the kidney was determined using BBMV. The vesicles were first analysed using Western Blot analysis for enrichment of the three amino acid transporters B^0AT1, B^0AT2 and ASCT2 from homogenate to BBMV. The vesicles were also tested for 4F2, a marker protein of the basolateral membrane. Kidney homogenate and BBMV samples were prepared and separated by SDS-PAGE. After transfer onto a nitrocellulose membrane, the proteins were observed by immunodetection.

The basolateral membrane protein 4F2 has been reported to have a molecular mass of 80 kDa (Nakamura *et al.*, 1999). Here, the 4F2 protein was detected as a 78 kDa band protein in kidney homogenate and in BBMV (Figure 4.5). Thus, the vesicles seem to have a significant basolateral membrane contamination. The protocol was later optimised and the amount of basolateral contamination was still present but varied (data not shown).

B^0AT1 was observed as a 63 kDa protein in the homogenate and was also enriched in the BBMV. B^0AT2 was detected as an 82 kDa protein in both the homogenate and the BBMV. However, no enrichment was discovered from homogenate to vesicle. The ASCT2 antisera detected a protein band at 47 kDa in homogenate and a 53 kDa protein in BBMV. Longer exposure time revealed a faint detection of the 53 kDa band in the homogenate as well (data not shown). The 53 kDa protein was enriched in BBMV in comparison to the homogenate.

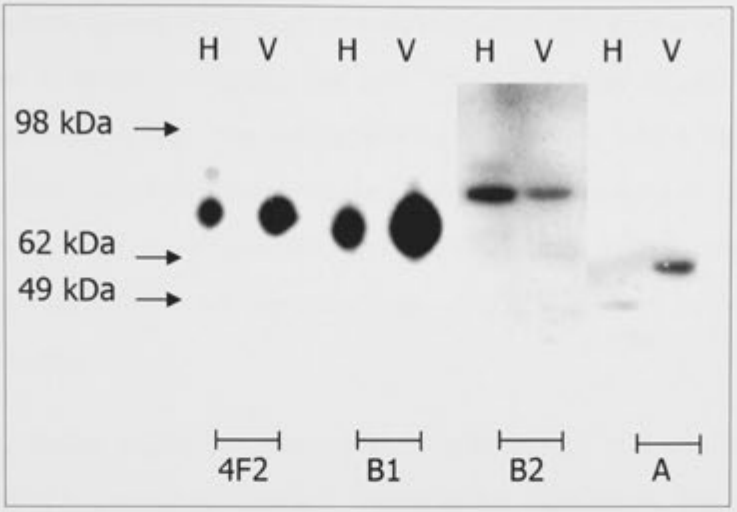

Figure 4.5 Detection of 4F2, B^0AT1, B^0AT2 and ASCT2 in kidney homogenate and brush border membrane vesicles.

Kidney homogenate, denoted as H and BBMV samples, denoted as V, were separated by SDS-PAGE and transferred onto a nitrocellulose membrane. The membrane was either incubated with rabbit-anti B^0AT1 (B1), rabbit-anti B^0AT2 (B2), rabbit-anti ASCT2 (A) or 4F2 antibody. The characterisation of the antibodies is described in Chapter 3. The BBMV preparation had a 10-fold AP enrichment. The bands were visualised using a chemiluminescent western detection kit.

4.3 Uptake experiments with brush border membrane vesicles

The Western Blot analysis showed that all three proteins are expressed in kidney. To investigate whether the proteins are functionally active, uptake of [^{3}H]labelled amino acid substrates was determined in the absence or presence of unlabelled amino acids.

For these experiments only BBMV that showed more than a twelve fold enrichment of the brush border membrane marker enzyme alkaline phosphatase were used. Since all three transporters are Na^+-dependent, the experiments were conducted in Na^+-based buffer, while K^+-based buffer was used as control and reference.

As shown above, leucine is a major substrate for the transporters B^0AT1 and B^0AT2 and was therefore chosen for BBMV uptake. The time point for amino acid transport (15 sec) was chosen after evaluation of a preliminary time course (data not shown) and is similar to time points chosen in previous studies (Ganapathy and Leibach, 1982; Chesney *et al.*, 1986). An equilibrium time point was taken after 4 to 10 min.

To start the uptake experiment, 20 µL of vesicle solution was added into 80 µL uptake buffer (Na^+- or K^+-based) containing 100 µM [^{3}H]leucine. After 15 sec, a sample was taken and the reaction was stopped by diluting the sample into 4 mL ice-cold stop buffer. The solution was immediately filtered through a pre-wetted nitrocellulose filter and washed with additional stop buffer. An equilibrium time point was taken after 4 to 10 min. The radioactivity on the filter was counted using a Beckman LS 6500 scintillation counter.

Uptake in Na^+-based buffer showed a higly significant 6.5 fold increase of leucine uptake ($p<0.001$) in comparison to the K^+-based buffer (Figure 4.6). The transport at 15 sec was 0.65 ± 0.1pmol/mg protein in Na^+-based buffer in contrast to 0.09 ± 0.001 pmol/mg protein in the absence of Na^+. After 10 min, a transport activity of 0.21 ± 0.01 pmol/mg protein was observed in Na^+-based buffer and of 0.33 ± 0.02 pmol/mg protein in K^+-based buffer.

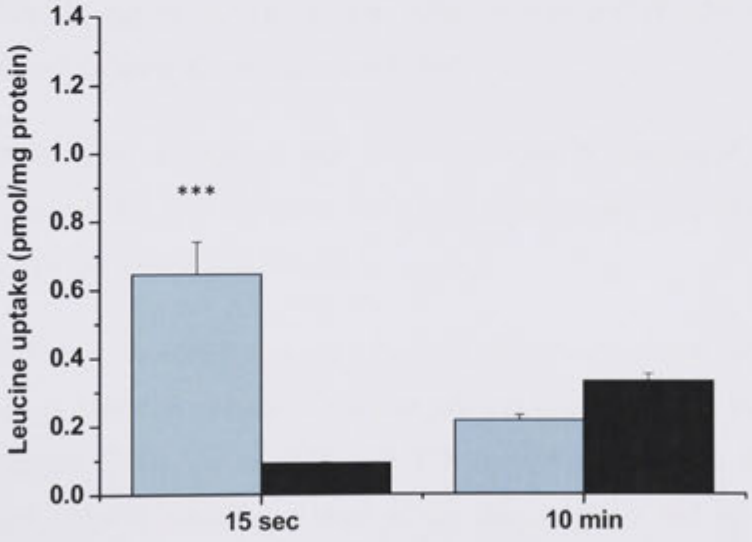

Figure 4.6: [^{3}H]leucine transport into mouse renal brush border membrane vesicles in Na^+-based and K^+-based buffer.

Renal BBMV were incubated with [^{3}H]leucine (10 µM) over a period of 10 min in Na^+-based buffer (blue bars) and K^+-based media (black bars). Each bar represents the average of duplicate measurements ± standard deviation, *** indicates statistical significance at $p<0.001$. Similar results were obtained in six different experiments. A 6.5 fold increase of [^{3}H]leucine uptake was observed with Na^+-based buffer in comparison to K^+-based buffer.

This transport is most likely to be facilitated only by the B^0AT1 or B^0AT2 transporters, because ASCT2 would require substrate inside the vesicles for its antiport mechanism. To detect ASCT2 activity, it was essential to preload the BBMV with an amino acid substrate. Furthermore, Oppedisano *et al.* reported an increase of the V_{max} of the transporter, decreasing the K_m of the transporter for external Na^+, in the presence of intra-vesicular ATP. For this reason, the BBMV were preloaded with ATP (4 mM) as well, which was complexed with $MgCl_2$ (4 mM).

First, the preloading process had to be validated. To this end the vesicles were preloaded with KCl. Preloading with K^+ can be verified by using the K^+-ionophore valinomycin. When vesicles are preloaded with K^+, the addition of valinomycin will render the membrane selectively permeable to K^+. Dilution of the vesicles into K^+-free buffer will generate a K^+-gradient, which in turn will generate a potassium diffusion potential. This method has frequently been used to identify rheogenic transport processes (Ganapathy and Leibach, 1982). Since the BBMV contain rheogenic Na^+-dependent B^0AT1 transporters, a potassium diffusion potential (inside negative) will enhance uptake of amino acids via this transporter.

Therefore, BBMV were preloaded with buffer containing potassium (K_2SO_4) and valinomycin (0.1 mg/ml) and subsequently [^{3}H]leucine uptake was analysed. Non-preloaded vesicles were used as a control.

The non-preloaded, renal BBMV showed a higly significant, close to 4 fold increase of leucine uptake ($p<0.001$) in comparison to the control in the absence of Na^+ (Figure 4.7). The transport at 15 sec was0.95 ± 0.003 pmol/mg protein in Na^+-buffer in contrast to 0.25 ± 0.002 pmol/mg protein in the absence from Na^+ (K^+-buffer). The valinomycin preloaded vesicle showed a higly significant 12 fold increase of leucine uptake ($p<0.001$) with a transport of 2.31 ± 0.1 pmol/mg protein in Na^+-based buffer in contrast to 0.19 ± 0.01 pmol/mg protein in K^+-based buffer.

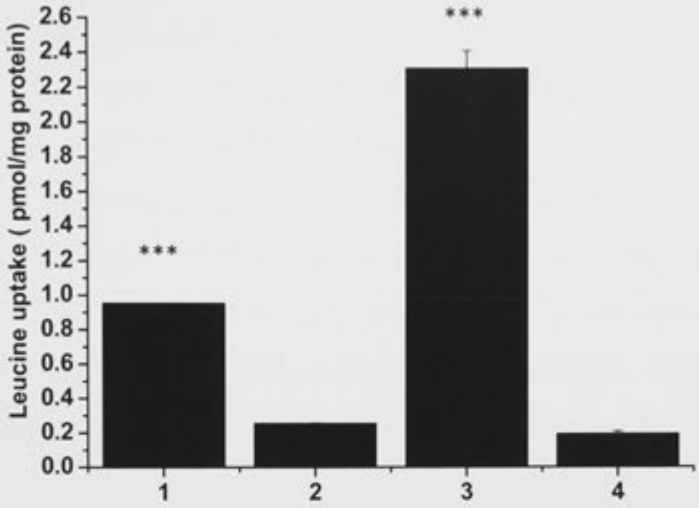

Figure 4.7: Effect on [^{3}H]leucine transport in mouse renal brush border membrane vesicles preloaded or not preloaded with valinomycin in Na^+-based and K^+-based buffer.

Non-preloaded renal BBMV were diluted into Na^+-based buffer, denoted as 1, or K^+-based buffer, denoted as 2, and [^{3}H]leucine (100 µM) was measured over a period of 0.25 min. Similarly, renal BBMV preloaded with K_2SO_4 and treated with valinomycin (0.1 mg/ml) were diluted into Na^+-based buffer, denoted as 3, or K^+-based buffer, denoted as 4. Each bar represents the average of duplicates ± standard deviation; *** indicates statistical significance at $p<0.001$). A 3.8 fold increase of [^{3}H]leucine uptake was observed with Na^+ buffer in comparison to K^+-based buffer for non-preloaded vesicles and a 12 fold increase was observed for preloaded BBMV.

This result confirmed that the procedure was suitable for preloading of the vesicles. In addition, it should be noted that the vesicles contain B^0AT1 transporters, which allow preloading with neutral amino acids. Preloading of vesicles with a substrate of ASCT2 would then allow determination of whether an ASCT2-like antiport activity is present in renal BBMV. It was expected that uptake into preloaded BBMV would reveal an additional activity not observed in non-preloaded vesicles.

To test for ASCT2 activity, renal BBMV preloaded with glutamine (30 mM) and ATP (4 mM) were added to uptake buffer containing 100 µM [^{3}H]leucine. As described above, non-preloaded vesicles were used as controls. A sample was taken after 15 sec and processed as described previously. Likewise, an equilibrium time point sample (data not shown) was processed.

The renal BBMV showed a significant 2.2 fold increase of leucine uptake in Na^+-based buffer ($p<0.01$) in comparison to their counterparts in K^+-based buffer. The preloaded BBMV, if anything, showed a smaller (1.8 fold) stimulation of leucine uptake in comparison to preloaded BBMV in K^+-based buffer (Figure 4.8). The transport at 15 sec was 0.72 ± 0.05 pmol/mg protein in Na^+-based buffer in contrast to 0.32 ± 0.03 pmol/mg protein in the absence of Na^+ for non-preloaded BBMV. For preloaded BBMV, a leucine transport of 0.57 ± 0.001 pmol/mg protein in Na^+-based buffer in contrast to 0.31 ± 0.07 pmol/mg protein in K^+-based buffer was detected. Thus no additional transport activity was detected in vesicles preloaded with ATP and glutamine.

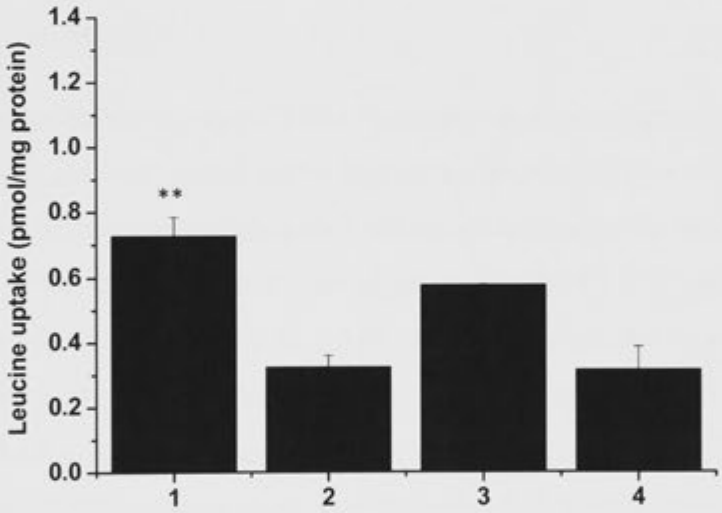

Figure 4.8: [^{3}H]leucine transport (15 sec time point) into mouse renal brush border membrane vesicles (preloaded with 30 mM glutamine and 4 mM ATP or non-preloaded) in Na^+-based and K^+-based buffer.

Non-preloaded renal BBMV were incubated with [^{3}H]leucine (100 µM) over a period of 15 sec in Na^+-based buffer), denoted as 1 or K^+-based buffer (2). Alternatively, renal BBMV were preloaded with 30 mM glutamine and [^{3}H]leucine uptake was determined in the same way in Na^+-based buffer(3), or K^+-based buffer(4). Each bar represents the average of duplicates ± standard deviation, ** indicates statistical significance at $p<0.01$. Similar results were obtained in five different experiments. A 2.2 fold increase of [^{3}H]leucine uptake was observed with Na^+-based buffer in comparison to K^+-based buffer in non-preloaded vesicles. In preloaded BBMV a 1.8 fold increase was observed for leucine uptake between the two buffers.

Since no additional leucine transport was observed in preloaded BBMV, it appears unlikely that ASCT2 contributes to leucine transport in mouse kidney. However as mentioned above, leucine is not a major substrate for ASCT2. Therefore the experiments were also conducted with glutamine, the major substrate of ASCT2, to fully confirm the lack of ASCT2 activity for neutral amino acid transport in mouse kidney.

Preloaded BBMV (glutamine (30 mM) and ATP (4 mM) complexed with 4 mM $MgCl_2$) were added to uptake buffer containing 100 µM [^{3}H]glutamine. As described above, non-preloaded vesicles were used as control. A sample was taken after 15 sec and processed as described previously. Likewise, an equilibrium time point sample (data not shown) was processed.

The non-preloaded BBMV showed a 3 fold increase of glutamine uptake in comparison to their counterparts in K^+-based buffer ($p<0.001$). In contrast the preloaded BBMV showed only a 2 fold increase of glutamine uptake in comparison to BBMV in K^+-based buffer (Figure 4.9) ($p<0.01$). The transport at 15 sec was 1.34 ± 0.07 pmol/mg protein in Na^+-based buffer in contrast to 0.41 ± 0.02 pmol/mg protein in K^+-based buffer. For preloaded BBMV a glutamine transport of 0.87 ± 0.02 pmol/mg protein was observed in Na^+-based buffer, in contrast to 0.38 ± 0.03 pmol/mg protein in K^+-based buffer. Thus, no additional glutamine transport was observed in glutamine-preloaded BBMV in comparison to non-preloaded vesicles.

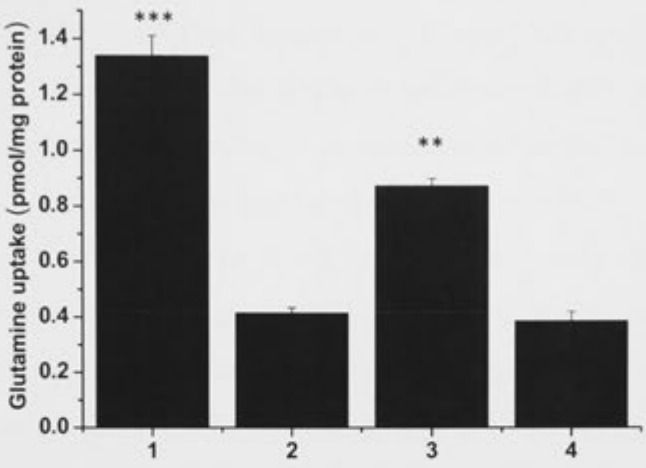

Figure 4.9: [^{3}H]glutamine transport (15 sec time point) into mouse renal brush border membrane vesicles (preloaded with 30 mM glutamine and 4 mM ATP or non-preloaded) in Na^+-based and K^+-based buffer.

Non-preloaded BBMV were incubated with [^{3}H]glutamine (100 µM) over a period of 15 sec in Na^+-based buffer (1) or K^+-based buffer (2). Glutamine uptake in BBMV preloaded with 30 mM glutamine was measured in the same way in Na^+-based buffer (3) or K^+-based buffer (4). Each bar represents the average of duplicates ± standard deviation. Statistical significance is indicated as *** ($p<0.001$) and ** ($p<0.01$). Similar results were obtained in five separate experiments. A 3 fold increase of [^{3}H]glutamine uptake was observed in Na^+-based buffer in comparison to K^+-based buffer for non-preloaded vesicles and a 2 fold increase was observed for preloaded BBMV.

The results of the previous experiments suggested that ASCT2 did not contribute to neutral amino acid transport in mouse kidney. In the following experiments, the relative contributions of B^0AT1 and B^0AT2 were investigated. In uptake experiments with [^{3}H]leucine, different non-labelled amino acid substrates were used to compete for leucine transport. Due to the overlapping substrate specificity of B^0AT1 and B^0AT2, substrates that discriminate between the two had to be chosen carefully. Leucine, glutamine and phenylalanine were chosen as substrates for both transporters. Glycine is only transported by B^0AT1, and not by B^0AT2 and hence was chosen as the substrate for B^0AT1 only, and proline is a better substrate for the B^0AT2 than for the B^0AT1 transporter as indicated in inhibition experiments (90% inhibition with B^0AT2, Figure 4.2 while B^0AT1 only showed 60% inhbition).

Renal BBMV (not preloaded) were used to examine the contribution of B^0AT1 and B^0AT2 transport by challenging the uptake of 100 µM [^{3}H]leucine with 30 mM of different unlabelled amino acids. The BBMV in Na^+-based buffer showed a 3.5 fold increase of leucine transport ($p<0.001$) in comparison to the potassium control. [^{3}H]leucine uptake was strongly inhibited (≥ 91 %) by leucine itself, phenylalanine and glycine ($p<0.001$). Weaker inhibition (79 %) was observed with glutamine ($p<0.01$). Proline inhibited 55 % of leucine uptake (Figure 4.10) ($p>0.5$). The strong inhibition of leucine transport by glycine, suggests that a B^0AT1-like transport activity is dominant in renal BBMV. Since proline inhibited leucine uptake is only partially, there could be another transporter involved in this uptake, for instance XT2.

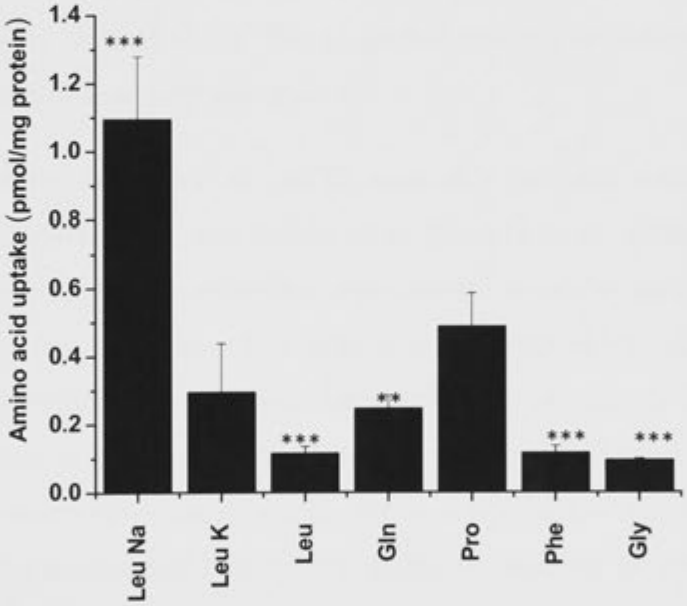

Figure 4.10: [^{3}H]leucine transport into mouse renal brush border membrane vesicles in the presence and absence of unlabelled amino acids in Na^+-based and K^+-based buffer.

BBMV were incubated with [^{3}H]leucine (100 µM) in the absence or presence of 30 mM unlabelled amino acids for 15 sec. [3H]leucine uptake in Na^+-based buffer, denoted as Leu Na and in K^+-based buffer, denoted as Leu K were used as a control. [3H]leucine uptake was then challenged by an excess of leucine (Leu), gutamine (Gln), proline (Pro), phenylalanine (Phe) and glycine (Gly) in Na^+-based buffer. Each bar represents the average of duplicates ± standard deviation. Statistical significance is indicated as *** ($p<0.001$) and ** ($p<0.01$). Similar results were obtained in five different experiments.

4.4 Discussion

4.4.1 Substrate specificity

As a first step, the substrate specificity of B^0AT1, B^0AT2 and ASCT2 was analysed to provide guidance for the selection of substrates used for competition experiments in BBMV. Since B^0AT1 and B^0AT2 have been characterised previously in our laboratory (Bohmer *et al.*, 2005; Broer *et al.*, 2006), these experiments were not repeated.

As mentioned above, ASCT2 substrate specificity was analysed by Utsunomiya-Tate *et al.* using competition and exchange experiments (Utsunomiya-Tate *et al.*, 1996). These results were confirmed, the results obtained in this thesis being consistent with Utsunomiya-Tate *et al.* cited above. This suggested that ASCT2 prefers neutral amino acids without bulky or branched side chains.

However, substrate specificity of ASCT2 was also analysed using competition experiments by Kekuda *et al.* and Pollard *et al.* (Kekuda *et al.*, 1996; Pollard *et al.*, 2002). The basic principle for competition experiments is to use an additional substrate to a normal labelled susbstrate. This additional substrate reacts as a competitive inhibitor since both substrates compete for binding and transport. In most cases the competing inhibitor is also a substrate of the transporter. However, it is know that in some cases the competitive inhibitor may not be a substrate of the transporter and hence may not be transported (Van Winkle, 1999). An example for this situation was observed by Thomas and Christensen where cationic amino acids are a competitive inhibitor of amino acid transport by system ASC but they are not transported by it (Thomas and Christensen, 1970). Another example was observe by van Winkle *et al.* where D-tryptophan competitively inhibits L-tryptophan transport by system T but D-tryptophan does not appear to be a susbtrate for system T (Van Winkle *et al.*, 1990). In the case of ASCT2 alanine transport was inhibited in the presence of phenylalanine in transfected HeLa cells (Kekuda *et al.*, 1996), indicating that phenylalanine is a preferred substrate of ASCT2. Pollard *et al.* showed that ASCT2 transport is inhibited

by phenylalanine transfected NBL-1 cells. In contrast, the inhibition of alanine transport with phenylalanine in JAR cells was not observed (Pollard *et al.*, 2002). As experienced here, inhibition and active uptake do not always correlate.

Therefore, to characterise a transporter both parts inhibition and active uptake should be measured in order to exclude discrepancies. In the case of ASCT2, the inhibition with phenylalanine obtained by Kekuda *et al.* caused the assumption that the transporter also transports aromatic amino acids and therefore could be the main B^0 activity in kidney and in the intestine (Avissar *et al.*, 2001; Sundaram *et al.*, 2007).

Almost all B^0AT2 substrates are also substrates of B^0AT1, and therefore it is difficult to find substrates for distinct competition experiments. To see the total activity of both transporters, leucine was chosen as a substrate which is accepted by both transporters. Phenylalanine and glutamine were chosen as competitors because they inhibit both transporters (Bohmer *et al.*, 2005; Broer *et al.*, 2006).

Glycine was chosen since it inhibits only B^0AT1, while proline is a better inhibitor for B^0AT2 than for B^0AT1 (Broer *et al.*, 2006). Therefore, the key substrate to distinguish between B^0AT1 and B^0AT2 transport activity is glycine. If glycine inhibits the amino acid uptake, B^0AT1 is the active transporter and if glycine does not inhibit the amino acid uptake, B^0AT2 is the active transporter.

Since glutamine seems to be the preferred ASCT2 substrate over leucine, it was chosen to analyse ASCT2 transport activity. Additionally, the antiport mechanism of ASCT2 has to be considered when undertaking uptake experiments, meaning that BBMV have to contain amino acids in order to show transport activity. To discriminate between B^0AT1, B^0AT2 and ASCT2, glutamine uptake with non-preloaded vesicles has to be conducted as reference. If additional glutamine transport occurs with amino acid preloaded vesicles, ASCT2 is responsible for this additional transport.

4.4.2 Western Blot analysis of brush border membrane vesicles

The Western Blot analysis showed that all three transporters were present in renal BBMV. Romeo *et al.* showed that B^0AT1, having a calculated relative molecular weight of 71 kDa, runs at about 60 kDa, probably due to the hydrophobic nature of transport proteins (Romeo et al., 2006). The B^0AT1-specific band detected in Figure 4.5 is thus consistent with the literature.

B^0AT2 has a calculated relative molecular weight of 82 kDa. Due to different glycosylation states it was observed to run between 85 to 96 kDa (Takanaga *et al.*, 2005). Thus, the protein detected as B^0AT2 in BBMV had the same weight as described in this previous study. Interestingly, B^0AT2 was not enriched in the BBMV suggesting that B^0AT2 is not located in the apical membrane. The lack of B^0AT2 enrichment in BBMV is at variance with the results obtained with immunofluorescence in Chapter 3, where B^0AT2 was detected in the apical membrane of the renal S2 and S3 segment. The principle of BBMV preparation is an enrichment of the apical membrane (Biber et al., 2007). Therefore, if the transporter is located in the apical membrane of the tubulus, it would be enriched in BBMV, even when it is not very abundant in the kidney, as observed with B^0AT2 in Chapter 3.

To further address this problem, *in situ* biotinylation could be used to biotinylate the extracellular surfaces of renal cells and examine apically targeted transporters after membrane solubilisation. To this end, kidneys are perfused in situ with biotinylation solution containing sulfosuccinimidobiotin (sulfo-NHS-biotin), a cell-impermeant biotin derivative that attaches covalently to free amino acid groups on lysines. After solubilisation and fractionation of the membranes, labelled proteins can be isolated using streptavidin beads and analysed using immunoblotting (Frindt *et al.*, 2008; Frindt and Palmer, 2009). This experimental method could help to determine if B^0AT2 is located in the apical membrane.

The different reported molecular weights of ASCT2 have been discussed before in Chapter 3. ASCT2 has a predicted theoretical relative molecular weight of 57 kDa. A band consistent with these findings was enriched in BBMV as depicted Figure 4.5 and therefore is likely to be ASCT2. Surprisingly, the 60 kDa band was not detected in kidney homogenate, where instead a 49 kDa protein was detected. This band has the same size as the protein detected with the antibody received from the Avissar laboratory. As discussed previously, truncated forms of ASCT2 have been reported (Tailor *et al.*, 2001), resulting from imprecise recognition of the first start codon. The lack of enrichment of this protein in BBMV suggests that it is not trafficked to the apical membrane. Another alternative would be that the homogenate was partially degraded and hence ASCT2 was detected at a different molecular weight. The first option appears more likely since the homogenate was used as a starting material to prepare the BBMV, which contained the higher molecular weight band.

The 4F2 heavy-chain of heterodimeric amino acid transporters forms a protein with a relative molecular weight of 80 kDa (Nakamura *et al.*, 1999). It is established a marker protein for the basolateral membrane. The presence of 4F2 in renal BBMV suggests a significant cross-contamination with basolateral membrane. This contamination has been reported before (Murer, 1984; Chung *et al.*, 1999; Lim *et al.*, 2005) and is difficult to avoid due to the procedure how BBMV are obtained. As mentioned above, the procedure makes use of the different composition of apical and basolateral membranes (Murer, 1984). The Mg^{2+}-precipitation plays an important role in the procedure.

The positive charge of the Mg^{2+} neutralises the negative charge of the membrane, allowing formation of cell membrane aggregates. However, the apical membrane is highly glycosylated (Lodish, 2000) and therefore would not form aggregations because the membranes cannot come into contact. Apical membranes can therefore be separated from basolateral and intra-cellular membranes and cell debris.

However, several components in the basolateral membrane also possess glycosylations, for instance 4F2 (Pineda *et al.*, 1999). Sometimes these glycosylations are sufficient enough to prevent aggregations with the rest of the basolateral membrane, resulting in the cross-contamination. Additionally, during the homogenisation process cells are disrupted at different parts of the membrane. Especially in the location around the tight junctions, which divides apical and basolateral compartments, contamination of the apical membrane by small pieces of basolateral membrane can occur.

4.4.3 Transport studies in BBMV

Under optimal conditions, [^{3}H]leucine uptake in BBMV showed a 6.5 fold higher uptake in Na^+-based buffer than in K^+-based buffer, indicating the presence of Na^+-dependent transport in those vesicles. It is not possible to determine just from this [^{3}H]leucine uptake experiment which of the two SLC6 family members is responsible for the transport since they display similar transport characteristics (Broer *et al.*, 2006).

[^{3}H]leucine uptake in valinomycin-treated vesicles showed that the Na^+-dependent transporter was also electrogenic. It further showed that the preloading procedure was useful for the analysis of ASCT2 activity. Valinomycin has been used extensively in previous studies to determine electrogenicity of transporters (Ghishan and Wilson, 1985; Sugawara *et al.*, 1992; Endo *et al.*, 1998). Since valinomycin is an ionophore selective to K^+ only, the vesicles could be successfully preloaded with K^+, resulting in an increase of [^{3}H]leucine uptake with K^+-preloaded vesicles.

Glutamine-preloaded vesicles were generated to examine ASCT2 contribution since the transporter requires amino acid on the inside of the vesicles for its obligatory antiport mechanism (Broer *et al.*, 2000). Since ASCT2 activity would be an additional transport activity on top of the symport activity of B^0AT1 and B^0AT2, an increase of leucine transport would be expected. However, [^{3}H]leucine transport in amino-acid free vesicles is higher (2.2 fold in comparison to uptake in K^+-based buffer) than in the preloaded vesicles (1.8 fold increase in comparison to uptake in K^+-based buffer).

The system L amino acid transporter LAT2/4F2 is located in the basolateral membrane and has an obligatory antiport mechanism as well. It transports a wide variety of neutral amino acids including leucine and glutamine in an ion-independent manner (Rossier *et al.*, 1999; Wagner *et al.*, 2000; Babu *et al.*, 2003; Bodoy *et al.*, 2005). If LAT2/4F2 had been present in the BBMV due to the cross-contaminations, leucine uptake would increase in glutamine-preloaded vesicles.

Glutamine is the preferred substrate for ASCT2. The [^{3}H]glutamine uptake was therefore analysed to further test for the presence of ASCT2. The same conditions were chosen as in [^{3}H]leucine uptake. [^{3}H]glutamine transport in amino acid-free vesicles was higher (3 fold in comparison to uptake in K^+-based buffer) than in the glutamine-preloaded vesicles (2 fold increase in comparison to uptake in K^+-based buffer), providing additional evidence for the lack of ASCT2 transport activity in kidney.

Similar to the experiments performed in the oocyte expression system, BBMV can be used to determine radioactive amino acid transport in the presence of unlabelled amino acids. The 3 fold increase of [^{3}H]leucine uptake under normal conditions showed that the vesicles were suitable for the experiment. The experiment showed that maximal inhibition of [^{3}H]leucine by unlabelled leucine amounted to 91 %, which is similar to previous studies of B^0AT1 and B^0AT2 transport activity in heterologous expression systems (Broer *et al.*, 2006).

Given that phenylalanine strongly inhibits both transporters, the 91 % inhibition by phenylalanine further validates the presence of B^0-like amino acid transporters. Glutamine, is a weak inhibitor of B^0AT2, but a good substrate of B^0AT1, and inhibited the transport less strongly than leucine and phenylalanine (79 % inhibition).

Proline is a substrate for both transporters but shows a preference for B^0AT2 (Broer *et al.*, 2006). The partial inhibition (55 %) therefore suggests that B^0AT1 prevails over B^0AT2 activity. Glycine is a substrate for B^0AT1 only. Thus, the inhibition of [^{3}H]leucine uptake by 91 % in the presence of glycine, provides strong evidence for leucine transport being predominantly mediated by B^0AT1. To fully confirm this analysis, the B^0AT1-deficient mouse was generated and its properties are analysed in Chapter 5.

Over the past decades, the mechanism of renal transport has been extensively studied by the use of BBMV (reviewed in (Murer and Gmaj, 1986). Those studies usually have been performed with membrane vesicles from whole cortex. However, some studies also have been performed with separated BBMV from the proximal convoluted part (pars convoluta) and the proximal straight part (pars recta) of proximal tubule (Kragh-Hansen *et al.*, 1984; Jorgensen *et al.*, 1990; Jessen and Sheikh, 1992).

For those studies, renal tissue has been examined using microscopes and the two parts of the tubule were separated by their anatomical localisation. Subsequently, tissue sections of the two parts of the proximal tubule were obtained and further processed to BBMV (Kragh-Hansen *et al.*, 1984). Transport studies with these BBMV showed the presence of different amino acid transport systems in the different part of the proximal tubulus consistent with the reported axial distribution of different amino acid transporters in the kidney (Scriver and Tenenhouse, 1985).

The BBMV studies in this thesis were conducted with vesicle of whole kidney cortex and therefore are a mixture of BBMV obtained from pars convoluta and pars recta. It would be interesting to investigate whether all neutral amino acid transport takes place via B^0AT1 in the early segments of the proximal tubule (as suggested in this chapter) or if some other activity is still observed in the S3 segment, where B^0AT1 is not located.

Chapter 5

Characterisation of the B^0AT1-deficient Mouse

5.1 Introduction and aim of the study

To investigate the contribution to neutral amino acid of the amino acid transporters B^0AT1, B^0AT2 and ASCT2 further, a B^0AT1-deficient mouse was employed and studied. The B^0AT1-deficient mouse was established by the biotech company Deltagen. To achieve this gene targeting in mouse embryonic stem cells was used. The method is based on the fact that homologous DNA sequences can align with genomic DNA and undergo recombination in low frequencies. Thus, directed mutation at any locus in the mouse genome can be generated (Torres, 1997). A cassette containing the *E. coli* β-galactosidase (LacZ) and a neomycin resistance gene (Neo) as selective markers, was inserted in to exon 3, resulting in a 28 bp deletion of the SLC6A19 gene in exon 3. Thus, no functional B^0AT1 protein can be translated. The principle is depicted in Figure 5.1. Subsequent PCR analysis and Southern Blot detection undertaken by Deltagen confirmed the deletion of the B^0AT1 gene (data not shown).

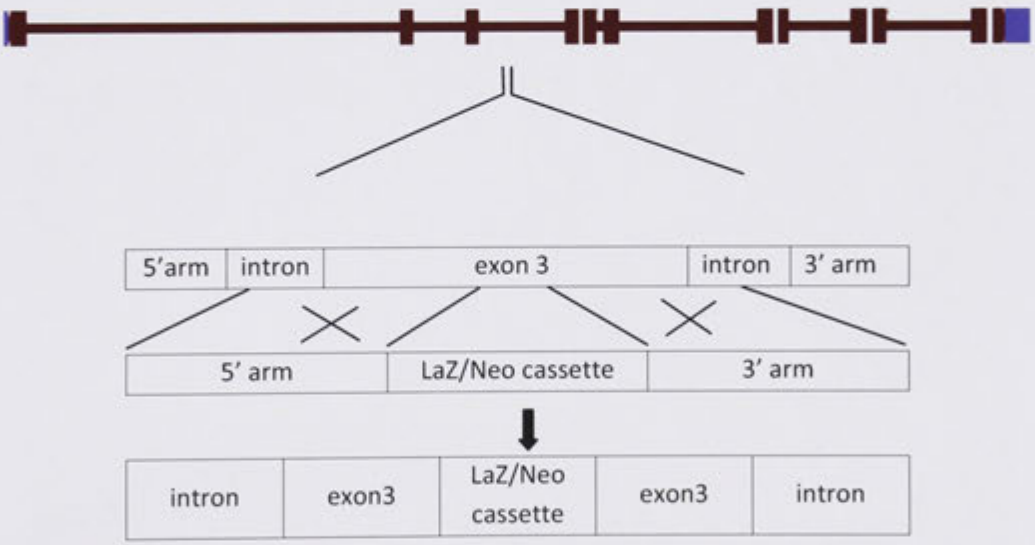

Figure 5.1: Principle of B^0AT1-deficient mouse generation.

The B^0AT1 gene is depicted with its coding sequences (red) and untranslated regions in blue. Boxes mark exons of the gene. A LacZ/Neo cassette was inserted into exon 3, disrupting the B^0AT1 gene and deleting 28 bp of the exon 3 sequence. Note, the Figure is not drawn to scale.

The phenotype of the B^0AT1-deficient mice showed a significant difference in size compared to wild type (wt) mice (Figure 5.2). An adult B^0AT1-deficient mouse was smaller in size than the wt sibling. Weight measurements and urine amino acid analysis were not available at the time this thesis was written..

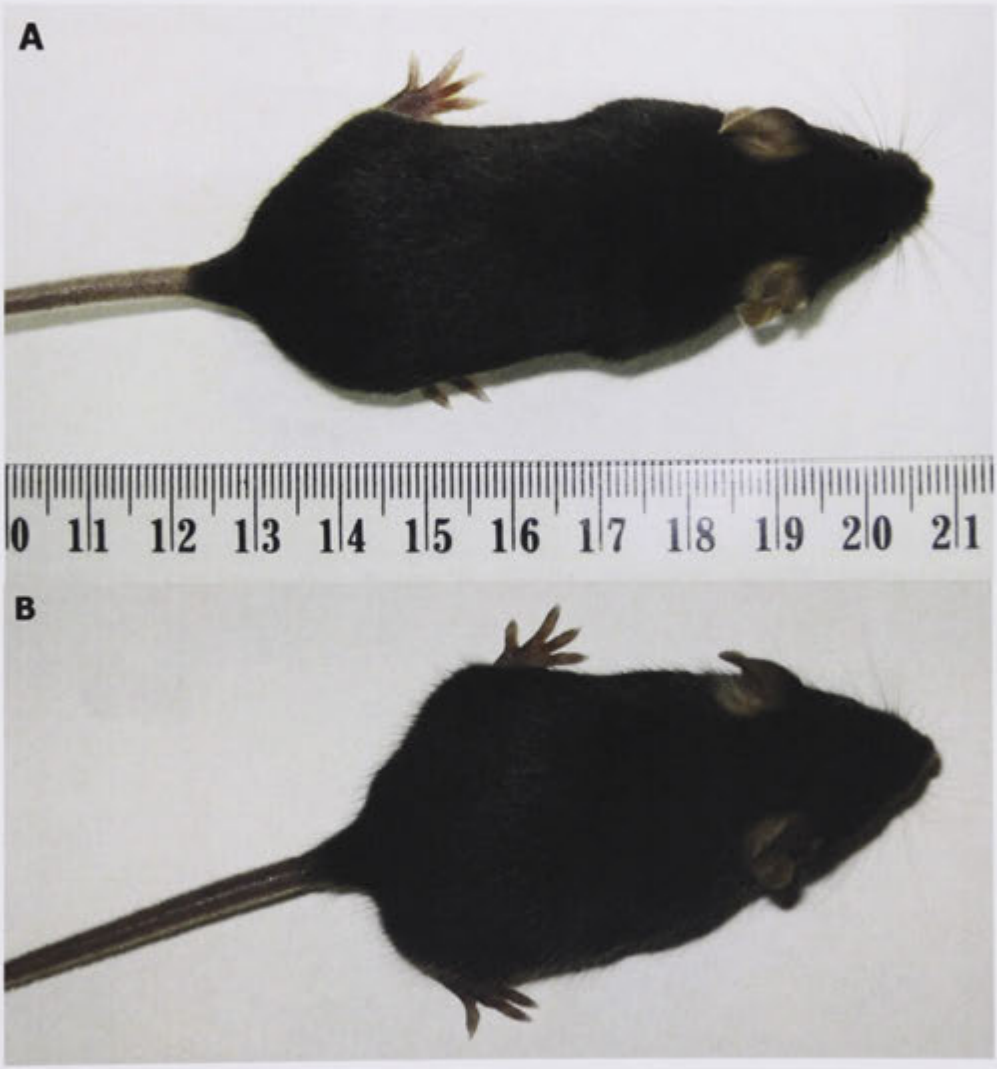

Figure 5.2: Phenotype of wild type C57/Bl6 and B^0AT1-deficient mouse.

The smaller size of the B^0AT1-deficient mouse (**B**) in comparison to the wt mouse (**A**) is shown by the measuring tape (Figure kindly provided by Angelika Bröer)

The aim of this chapter was to study amino acid transport in the B^0AT1-deficient mouse. Firstly, the lack of the B^0AT1 protein was confirmed by immunofluorescence studies. Paraffin embedded kidney and intestinal sections of B^0AT1-deficient mice were stained in parallel with sections of wt mice. Secondly, vesicle experiments were conducted with vesicles derived from B^0AT1-deficient mice kidneys. These experiments were undertaken in order to investigate changes in neutral amino acid transport and possible compensations for the lack of B^0AT1.

5.2 Results

5.2.1 Determination of B^0AT1 localisation in mouse kidney and intestine

B^0AT1-deficient mouse kidney and intestine were investigated using immunofluorescence microscopy to confirm whether B^0AT1 was lacking or not. The mouse kidney and intestine specimens were pre-fixed with 10 % NBF, then embedded in paraffin, sectioned and de-paraffined. Boiling sodium citrate buffer (1 mM) at pH 6 was subsequently applied to retrieve the cross-linked antigenic sites formed during the fixation. Subsequently, the slides were incubated with rabbit anti-mB^0AT1 antibody, which was detected by donkey anti-rabbit secondary antibody conjugated to AF 488. The kidney proximal tubules were identified, as described in Chapter 3 by co-staining with biotinylated LTL, which was detected by Steptavidin-Texas Red. No marker was used in intestinal staining.

Immunofluorescence staining of the B^0AT1-deficient mouse kidney sections detected no signal for B^0AT1 (Figure 5.3 A). Positive controls consisted of wt mouse kidney sections stained in parallel with the B^0AT1-deficient mouse kidney slides. The positive control showed B^0AT1 staining in the S1 and S2 segments of the mouse kidney (Figure 5.3 B), as described in Chapter 3. A negative control consisting of stained wt mouse sections with the secondary antibody only demonstrated no distinct staining (Figure 5.3 C).

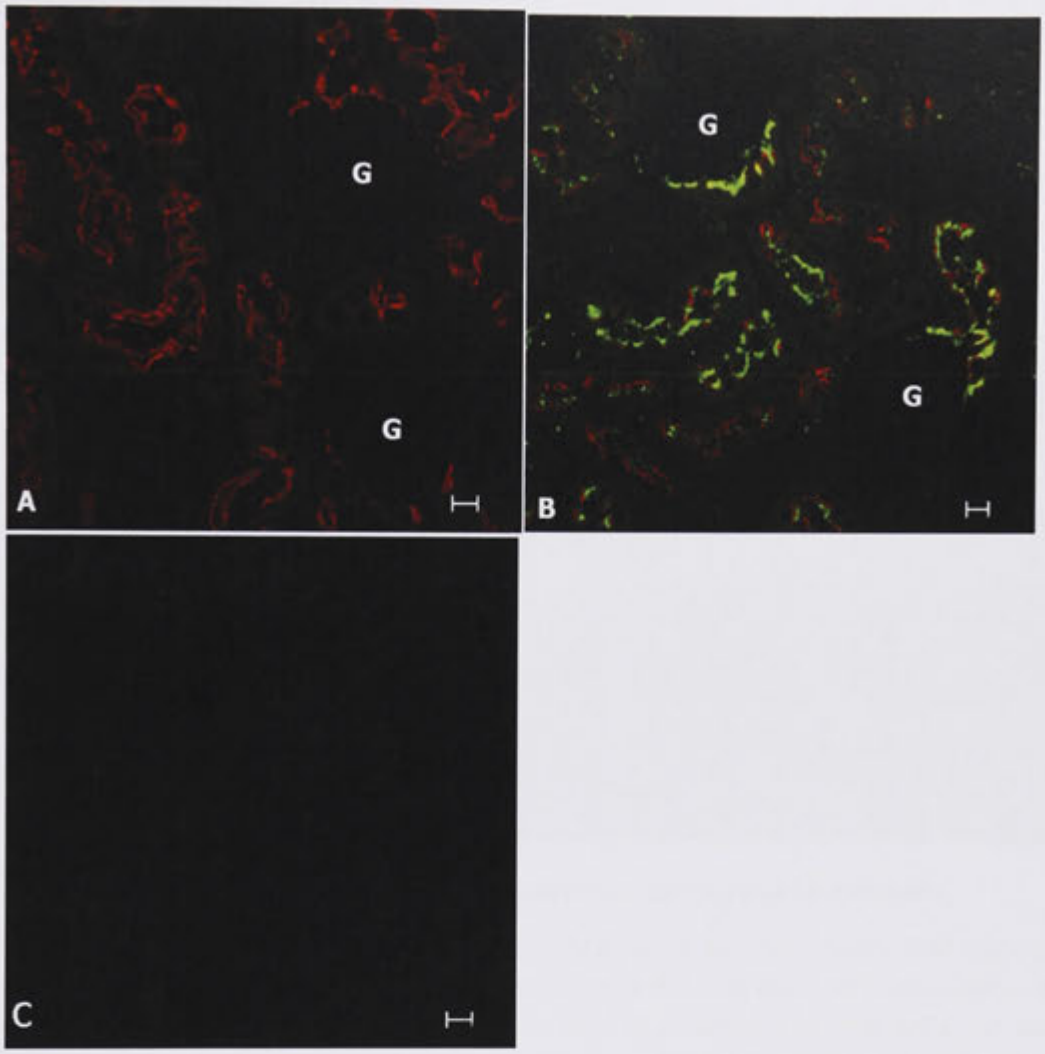

Figure 5.3: Localisation of B^0AT1 in B^0AT1-deficient and wt C57Bl/6 mouse kidney.

Slides were stained using a rabbit primary B^0AT1 antibody detected by a donkey-anti rabbit secondary antibody conjugated to AF 488 (green). Kidney proximal tubules were co-stained with biotinylated Lotus Tetragonobolus lectine as marker followed by detection with Streptavidine-Texas Red (red). The glomeruli are denoted as G. **A**: No B^0AT1-specific immunoreactivity was detected in the B^0AT1-deficient mouse kidney sections. Only the marker was visible. **B**: B^0AT1 staining was detected in the wt mouse slides as described above in the S1 and S2 segments of the kidney proximal tubule. **C**: No specific staining of mouse tissue was observed with the usage of only secondary antibody. Original magnification, x40. Bars represent 10 µm.

Immunofluorescence staining of intestinal sections from B^0AT1-deficient mice also failed to detect a signal for B^0AT1 (Figure 5.4 A). As with the experiments on kidney sections, wt mouse intestine sections were stained in parallel with sections from the B^0AT1-deficient mouse. The positive control showed B^0AT1 staining in the apical membrane of the intestinal villi with more B^0AT1 being expressed at the top of the villi gradually decreasing to the crypts (Figure 5.4 B).

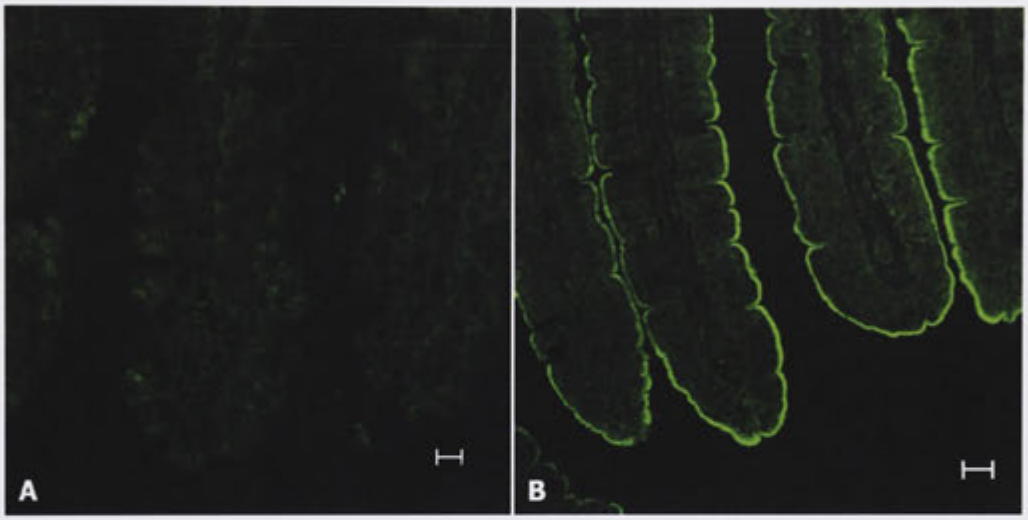

Figure 5.4: Localisation of B^0AT1 in B^0AT1-deficient and wt mouse intestine.

B^0AT1 was stained using a rabbit primary antibody detected by donkey-anti rabbit secondary antibody conjugated to AF 488 (green). **A**: No distinct B^0AT1-specific immunoreactivity was detected in the B^0AT1-deficient mouse sections. **B**: B^0AT1 staining was detected in the apical membrane of the villi of wt mouse sections. Original magnification, x40. Bars represent 10 µm.

5.2.2 Amino acid transport of leucine and glutamine in B^0AT1-deficient mice

After confirmation of B^0AT1 deletion in the B^0AT1-deficient mice, the amino acid transport in the B^0AT1-deficient mice was examined to determine the contribution to neutral amino acid transport by other proteins and a possible compensation for the lack of B^0AT1. Renal BBMV were generated as described in Chapter 4 and immediately used for radioactive uptake studies as described in Chapter 4. Uptake was measured in NaCl-based and KCl-based buffer. Furthermore, the uptake studies were undertaken with and without preloading of the vesicles in order to examine the contribution of ASCT2 transport due to the antiport mechanism of ASCT2.

As before [^{3}H]leucine uptake (100 µM) was measured in BBMV generated from B^0AT1-deficient mice not preloaded or preloaded with 30 mM glutamine and 4 mM ATP.

In contrast to BBMV from wt kidneys, [^{3}H]leucine uptake was the same under all conditions. (Figure 5.5). The transport at 15 sec was 0.24 ± 0.01 pmol/mg protein in Na^+-based buffer in contrast to 0.25 ± 0.01 pmol/mg protein in the absence of Na^+ for non-preloaded BBMV. For preloaded BBMV a leucine transport of 0.28 ± 0.02 pmol/mg protein in Na^+-based buffer in contrast to 0.23 ± 0.003 pmol/mg protein in K^+-based buffer was detected. A small additional leucine transport was observed in preloaded BBMV in comparison to non-preloaded vesicles.

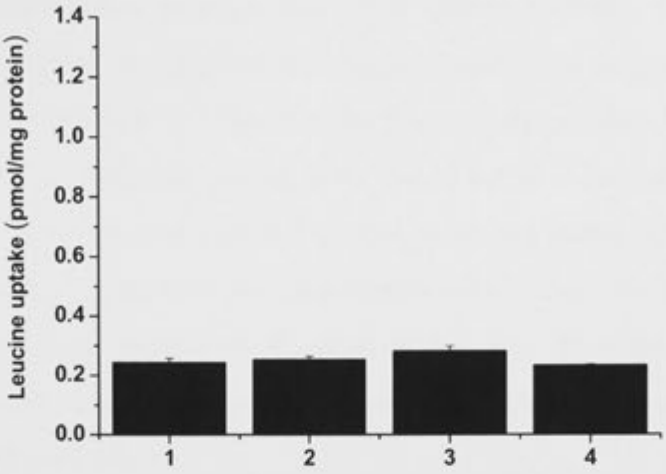

Figure 5.5: [^{3}H]leucine transport into mouse renal brush border membrane vesicles (preloaded with 30 mM glutamine or not preloaded) in NaCl-based and KCl-based buffer.

Non-preloaded renal BBMV were incubated with [^{3}H]leucine (100 µM) for 15 sec in NaCl-based buffer, denoted as 1 or KCl-based buffer, denotes as 2. The transport activity of BBMV preloaded with 30 mM glutamine was determined in the same way in NaCl-based buffer, denoted as 3, or KCl-based buffer, denoted as 4. Each bar represents the average of duplicates ± standard deviation. Similar results were obtained in four different experiments. No increase of [^{3}H]leucine uptake was observed with NaCl-based buffer in comparison to KCl-based buffer for non-preloaded vesicles and a 1.2 increase was observed for preloaded BBMV.

Additionally, [^{3}H]glutamine uptake was investigated, since it is the main substrate for ASCT2 (Figure 4.3). Preloaded and non-preloaded l BBMV were added to NaCl-based or KCl-based uptake buffer containing [^{3}H]glutamine (100 µM). Non-preloaded vesicles were used as controls. A sample was taken after 15 sec and processed as described above.

The renal BBMV from B^0AT1-deficient mice showed a 1.5 fold increase of glutamine uptake in Na^+-based buffer to KCl-based buffer control ($p<0.05$). Preloaded BBMV showed only a marginal, not significant increase of glutamine uptake in NaCl-based buffer to preloaded BBMV in KCl-based buffer (Figure 5.6) ($p>0.05$). The transport at 15 sec was 0.36 ± 0.02 pmol/mg protein in Na^+-based buffer in contrast to 0.24 ± 0.01 pmol/mg protein in the absence from Na^+ for non-preloaded BBMV. Preloaded BBMV a glutamine transport of 0.29 ± 0.04 pmol/mg protein in NaCl-based buffer in contrast to 0.25 ± 0.008 pmol/mg protein in K^+-based buffer was detected. No additional glutamine transport was observed for preloaded BBMV in comparison to non preloaded vesicles ($p>0.05$).

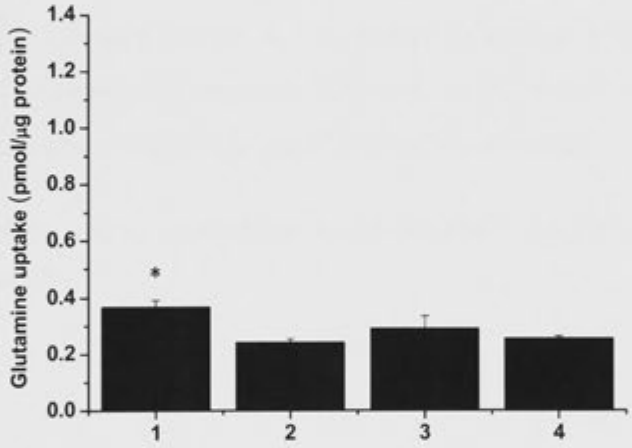

Figure 5.6: [^{3}H]glutamine transport into mouse renal brush border membrane vesicles (preloaded with 30 mM glutamine or non-preloaded) in NaCl and KCl buffer.

Non-preloaded BBMV were incubated with [^{3}H]glutamine (100 µM) for of 15 sec in NaCl-based buffer, denoted as 1 and KCl-based buffer, denoted as 2. Renal BBMV preloaded with 30 mM glutamine were treated in the same way in NaCl-based buffer are denoted as 3, and 4 in KCl-based media. Each bar represents the average of duplicates ± standard deviation; * indicates statistical significance at $p<0.05$. Similar results were obtained in five different experiments. A 1.5 fold increase of [^{3}H]glutamine uptake was observed in NaCl-based buffer in comparison to KCl-based buffer for non-preloaded vesicles and a 1.16 fold increase was observed for preloaded BBMV.

5.3 Discussion

5.3.1 Localisation of B^0AT1 in B^0AT1-deficient mice:

Immunofluorescence studies with B^0AT1-deficient mice in comparison to wt mice confirmed the lack of B^0AT1 in B^0AT1-deficient mice. No B^0AT1 staining was observed in all segments of the kidney while in B^0AT1 wt mice staining was detected in the S1 and S2 segments as observed in Chapter 3. This represents the first characterisation of an SLC6A19-deficient mouse. A B^0AT2-deficient mouse has been characterised by Drgonova *et al.*, however, this study only focused on the localisation of B^0AT2 in brain and not in kidney (Drgonova *et al.*, 2007). Therefore, it would be very interesting to investigate the B^0AT2-defient mouse in this matter to compare the B^0AT2-deficient mouse to the B^0AT1-deficient mouse. Furthermore it would be interesting to investigate the localisation of B^0AT2 in the B^0AT1-deficient mouse.

The amino acid uptake into renal BBMV derived from B^0AT1-deficient mice will be discussed in Chapter 6.

Chapter 6

General Discussion and Future Directions

Amino acids are one of the basic building blocks for life and are crucially involved in most if not all biological processes. As a result, it is important to understand amino acid transport and reabsorption in organisms. In the last 10 to 15 years nearly all physiologically described amino acid transport systems (outlined in Table 1.1) in the kidney and the intestine have been identified at on the molecular level and characterised in different expression systems in some detail. By contrast, much less is known about their physiological contribution to amino acid transport *in vivo*.

As outlined in the introduction, this thesis focuses on the neutral amino acid transport and reabsorption in mammals in the kidney and the intestine. More precisely, it investigates the relative contribution to neutral amino acid uptake of the transporters B^0AT1, B^0AT2 and ASCT2.

Mutations in neutral amino acid transporters have been linked to diseases such as Hartnup Disorder (Kleta *et al.*, 2004; Seow *et al.*, 2004; Kowalczuk *et al.*, 2008). A thorough analysis of epithelial amino acid transporters could not only elucidate the molecular correlation to diseases but also identify routes for drug delivery.

Previous studies by Kleta *et al.* and Romeo *et al.* have examined the localisation of B^0AT1 in mouse tissue via the use of immunofluorescence (Kleta *et al.*, 2004; Romeo *et al.*, 2006). They reported the presence of the transporter in the apical membrane of mouse proximal tubules. Both studies suggested expression of B^0AT1 in the S1 segment, but not in other segments of the kidney.

These data are in agreement with earlier in-situ hybridisation studies by Broer *et al.* (2004), which reported expression of B^0AT1 being restricted to S1 and S2 segments of the kidney nephron. Finally, high levels of B^0AT1 mRNA in mouse kidney were confirmed with RT-PCR (Romeo *et al.*, 2006).

The results in Chapter 3 are consistent with this literature in terms of identifying the apical expression of the amino acid transporter B^0AT1 in the S1 and S2 segment of the mouse proximal nephron. B^0AT1 was not observed in the S3 segment. These results are at variance with an RT-PCR analysis, where B^0AT1 mRNA was detected in all segment of the mouse nephron except the glomerulus, the thick ascending limb and the distal tubules (Kleta *et al.*, 2004). The tissue isolation required for RT-PCR analysis does not provide the same cellular resolution as *in situ*-hybridisation and immunofluorescence. As a result the discrepancy is likely to result from technical problems rather than refuting the more detailed localisation studies generated in this thesis and other more recent publications.

In contrast to B^0AT1, very little information was available about the B^0AT2 biodistribution in kidney. Previously, it was assumed that B^0AT2 is a brain-specific transporter (Takanaga *et al.*, 2005). However, RT-PCR analysis revealed the presence of B^0AT2 mRNA not only in mouse brain but also in mouse kidney and lung (Broer *et al.*, 2006). Thus a central question of this thesis was to determine the possible activity of B^0AT2 in kidney. Utilising immunofluorescence techniques and proximal tubule specific markers, expression of B^0AT2 protein was detected in the proximal tubule. Based on cell anatomy, expression was confined to the S2 and S3 segment (Figure 3.17). However, my results suggest low expression levels of B^0AT2 in the kidney overall. The transporter is not expressed in the intestine.

In comparison to B^0AT1, B^0AT2 seems to have a less important role due to the lower expression level and the more distal localisation along the proximal tubule. It has been known that amino acids transporters have a distinct distribution along the axis of the proximal tubule (Scriver and Tenenhouse, 1985). Transporters in the earlier segments of the proximal tubule tend to have higher capacity and broader specificity but lower affinity for their substrates, while transporters in the later segments of the proximal tubule possess lower capacity but higher affinity for a more select group of substrates.

B^0AT1 and B^0AT2 fit this pattern. B^0AT1 accepts all neutral amino acids, has a low affinity for its substrates and is abundantly expressed in the S1/S2 segment of the proximal tubule. B^0AT2, by contrast prefers branched-chain amino acids, has a higher affinity for its substrates and is expressed in smaller amounts in the S2/S3 segment of the proximal tubule.

It has been suggested that in the early segments, where amino acid concentration is similar to that found in plasma, the reabsorption by transporters needs to be controlled or limited in order to protect the cells from osmotic overload. In later segments of the kidney, where the substrate concentration is lower, the transporters need to be of higher affinity in order to effectively retrieve the amino acids from the primary urine (Verrey, 2003).

Similar to B^0AT2, limited information was available about the ASCT2 expression in the kidney. Avissar *et al.* localised ASCT2 in rabbit kidney via immunohistochemistry in the apical membrane of the S1 segment of the proximal convoluted tubule (Avissar *et al.*, 2001). In contrast, studies undertaken by Green *et al.* suggested localisation of ASCT2 in the basolateral membrane of the proximal tubule in human kidney (Green *et al.*, 2004).

In the study conducted by Vanslambrouck (2006) immunofluorescent techniques were used in combination with segment specific markers of the human nephron to clarify previous contradictions (Breedan, 2006). ASCT2 expression was detected in the apical membrane of the S2 and the S3 segments of the proximal convoluted tubule. Furthermore, the presence of the transporter was also observed in the basolateral membrane of the distal convoluted tubule.

The observed localisation in the apical membrane is contrary to the observations of Avissar *et al.* (2001). However, the results of this study suggest that the ASCT2 antibody does not recognise a specific epitope in paraformaldehyde-fixed tissue and therefore the results need to be interpreted with caution. In addition it has to be considered that the antibody for ASCT2 was raised against a synthetic peptide.

Holmseth *et al.* (2005) showed that with the use of these antibodies cross-reactivity to unrelated proteins is frequently observed and therefore interpretation of immunolocalisation should be done with caution.

Previous investigations also showed that the cell surface expression of ASCT2 was significant higher at lower pH values of 6.2 to 6.7 in rat lenses (Lim *et al.*, 2005) and foetal astrocytes (Gegelashvili *et al.*, 2006). It is known that the pH of the kidney ultrafiltrate changes gradually from 7.4 to approximately 6.8 and therefore could explain the different localisations of ASCT2 on the apical membrane. Although these results would not explain the basolateral expression of ASCT2 and therefore the results should be interpreted with caution.

As an amino acid exchanger ASCT2 is unlikely to have a prominent role in transepithelial transport of amino acids. A possible role of ASCT2 at the basolateral membrane of the distal tubules could be to equilibrate cytoplasmatic amino acids by releasing excess amino acids. This role has been discussed, but experimental proof is missing and needs further investigation (Verrey *et al.*, 2005). Future experiments could be conducted using transwell plates. These plates allow the cells to differentiate and form apical and basolateral sides to the cell layer as they polarise allowing access to investigate expression and functional activity of the transporters on both sides of the membrane. OK is a cell line derived from possum kidney, showing characteristics of the proximal tubule, such as Na^+-dependent transport systems and enzymes located in the apical membrane such as alkaline phosphatase (Koyama *et al.*, 1978; Cheng *et al.*, 1988) and could be used for these experiments.

The detection of ASCT2 in the basolateral membrane of crypt cells in the intestine is also at variance to the report of Avissar *et al.* (2001), where ASCT2 was suggested to be expressed in the apical membrane of the ileum but only weakly in the crypt cells. An ASCT2-like transport activity has been detected in rabbit small intestine and has been suggested to contribute to L-glutamate uptake. This is consistent with uptake of L-glutamate transport via ASCT2 at lower pH (Utsunomiya-Tate *et al.*, 1996).

Thus, it appears likely that ASCT2 corresponds to the glutamate transport activity described in rabbit ileum (Munck and Munck, 1999). With the localisation in the intestinal crypt cells, ASCT2 cannot accomplish this transport.

According to the results obtained with the different fixation methods it would be worthwhile to repeat the immunofluorescence experiments with specimens fixed in acetone instead of paraformaldehyde to exclude possible damage of the antigens. It also has to be considered, that the ASCT2 localisation conducted by Vanslambrouck was conducted with human specimens. Therefore, it would be interesting to investigate, if localisation studies in different species obtain different results.

As outlined above, the biodistribution data did not provide an unambiguous answer as to the role of ASCT2 in amino acid reabsorption. The substrate specificies of all three neutral amino acid transporters have been characterised in the *Xenopus laevis* expression system in some detail (Utsunomiya-Tate *et al.*, 1996; Bohmer *et al.*, 2005; Broer *et al.*, 2006). However, to date no study has been conducted to reveal their contribution to neutral amino acid transporter *in vivo*. However, studies with BBMV have been conducted for amino acid transport without knowing the substrate specificity of the different systems (Murer and Kinne, 1980; Murer and Gmaj, 1986; Satoh *et al.*, 1989).

In particular both B^0AT1 (Verrey *et al.*, 2005; Broer, 2008) and ASCT2 (Kekuda *et al.*, 1996; Avissar *et al.*, 2001) have been suggested to represent the main Na^+-dependent transport activity for neutral amino acids in kidney and intestine (system B^0). Chapter 4 thus analysed the contribution to epithelial neutral amino acid transport by B^0AT1, B^0AT2 and ASCT2 using BBMV derived from mouse kidney.

The lack of stimulation of [^{3}H]leucine or [^{3}H]glutamine uptake in preloaded vs non-preloaded vesicles, was inconsistent with a significant contribution of ASCT2 to neutral amino acid transport. This result refutes the suggestion of Avissar *et al.* that ASCT2 represents the B^0 activity in kidney and intestine (Avissar *et al.*, 2001).

Further weight to this argument was added by the use of BBMV derived from kidneys of B^0AT1-deficient mice. The reduction of Na^+-dependent glutamine transport by more than 70 % in comparison to BBMV derived from wildtype mice (Figure 4.9) confirms that B^0AT1 is the main Na^+-dependent glutamine transporter in kidney.

However, the slight increase in glutamine uptake with non-preloaded, renal BBMV indicated the possible presence of another Na^+-dependent glutamine transporter. Since no additional transport is observed in preloaded BBMV, ASCT2 is unlikely to be a candidate for this transporter.

To discriminate between the contribution of B^0AT1 and B^0AT2, [^{14}C]leucine-uptake was challenged by unlabelled substrates The key substrate in this experiment was glycine, which is a substrate for B^0AT1 only. The strong inhibition of leucine uptake by glycine further confirms that B^0AT1 is the predominant neutral amino acid transporter in the apical membrane of the kidney proximal tubule. The lack of B^0AT2 activity was confirmed in BBMV derived from B^0AT1-deficient mice, showing a lack of Na^+-dependent [^{3}H]leucine uptake. Recently a B^0AT2-deficient mouse was characterised by Drgonova *et al.* However, only amino acid uptake in synaptosomes was studied in these mice (Drgonova *et al.*, 2007). Transport studies with this mouse using kidney BBMV or sections of intestine were unfortunately missing but would be interesting to investigate the possible role of B^0AT2.

In summary the results of this thesis strongly support the notion that B^0AT1 is the major if not only Na^+-dependent, broad neutral amino acid transport activity in kidney cortex. However, another possible candidate is B^0AT3 because recent investigations showed it is mainly an alanine and glycine transporter (Vanslambrouck *et al.*, 2010) that is expressed in the kidney. It could therefore, be involved in transport of those neutral amino acids. It would be worthwhile conducting transport experiments with BBMV derived from B^0AT1-deficient mice with the different substrate for B^0AT3. Na^+-dependent transport of those substrates would be likely to be from B^0AT3 since B^0AT2 and ASCT2 were excluded in this thesis.

Leucine uptake into renal BBMV derived from B^0AT1-deficient mice showed no evidence of Na^+-dependent leucine transport. Therefore, B^0AT1 seems to be the only, functional Na^+-dependent leucine transporter in the kidney. However, it needs to be analysed if the low levels of leucine transport observed in both NaCl- and KCl-based buffer reflects Na^+-independent transport or binding of radioactive substrate to the vesicles.

A possible candidate for the remaining leucine transport is B^0AT3. As described previously, B^0AT3 is mainly an alanine and glycine transporter but also shows low transport activity for leucine (Vanslambrouck *et al.*, 2010). To investigate the role of B^0AT3, leucine uptake in competition with glycine should be measured in BBMV derived from B^0AT1-deficient mice. Another possible candidate for the remaining transport activity is the system L-like transporter LAT2/4F2 arising from cross-contamination of the vesicles with basolateral membrane fragments.

As described in the introduction, LAT2/4F2 is a Na^+-independent transporter for large neutral amino acids, which in the kidney is made up of a heterodimer of the LAT2 light chain and the 4F2 heavy chain. However, its activity would only be revealed in preloaded vesicles because it catalyses an antiport mechanism (Kanai *et al.*, 1998; Pineda *et al.*, 1999). This would also be consistent with the marginal increase of leucine transport in preloaded BBMV. However, only LAT2/4F2 would explain this transport activity but not the non-identified uniporter with system L activity. One possibility to investigate the involvement of LAT2/4F2 is to test radio-labelled leucine uptake in the presence of system L inhibitors, such as BCH.

In contrast to leucine uptake, BBMV derived from B^0AT1-deficient mice still showed a significant amount of Na^+-dependent glutamine uptake. A possible candidate for this Na^+-dependent glutamine transporter in the kidney could be SNAT2. The Na^+-dependent, system A transporter SNAT2 is a symporter and has been found in the kidney, but is not known to be expressed in the apical membrane. (Hatanaka *et al.*, 2000; Reimer *et al.*, 2000; Sugawara *et al.*, 2000; Yao *et al.*, 2000; Hatanaka *et al.*, 2001; Armano *et al.*, 2002; Chaudhry *et al.*, 2002; Mackenzie *et al.*, 2003).

Uptake experiments with the system A substrate analogue MeAIB could provide indication for the presence of SNAT2 in the apical membrane. LAT2/4F2 can be excluded as a possible candidate since it is Na^+- independent and therefore would show similar levels of activity in NaCl-based and KCl-based buffer (Rossier *et al.*, 1999).

In summary, the studies presented in this thesis have determined the distribution and contribution of neutral amino acid transporter B^0AT1, B^0AT2 and ASCT2 *in vivo*. It is now without doubt that the neutral amino acid transporter B^0AT1 is the main, Na^+-dependent neutral amino acid transporter in the kidney. Therefore, B^0AT1 and not ASCT2, as suggested by Avissar *et al.*, is the actual B^0 activity in the kidney (Avissar *et al.*, 2001).

#

Bibliography

Bibliography

al-Mahroos, F. T., N. Abumrad and F. K. Ghishan (1990). "Developmental changes in glutamine transport by rat jejunal basolateral membrane vesicles." *Proc Soc Exp Biol Med* **194**(3): 186-92.

Altschul, S. F., T. L. Madden, A. A. Schaffer, J. Zhang, Z. Zhang, W. Miller and D. J. Lipman (1997). "Gapped BLAST and PSI-BLAST: a new generation of protein database search programs." *Nucleic Acids Res* **25**(17): 3389-402.

Armano, S., S. Coco, A. Bacci, E. Pravettoni, U. Schenk, C. Verderio, H. Varoqui, J. D. Erickson and M. Matteoli (2002). "Localization and functional relevance of system a neutral amino acid transporters in cultured hippocampal neurons." *J Biol Chem* **277**(12): 10467-73.

Arriza, J. L., S. Eliasof, M. P. Kavanaugh and S. G. Amara (1997). "Excitatory amino acid transporter 5, a retinal glutamate transporter coupled to a chloride conductance." *Proc Natl Acad Sci U S A* **94**(8): 4155-60.

Arriza, J. L., M. P. Kavanaugh, W. A. Fairman, Y. N. Wu, G. H. Murdoch, R. A. North and S. G. Amara (1993). "Cloning and expression of a human neutral amino acid transporter with structural similarity to the glutamate transporter gene family." *J Biol Chem* **268**(21): 15329-32.

Avissar, N. E., C. K. Ryan, V. Ganapathy and H. C. Sax (2001). "Na(+)-dependent neutral amino acid transporter ATB(0) is a rabbit epithelial cell brush-border protein." *Am J Physiol Cell Physiol* **281**(3): C963-71.

Avissar, N. E., H. C. Sax and L. Toia (2008). "In human entrocytes, GLN transport and ASCT2 surface expression induced by short-term EGF are MAPK, PI3K, and Rho-dependent." *Dig Dis Sci* **53**(8): 2113-25.

Azmanov, D. N., S. Kowalczuk, H. Rodgers, C. Auray-Blais, R. Giguere, J. E. Rasko, S. Broer and J. A. Cavanaugh (2008). "Further evidence for allelic heterogeneity in Hartnup disorder." *Hum Mutat* **29**(10): 1217-21.

Babu, E., Y. Kanai, A. Chairoungdua, D. K. Kim, Y. Iribe, S. Tangtrongsup, P. Jutabha, Y. Li, N. Ahmed, S. Sakamoto, N. Anzai, S. Nagamori and H. Endou (2003). "Identification of a novel system L amino acid transporter structurally distinct from heterodimeric amino acid transporters." *J Biol Chem* **278**(44): 43838-45.

Baron, D. N., C. E. Dent, H. Harris, E. W. Hart and J. B. Jepson (1956). "Hereditary pellagra-like skin rash with temporary cerebellar ataxia, constant renal amino-aciduria, and other bizarre biochemical features." *Lancet* **271**(6940): 421-8.

Biber, J., B. Stieger, G. Stange and H. Murer (2007). "Isolation of renal proximal tubular brush-border membranes." *Nat Protoc* **2**(6): 1356-9.

Bodoy, S., L. Martin, A. Zorzano, M. Palacin, R. Estevez and J. Bertran (2005). "Identification of LAT4, a novel amino acid transporter with system L activity." *J Biol Chem* **280**(12): 12002-11.

Bohmer, C., A. Broer, M. Munzinger, S. Kowalczuk, J. E. Rasko, F. Lang and S. Broer (2005). "Characterization of mouse amino acid transporter B0AT1 (slc6a19)." *Biochem J* **389**(Pt 3): 745-51.

Boron, W., F.; and E. L. Boulpaep (2005). Medical Physiology: A Cellular and Molecular Approach, Elsevier Ltd.

Bradford, M. M. (1976). "A rapid and sensitive method for the quantitation of microgram quantities of protein utilizing the principle of protein-dye binding." *Anal Biochem* **72**: 248-54.

Breedan, J. (2006). "The biodistribution of amino acid transporters in mammalian kidney and small intestine." *Honours Thesis*.

Broer, A., K. Klingel, S. Kowalczuk, J. E. Rasko, J. Cavanaugh and S. Broer (2004). "Molecular cloning of mouse amino acid transport system B0, a neutral amino acid transporter related to Hartnup disorder." *J Biol Chem* **279**(23): 24467-76.

Broer, A., N. Tietze, S. Kowalczuk, S. Chubb, M. Munzinger, L. K. Bak and S. Broer (2006). "The orphan transporter v7-3 (slc6a15) is a Na+-dependent neutral amino acid transporter (B0AT2)." *Biochem J* **393**(Pt 1): 421-30.

Broer, A., C. Wagner, F. Lang and S. Broer (2000). "Neutral amino acid transporter ASCT2 displays substrate-induced Na+ exchange and a substrate-gated anion conductance." *Biochem J* **346 Pt 3**: 705-10.

Broer, S. (2002). "Adaptation of plasma membrane amino acid transport mechanisms to physiological demands." *Pflugers Arch* **444**(4): 457-66.

Broer, S. (2003). "Xenopus laevis Oocytes." *Methods Mol Biol* **227**: 245-58.

Broer, S. (2006). "The SLC6 orphans are forming a family of amino acid transporters." *Neurochem Int* **48**(6-7): 559-67.

Broer, S. (2008). "Amino acid transport across mammalian intestinal and renal epithelia." *Physiol Rev* **88**(1): 249-86.

Broer, S. (2009). "The role of the neutral amino acid transporter B0AT1 (SLC6A19) in Hartnup disorder and protein nutrition." *IUBMB Life* **61**(6): 591-9.

Bungard, C. I. and J. D. McGivan (2004). "Glutamine availability up-regulates expression of the amino acid transporter protein ASCT2 in HepG2 cells and stimulates the ASCT2 promoter." *Biochem J* **382**(Pt 1): 27-32.

Camargo, S. M., V. Makrides, L. V. Virkki, I. C. Forster and F. Verrey (2005). "Steady-state kinetic characterization of the mouse B(0)AT1 sodium-dependent neutral amino acid transporter." *Pflugers Arch* **451**(2): 338-48.

Chaudhry, F. A., D. Schmitz, R. J. Reimer, P. Larsson, A. T. Gray, R. Nicoll, M. Kavanaugh and R. H. Edwards (2002). "Glutamine uptake by neurons: interaction of protons with system a transporters." *J Neurosci* **22**(1): 62-72.

Chen, N. H., M. E. Reith and M. W. Quick (2004). "Synaptic uptake and beyond: the sodium- and chloride-dependent neurotransmitter transporter family SLC6." *Pflugers Arch* **447**(5): 519-31.

Cheng, L., C. T. Liang, P. Precht and B. Sacktor (1988). "Alpha-2-adrenergic modulation of the parathyroid hormone-inhibition of phosphate uptake in cultured renal (OK) cells." *Biochem Biophys Res Commun* **155**(1): 74-82.

Chesney, R. W., N. Gusowski, M. Padilla and S. Lippincott (1986). "Effect of amino acid intake on brush-border membrane uptake of sulfur amino acids." *Am J Physiol* **251**(1 Pt 2): F125-31.

Choudry, H. A., W. W. Souba, C. Lin, Q. Meng, A. M. Karinch, J. Huang and M. Pan (2006). "Stimulation of expression of the intestinal glutamine transporter ATB0 in tumor-bearing rats." *Ann Surg Oncol* **13**(12): 1747-53.

Christensen, H. N. (1984). "Organic ion transport during seven decades. The amino acids." *Biochim Biophys Acta* **779**(3): 255-69.

Christensen, H. N. (1990). "Role of amino acid transport and countertransport in nutrition and metabolism." *Physiol Rev* **70**(1): 43-77.

Christensen, H. N., M. Liang and E. G. Archer (1967). "A distinct Na+-requiring transport system for alanine, serine, cysteine, and similar amino acids." *J Biol Chem* **242**(22): 5237-46.

Chung, B. M., J. K. Wong, J. A. Hardin and D. G. Gall (1999). "Role of actin in EGF-induced alterations in enterocyte SGLT1 expression." *Am J Physiol* **276**(2 Pt 1): G463-9.

Cohen, L. L. and K. C. Huang (1964). "Intestinal Transport of Tryptophan and Its Derivatives." *Am J Physiol* **206**: 647-52.

Crane, R. (1965). "Na+ -dependent tansport in the intestine and other animal tisses." *Fred Proc* **24**: 1000-1006.

Curran, P. F., S. G. Schultz, R. A. Chez and R. E. Fuisz (1967). "Kinetic relations of the Na-amino acid interaction at the mucosal border of intestine." *J Gen Physiol* **50**(5): 1261-86.

Danbolt, N. C., J. Storm-Mathisen and B. I. Kanner (1992). "An [Na+ + K+]coupled L-glutamate transporter purified from rat brain is located in glial cell processes." *Neuroscience* **51**(2): 295-310.

Danilczyk, U. and J. M. Penninger (2006). "Angiotensin-converting enzyme II in the heart and the kidney." *Circ Res* **98**(4): 463-71.

Danilczyk, U., R. Sarao, C. Remy, C. Benabbas, G. Stange, A. Richter, S. Arya, J. A. Pospisilik, D. Singer, S. M. Camargo, V. Makrides, T. Ramadan, F. Verrey, C. A. Wagner and J. M. Penninger (2006). "Essential role for collectrin in renal amino acid transport." *Nature* **444**(7122): 1088-91.

Doyle, F. A. and J. D. McGivan (1992a). "The bovine renal epithelial cell line NBL-1 expresses a broad specificity Na(+)-dependent neutral amino acid transport system (System Bo) similar to that in bovine renal brush border membrane vesicles." *Biochim Biophys Acta* **1104**(1): 55-62.

Doyle, F. A. and J. D. McGivan (1992b). "Reconstitution and identification of the major Na(+)-dependent neutral amino acid-transport protein from bovine renal brush-border membrane vesicles." *Biochem J* **281 (Pt 1)**: 95-102.

Drgonova, J., Q. R. Liu, F. S. Hall, R. M. Krieger and G. R. Uhl (2007). "Deletion of v7-3 (SLC6A15) transporter allows assessment of its roles in synaptosomal proline uptake, leucine uptake and behaviors." *Brain Res* **1183**: 10-20.

Endo, T., O. Kimura and M. Sakata (1998). "pH-dependent transport of cadmium in rat renal brush border membrane vesicles: cadmium efflux via H+-antiport." *Toxicol Lett* **99**(2): 99-107.

Evans, B. K. L., P. Y; and J. A. McKenzie (1995). Heinemann Biology in Context Biology One Melbourne, Heinemann Educational Australia.

Evers, J., H. Murer and R. Kinne (1976). "Phenylalanine uptake in isolated renal brush border vesicles." *Biochim Biophys Acta* **426**(4): 598-615.

Fairman, W. A., R. J. Vandenberg, J. L. Arriza, M. P. Kavanaugh and S. G. Amara (1995). "An excitatory amino-acid transporter with properties of a ligand-gated chloride channel." *Nature* **375**(6532): 599-603.

Farmer, M. K., M. J. Robbins, A. D. Medhurst, D. A. Campbell, K. Ellington, M. Duckworth, A. M. Brown, D. N. Middlemiss, G. W. Price and M. N. Pangalos (2000). "Cloning and characterization of human NTT5 and v7-3: two orphan transporters of the Na+/Cl- -dependent neurotransmitter transporter gene family." *Genomics* **70**(2): 241-52.

Fass, S. J., M. R. Hammerman and B. Sacktor (1977). "Transport of amino acids in renal brush border membrane vesicles. Uptake of the neutral amino acid L-alanine." *J Biol Chem* **252**(2): 583-90.

Fernandez, E., D. Torrents, J. Chillaron, R. Martin Del Rio, A. Zorzano and M. Palacin (2003). "Basolateral LAT-2 has a major role in the transepithelial flux of L-cystine in the renal proximal tubule cell line OK." *J Am Soc Nephrol* **14**(4): 837-47.

Frindt, G., Z. Ergonul and L. G. Palmer (2008). "Surface expression of epithelial Na channel protein in rat kidney." *J Gen Physiol* **131**(6): 617-27.

Frindt, G. and L. G. Palmer (2009). "Surface expression of sodium channels and transporters in rat kidney: effects of dietary sodium." *Am J Physiol Renal Physiol* **297**(5): F1249-55.

Ganapathy, V. and F. H. Leibach (1982). "Transport and utilization of methionine sulfoxide in the rabbit." *Biochim Biophys Acta* **693**(2): 305-14.

Gegelashvili, M., A. Rodriguez-Kern, I. Pirozhkova, J. Zhang, L. Sung and G. Gegelashvili (2006). "High-affinity glutamate transporter GLAST/EAAT1 regulates cell surface expression of glutamine/neutral amino acid transporter ASCT2 in human fetal astrocytes." *Neurochem Int* **48**(6-7): 611-5.

Ghishan, F. K. and F. A. Wilson (1985). "Developmental maturation of D-glucose transport by rat jejunal brush-border membrane vesicles." *Am J Physiol* **248**(1 Pt 1): G87-92.

Green, B. J., C. S. Lee and J. E. Rasko (2004). "Biodistribution of the RD114/mammalian type D retrovirus receptor, RDR." *J Gene Med* **6**(3): 249-59.

Grunewald, M., A. Bendahan and B. I. Kanner (1998). "Biotinylation of single cysteine mutants of the glutamate transporter GLT-1 from rat brain reveals its unusual topology." *Neuron* **21**(3): 623-32.

Grunewald, M. and B. I. Kanner (2000). "The accessibility of a novel reentrant loop of the glutamate transporter GLT-1 is restricted by its substrate." *J Biol Chem* **275**(13): 9684-9.

Guastella, J., N. Nelson, H. Nelson, L. Czyzyk, S. Keynan, M. C. Miedel, N. Davidson, H. A. Lester and B. I. Kanner (1990). "Cloning and expression of a rat brain GABA transporter." *Science* **249**(4974): 1303-6.

Gurdon, J. B., C. D. Lane, H. R. Woodland and G. Marbaix (1971). "Use of frog eggs and oocytes for the study of messenger RNA and its translation in living cells." *Nature* **233**(5316): 177-82.

Hatanaka, T., W. Huang, R. Ling, P. D. Prasad, M. Sugawara, F. H. Leibach and V. Ganapathy (2001). "Evidence for the transport of neutral as well as cationic amino acids by ATA3, a novel and liver-specific subtype of amino acid transport system A." *Biochim Biophys Acta* **1510**(1-2): 10-7.

Hatanaka, T., W. Huang, H. Wang, M. Sugawara, P. D. Prasad, F. H. Leibach and V. Ganapathy (2000). "Primary structure, functional characteristics and tissue expression pattern of human ATA2, a subtype of amino acid transport system A." *Biochim Biophys Acta* **1467**(1): 1-6.

Heckel, T. H. (2002). Charakterisierund des Glutamintransports in Zellen mit neuronalen Eigenschaften. Tuebingen, Univsersitaet Tuebingen. **Diplom/ Honours**.

Hediger, M. A., M. F. Romero, J. B. Peng, A. Rolfs, H. Takanaga and E. A. Bruford (2004). "The ABCs of solute carriers: physiological, pathological and therapeutic implications of human membrane transport proteinsIntroduction." *Pflugers Arch* **447**(5): 465-8.

Holmseth, S., Y. Dehnes, L. P. Bjornsen, J. L. Boulland, D. N. Furness, D. Bergles and N. C. Danbolt (2005). "Specificity of antibodies: unexpected cross-reactivity of antibodies directed against the excitatory amino acid transporter 3 (EAAT3)." *Neuroscience* **136**(3): 649-60.

Hopfer, U., K. Nelson, J. Perrotto and K. J. Isselbacher (1973). "Glucose transport in isolated brush border membrane from rat small intestine." *J Biol Chem* **248**(1): 25-32.

Hopfer, U., K. Sigrist-Nelson, E. Ammann and H. Murer (1976). "Differences in neutral amino acid and glucose transport between brush border and basolateral plasma membrane of intestinal epithelial cells." *J Cell Physiol* **89**(4): 805-10.

Inoue, K., K. Sato, M. Tohyama, S. Shimada and G. R. Uhl (1996). "Widespread brain distribution of mRNA encoding the orphan neurotransmitter transporter v7-3." *Brain Res Mol Brain Res* **37**(1-2): 217-23.

Jessen, H. and M. I. Sheikh (1992). "L-tryptophan uptake by segment-specific membrane vesicles from the proximal tubule of rabbit kidney." *Biochem J* **286 (Pt 1)**: 103-10.

Jorgensen, K. E., U. Kragh-Hansen and M. I. Sheikh (1990). "Transport of leucine, isoleucine and valine by luminal membrane vesicles from rabbit proximal tubule." *J Physiol* **422**: 41-54.

Kanai, Y. and M. A. Hediger (1992). "Primary structure and functional characterization of a high-affinity glutamate transporter." *Nature* **360**(6403): 467-71.

Kanai, Y. and M. A. Hediger (2004). "The glutamate/neutral amino acid transporter family SLC1: molecular, physiological and pharmacological aspects." *Pflugers Arch* **447**(5): 469-79.

Kanai, Y., H. Segawa, K. Miyamoto, H. Uchino, E. Takeda and H. Endou (1998). "Expression cloning and characterization of a transporter for large neutral amino acids activated by the heavy chain of 4F2 antigen (CD98)." *J Biol Chem* **273**(37): 23629-32.

Kanazawa, K., Y. Tamura and H. Ito (1953). "Effect of cortisone and hyaluronidase on the production of hemagglutinin of influenza and vaccinia viruses in suspended cell cultures." *Jpn J Exp Med* **23**(3): 249-53.

Kekuda, R., P. D. Prasad, Y. J. Fei, V. Torres-Zamorano, S. Sinha, T. L. Yang-Feng, F. H. Leibach and V. Ganapathy (1996). "Cloning of the sodium-dependent, broad-scope, neutral amino acid transporter Bo from a human placental choriocarcinoma cell line." *J Biol Chem* **271**(31): 18657-61.

Kekuda, R., V. TorresZamorano, Y. J. Fei, P. D. Prasad, H. W. Li, L. D. Mader, F. H. Leibach and V. Ganapathy (1997). "Molecular and functional characterization of intestinal Na+-dependent neutral amino acid transporter B-o." *American Journal of Physiology-Gastrointestinal and Liver Physiology* **35**(6): G1463-G1472.

Kilberg, M. S. (1982). "Amino acid transport in isolated rat hepatocytes." *J Membr Biol* **69**(1): 1-12.

Kim, J. W., E. I. Closs, L. M. Albritton and J. M. Cunningham (1991). "Transport of cationic amino acids by the mouse ecotropic retrovirus receptor." *Nature* **352**(6337): 725-8.

Kleta, R., E. Romeo, Z. Ristic, T. Ohura, C. Stuart, M. Arcos-Burgos, M. H. Dave, C. A. Wagner, S. R. Camargo, S. Inoue, N. Matsuura, A. Helip-Wooley, D. Bockenhauer, R. Warth, I. Bernardini, G. Visser, T. Eggermann, P. Lee, A. Chairoungdua, P. Jutabha, E. Babu, S. Nilwarangkoon, N. Anzai, Y. Kanai, F. Verrey, W. A. Gahl and A. Koizumi (2004). "Mutations in SLC6A19, encoding B0AT1, cause Hartnup disorder." *Nat Genet* **36**(9): 999-1002.

Koser, B. H. and H. N. Christensen (1971). "Effect of substrate structure on coupling ratio for Na + -dependent transport of amino acids." *Biochim Biophys Acta* **241**(1): 9-19.

Kotewicz, M. L., C. M. Sampson, J. M. D'Alessio and G. F. Gerard (1988). "Isolation of cloned Moloney murine leukemia virus reverse transcriptase lacking ribonuclease H activity." *Nucleic Acids Res* **16**(1): 265-77.

Kowalczuk, S., A. Broer, N. Tietze, J. M. Vanslambrouck, J. E. Rasko and S. Broer (2008). "A protein complex in the brush-border membrane explains a Hartnup disorder allele." *Faseb J* **22**(8): 2880-7.

Koyama, H., C. Goodpasture, M. M. Miller, R. L. Teplitz and A. D. Riggs (1978). "Establishment and characterization of a cell line from the American opossum (Didelphys virginiana)." *In Vitro* **14**(3): 239-46.

Kragh-Hansen, U., H. Roigaard-Petersen, C. Jacobsen and M. I. Sheikh (1984). "Renal transport of neutral amino acids. Tubular localization of Na+-dependent phenylalanine- and glucose-transport systems." *Biochem J* **220**(1): 15-24.

Kragh-Hansen, U. and M. I. Sheikh (1984). "Serine uptake by luminal and basolateral membrane vesicles from rabbit kidney." *J Physiol* **354**: 55-67.

Kriz, W. and L. Bankir (1988). "A standard nomenclature for structures of the kidney. The Renal Commission of the International Union of Physiological Sciences (IUPS)." *Kidney Int* **33**(1): 1-7.

Lash, L. H. and D. P. Jones (1984). "Characteristics of cysteine uptake in intestinal basolateral membrane vesicles." *Am J Physiol* **247**(4 Pt 1): G394-401.

Le Cam, A. and P. Freychet (1977). "Neutral amino acid transport. Characterization of the A and L systems in isolated rat hepatocytes." *J Biol Chem* **252**(1): 148-56.

Levy, H. L. (2001). Hartnup Disorder. New York.

Lim, J., Y. C. Lam, J. Kistler and P. J. Donaldson (2005). "Molecular characterization of the cystine/glutamate exchanger and the excitatory amino acid transporters in the rat lens." *Invest Ophthalmol Vis Sci* **46**(8): 2869-77.

Lim, J., K. A. Lorentzen, J. Kistler and P. J. Donaldson (2006). "Molecular identification and characterisation of the glycine transporter (GLYT1) and the glutamine/glutamate transporter (ASCT2) in the rat lens." *Exp Eye Res* **83**(2): 447-55.

Liman, E. R., J. Tytgat and P. Hess (1992). "Subunit stoichiometry of a mammalian K+ channel determined by construction of multimeric cDNAs." *Neuron* **9**(5): 861-71.

Lodish, H. B., A.; Zipursky, S. L.; Matsudaira, P.; Baltimore, D. and Darnell, J (2000). Molecular Cell Biology (4th edition). New York, Freeman & Co.

Loo, D. D., S. Eskandari, K. J. Boorer, H. K. Sarkar and E. M. Wright (2000). "Role of Cl- in electrogenic Na+-coupled cotransporters GAT1 and SGLT1." *J Biol Chem* **275**(48): 37414-22.

Mackenzie, B., M. K. Schafer, J. D. Erickson, M. A. Hediger, E. Weihe and H. Varoqui (2003). "Functional properties and cellular distribution of the system A glutamine transporter SNAT1 support specialized roles in central neurons." *J Biol Chem* **278**(26): 23720-30.

Maenz, D. D., C. Chenu, S. Breton and A. Berteloot (1992). "pH-dependent heterogeneity of acidic amino acid transport in rabbit jejunal brush border membrane vesicles." *J Biol Chem* **267**(3): 1510-6.

Maenz, D. D. and J. F. Patience (1992). "L-threonine transport in pig jejunal brush border membrane vesicles. Functional characterization of the unique system B in the intestinal epithelium." *J Biol Chem* **267**(31): 22079-86.

Malakauskas, S. M., H. Quan, T. A. Fields, S. J. McCall, M. J. Yu, W. M. Kourany, C. W. Frey and T. H. Le (2007). "Aminoaciduria and altered renal expression of luminal amino acid transporters in mice lacking novel gene collectrin." *Am J Physiol Renal Physiol* **292**(2): F533-44.

Marieb, E. N. and K. Hoehn (2008). Anatomy & Physiology, Benjamin Cummings Pub Co.

Masson, J., C. Sagne, M. Hamon and S. El Mestikawy (1999). "Neurotransmitter transporters in the central nervous system." *Pharmacol Rev* **51**(3): 439-64.

Matthews, D. M. (1991). Protein Absorption- Development and Present State of the Subject. New York, Wiley-Liss.

Mbassa, G., M. Elger and W. Kriz (1988). "The ultrastructural organization of the basement membrane of Bowman's capsule in the rat renal corpuscle." *Cell Tissue Res* **253**(1): 151-63.

McCarthy, C. (1998). Chromas. Southport, Queensland, Australia: Griffith University.

Mircheff, A. K., C. H. van Os and E. M. Wright (1980). "Pathways for alanine transport in intestinal basal lateral membrane vesicles." *J Membr Biol* **52**(1): 83-92.

Munck, B. G. and L. K. Munck (1999). "Effects of pH changes on systems ASC and B in rabbit ileum." *Am J Physiol* **276**(1 Pt 1): G173-84.

Murer, H. (1984). "Advantages and disadvantages of studies with vesicles on the cellular mechanisms in epithelial transport." *Boll Soc Ital Biol Sper* **60 Suppl 4**: 123-41.

Murer, H., G. Ahearn, J. Biber, G. Cassano, P. Gmaj and B. Stieger (1983). "Co- and counter-transport mechanisms in brush border membranes and basal-lateral membranes of intestine and kidney." *J Exp Biol* **106**: 163-80.

Murer, H. and P. Gmaj (1986). "Transport studies in plasma membrane vesicles isolated from renal cortex." *Kidney Int* **30**(2): 171-86.

Murer, H., U. Hopfer and R. Kinne (1976). "Sodium/proton antiport in brush-border-membrane vesicles isolated from rat small intestine and kidney." *Biochem J* **154**(3): 597-604.

Murer, H. and R. Kinne (1980). "The use of isolated membrane vesicles to study epithelial transport processes." *J Membr Biol* **55**(2): 81-95.

Nakamura, E., M. Sato, H. Yang, F. Miyagawa, M. Harasaki, K. Tomita, S. Matsuoka, A. Noma, K. Iwai and N. Minato (1999). "4F2 (CD98) heavy chain is associated covalently with an amino acid transporter and controls intracellular trafficking and membrane topology of 4F2 heterodimer." *J Biol Chem* **274**(5): 3009-16.

Nash, S. R., B. Giros, S. F. Kingsmore, K. M. Kim, S. el-Mestikawy, Q. Dong, F. Fumagalli, M. F. Seldin and M. G. Caron (1998). "Cloning, gene structure and genomic localization of an orphan transporter from mouse kidney with six alternatively-spliced isoforms." *Receptors Channels* **6**(2): 113-28.

Newey, H. and D. H. Smyth (1964). "The Transfer System for Neutral Amino Acids in the Rat Small Intestine." *J Physiol* **170**: 328-43.

Nozaki, J., M. Dakeishi, T. Ohura, K. Inoue, M. Manabe, Y. Wada and A. Koizumi (2001). "Homozygosity mapping to chromosome 5p15 of a gene responsible for Hartnup disorder." *Biochem Biophys Res Commun* **284**(2): 255-60.

O'Mara, M., A. Oakley and S. Broer (2006). "Mechanism and putative structure of B(0)-like neutral amino acid transporters." *J Membr Biol* **213**(2): 111-8.

Oliver, C. J., M. C., Ed. (2010). Immunocytochemical Methods and Protocols (3rd edition). Methods in Molecular Biology. New York, Humana Press.

Oppedisano, F., L. Pochini, M. Galluccio, M. Cavarelli and C. Indiveri (2004). "Reconstitution into liposomes of the glutamine/amino acid transporter from renal cell plasma membrane: functional characterization, kinetics and activation by nucleotides." *Biochim Biophys Acta* **1667**(2): 122-31.

Oxender, D. L. and H. N. Christensen (1963). "Evidence for two types of mediation of neutral and amino-acid transport in Ehrlich cells." *Nature* **197**: 765-7.

Palacin, M., R. Estevez, J. Bertran and A. Zorzano (1998). "Molecular biology of mammalian plasma membrane amino acid transporters." *Physiol Rev* **78**(4): 969-1054.

Peel, A. L. (2004). "Transfection of mammalian cells." *Methods Find Exp Clin Pharmacol* **33**(2): 93- 94.

Pineda, M., E. Fernandez, D. Torrents, R. Estevez, C. Lopez, M. Camps, J. Lloberas, A. Zorzano and M. Palacin (1999). "Identification of a membrane protein, LAT-2, that Co-expresses with 4F2 heavy chain, an L-type amino acid transport activity with broad specificity for small and large zwitterionic amino acids." *J Biol Chem* **274**(28): 19738-44.

Pollard, M., D. Meredith and J. D. McGivan (2002). "Characterisation and cloning of a Na(+)-dependent broad-specificity neutral amino acid transporter from NBL-1 cells: a novel member of the ASC/B(0) transporter family." *Biochim Biophys Acta* **1561**(2): 202-8.

Pontoglio, M., J. Barra, M. Hadchouel, A. Doyen, C. Kress, J. P. Bach, C. Babinet and M. Yaniv (1996). "Hepatocyte nuclear factor 1 inactivation results in hepatic dysfunction, phenylketonuria, and renal Fanconi syndrome." *Cell* **84**(4): 575-85.

Preston, R. L., J. F. Schaeffer and P. F. Curran (1974). "Structure-affinity relationships of substrates for the neutral amino acid transport system in rabbit ileum." *J Gen Physiol* **64**(4): 443-67.

Quan, H., K. Athirakul, W. C. Wetsel, G. E. Torres, R. Stevens, Y. T. Chen, T. M. Coffman and M. G. Caron (2004). "Hypertension and impaired glycine handling in mice lacking the orphan transporter XT2." *Mol Cell Biol* **24**(10): 4166-73.

Rajan, D. P., R. Kekuda, W. Huang, L. D. Devoe, F. H. Leibach, P. D. Prasad and V. Ganapathy (2000). "Cloning and functional characterization of a Na(+)-independent, broad-specific neutral amino acid transporter from mammalian intestine." *Biochim Biophys Acta* **1463**(1): 6-14.

Reimer, R. J., F. A. Chaudhry, A. T. Gray and R. H. Edwards (2000). "Amino acid transport system A resembles system N in sequence but differs in mechanism." *Proc Natl Acad Sci U S A* **97**(14): 7715-20.

Ringer, S. (1880). "On the Antagonisms of Aconitia on the Frog's Heart." *J Physiol* **2**(5-6): 436-42.

Rogers, A. B., K. S. Cormier and J. G. Fox (2006). "Thiol-reactive compounds prevent nonspecific antibody binding in immunohistochemistry." *Lab Invest* **86**(5): 526-33.

Romeo, E., M. H. Dave, D. Bacic, Z. Ristic, S. M. Camargo, J. Loffing, C. A. Wagner and F. Verrey (2006). "Luminal kidney and intestine SLC6 amino acid transporters of B0AT-cluster and their tissue distribution in Mus musculus." *Am J Physiol Renal Physiol* **290**(2): F376-83.

Rossier, G., C. Meier, C. Bauch, V. Summa, B. Sordat, F. Verrey and L. C. Kuhn (1999). "LAT2, a new basolateral 4F2hc/CD98-associated amino acid transporter of kidney and intestine." *J Biol Chem* **274**(49): 34948-54.

Rudnick, G. (1998). "Bioenergetics of neurotransmitter transport." *J Bioenerg Biomembr* **30**(2): 173-85.

Saier, M. H., Jr. (2000). "Families of transmembrane transporters selective for amino acids and their derivatives." *Microbiology* **146 (Pt 8)**: 1775-95.

Sakata, K., S. Shimada, T. Yamashita, K. Inoue and M. Tohyama (1999). "Cloning of a bovine orphan transporter and its short splicing variant." *FEBS Lett* **443**(3): 267-70.

Sambrook, J. R., D.W. (2001). Molecular Cloning: A laboratory manual. New York, Cold Spring Harbor Laboratory.

Satoh, O., Y. Kudo, H. Shikata, K. Yamada and T. Kawasaki (1989). "Characterization of amino-acid transport systems in guinea-pig intestinal brush-border membrane." *Biochim Biophys Acta* **985**(2): 120-6.

Schultz, S. G., P. F. Curran, R. A. Chez and R. E. Fuisz (1967). "Alanine and sodium fluxes across mucosal border of rabbit ileum." *J Gen Physiol* **50**(5): 1241-60.

Scriver, C. R., B. Mahon, H. L. Levy, C. L. Clow, T. M. Reade, J. Kronick, B. Lemieux and C. Laberge (1987). "The Hartnup phenotype: Mendelian transport disorder, multifactorial disease." *Am J Hum Genet* **40**(5): 401-12.

Scriver, C. R. and H. S. Tenenhouse (1985). "Genetics and mammalian transport systems." *Ann N Y Acad Sci* **456**: 384-97.

Seldin, D. W. (2000). The Kidney: Physiology and Pathophysiology. Philadelphia, Lippicott Williams & Wilkins.

Seow, H. F., S. Broer, A. Broer, C. G. Bailey, S. J. Potter, J. A. Cavanaugh and J. E. Rasko (2004). "Hartnup disorder is caused by mutations in the gene encoding the neutral amino acid transporter SLC6A19." *Nat Genet* **36**(9): 1003-7.

Sepulveda, F. V. and M. W. Smith (1978). "Discrimination between different entry mechanisms for neutral amino acids in rabbit ileal mucosa." *J Physiol* **282**: 73-90.

Shafqat, S., M. Velaz-Faircloth, A. Guadano-Ferraz and R. T. Fremeau, Jr. (1993). "Molecular characterization of neurotransmitter transporters." *Mol Endocrinol* **7**(12): 1517-29.

Silbernagl, S., E. C. Foulkes and P. Deetjen (1975). "Renal transport of amino acids." *Rev Physiol Biochem Pharmacol* **74**: 105-67.

Singer, D., S. M. Camargo, K. Huggel, E. Romeo, U. Danilczyk, K. Kuba, S. Chesnov, M. G. Caron, J. M. Penninger and F. Verrey (2009). "Orphan transporter SLC6A18 is renal neutral amino acid transporter B0AT3." *J Biol Chem* **284**(30): 19953-60.

Smith, H. (1951). The Kidney: Structure and Function in Health and Disease. New York, Oxford University Press.

Storck, T., S. Schulte, K. Hofmann and W. Stoffel (1992). "Structure, expression, and functional analysis of a Na(+)-dependent glutamate/aspartate transporter from rat brain." *Proc Natl Acad Sci U S A* **89**(22): 10955-9.

Sugawara, M., T. Nakanishi, Y. J. Fei, W. Huang, M. E. Ganapathy, F. H. Leibach and V. Ganapathy (2000). "Cloning of an amino acid transporter with functional characteristics and tissue expression pattern identical to that of system A." *J Biol Chem* **275**(22): 16473-7.

Sugawara, M., M. Sasaki, K. Iseki and K. Miyazaki (1992). "Membrane-potential-dependent uptake of tryptamine by rat intestinal brush-border membrane vesicles." *Biochim Biophys Acta* **1111**(2): 145-50.

Sundaram, U., S. Wisel and S. Coon (2007). "Neutral Na-amino acid cotransport is differentially regulated by glucocorticoids in the normal and chronically inflamed rabbit small intestine." *Am J Physiol Gastrointest Liver Physiol* **292**(2): G467-74.

Tailor, C. S., M. Marin, A. Nouri, M. P. Kavanaugh and D. Kabat (2001). "Truncated forms of the dual function human ASCT2 neutral amino acid transporter/retroviral receptor are translationally initiated at multiple alternative CUG and GUG codons." *J Biol Chem* **276**(29): 27221-30.

Takanaga, H., B. Mackenzie, J. B. Peng and M. A. Hediger (2005). "Characterization of a branched-chain amino-acid transporter SBAT1 (SLC6A15) that is expressed in human brain." *Biochem Biophys Res Commun* **337**(3): 892-900.

Taylor, P. M., C. J. Egan and M. J. Rennie (1989). "Transport of glutamine across blood-facing membranes of perfused rat jejunum." *Am J Physiol* **256**(4 Pt 1): E550-8.

Terada, T., Y. Shimada, X. Pan, K. Kishimoto, T. Sakurai, R. Doi, H. Onodera, T. Katsura, M. Imamura and K. Inui (2005). "Expression profiles of various transporters for oligopeptides, amino acids and organic ions along the human digestive tract." *Biochem Pharmacol* **70**(12): 1756-63.

Thomas, E. L. and H. N. Christensen (1970). "Indications of spatial relations among structures recognizing amino acids and Na+ at a transport receptor site." *Biochem Biophys Res Commun* **40**(2): 277-83.

Torres, R. M. a. K., R. (1997). Laboratory protocols for conditional gene targeting New York, Oxford University Press.

Tortora, G. J. and B. Derrickson (2009). Principles of Anatomy and Physiology, John Wiley & Sons, Inc.

Utsunomiya-Tate, N., H. Endou and Y. Kanai (1996). "Cloning and functional characterization of a system ASC-like Na+-dependent neutral amino acid transporter." *J Biol Chem* **271**(25): 14883-90.

Van Slyke, D. D. a. M., G.M. (1913). "The Fate of Protein DigestionProducts in The Body. III. The Absorption of Amino- Acid from the Blood by the Tissues." *J Biol Chem* **16**(2): 197-212.

Van Winkle, L. J., D. F. Mann, A. L. Campione and B. H. Farrington (1990). "Transport of benzenoid amino acids by system T and four broad scope systems in preimplantation mouse conceptuses." *Biochim Biophys Acta* **1027**(3): 268-77.

Van Winkle, L. J. (1999). Biomembrane Transport. San Diego, Academic Press.

Vanslambrouck, J. M., A. Broer, T. Thavyogarajah, J. Holst, C. G. Bailey, S. Broer and J. E. Rasko (2010). "Renal imino acid and glycine transport system ontogeny and involvement in developmental iminoglycinuria." *Biochem J.*

Veljkovic, E., S. Stasiuk, P. J. Skelly, C. B. Shoemaker and F. Verrey (2004). "Functional characterization of Caenorhabditis elegans heteromeric amino acid transporters." *J Biol Chem* **279**(9): 7655-62.

Verrey, F., Z. Ristic, E. Romeo, T. Ramadan, V. Makrides, M. H. Dave, C. A. Wagner and S. M. Camargo (2005). "Novel renal amino acid transporters." *Annu Rev Physiol* **67**: 557-72.

Wagner, C. A., A. Broer, A. Albers, N. Gamper, F. Lang and S. Broer (2000). "The heterodimeric amino acid transporter 4F2hc/LAT1 is associated in Xenopus oocytes with a non-selective cation channel that is regulated by the serine/threonine kinase sgk-1." *J Physiol* **526 Pt 1**: 35-46.

Wang, H., M. P. Kavanaugh, R. A. North and D. Kabat (1991). "Cell-surface receptor for ecotropic murine retroviruses is a basic amino-acid transporter." *Nature* **352**(6337): 729-31.

Wasserman, J. C., E. Delpire, W. Tonidandel, R. Kojima and S. R. Gullans (1994). "Molecular characterization of ROSIT, a renal osmotic stress-induced Na(+)-Cl(-)-organic solute cotransporter." *Am J Physiol* **267**(4 Pt 2): F688-94.

Wilde, S. W. and M. S. Kilberg (1991). "Glutamine transport by basolateral plasma-membrane vesicles prepared from rabbit intestine." *Biochem J* **277 (Pt 3)**: 687-91.

Yamashita, A., S. K. Singh, T. Kawate, Y. Jin and E. Gouaux (2005). "Crystal structure of a bacterial homologue of Na+/Cl--dependent neurotransmitter transporters." *Nature* **437**(7056): 215-23.

Yao, D., B. Mackenzie, H. Ming, H. Varoqui, H. Zhu, M. A. Hediger and J. D. Erickson (2000). "A novel system A isoform mediating Na+/neutral amino acid cotransport." *J Biol Chem* **275**(30): 22790-7.

Yernool, D., O. Boudker, Y. Jin and E. Gouaux (2004). "Structure of a glutamate transporter homologue from Pyrococcus horikoshii." *Nature* **431**(7010): 811-8.

Young, J. A. and K. D. Edwards (1966). "Clearance and stop-flow studies on histidine and methyldopa transport by rat kidney." *Am J Physiol* **210**(3): 667-75.

Young, J. A. and B. S. Freedman (1971). "Renal tubular transport of amino acids." *Clin Chem* **17**(4): 245-66.

Zerangue, N. and M. P. Kavanaugh (1996). "ASCT-1 is a neutral amino acid exchanger with chloride channel activity." *J Biol Chem* **271**(45): 27991-4.

Zhang, H., J. Wada, K. Hida, Y. Tsuchiyama, K. Hiragushi, K. Shikata, H. Wang, S. Lin, Y. S. Kanwar and H. Makino (2001). "Collectrin, a collecting duct-specific transmembrane glycoprotein, is a novel homolog of ACE2 and is developmentally regulated in embryonic kidneys." *J Biol Chem* **276**(20): 17132-9.

Appendix A

Plasmid maps

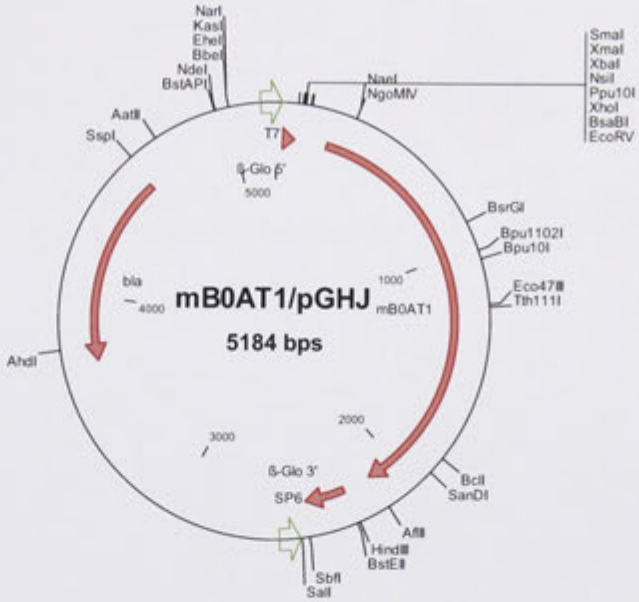
NarI
KasI
EheI
BbeI
NdeI
BstAPI
AatII
SspI
AhdI
NaeI
NgoMIV
SmaI
XmaI
XbaI
NsiI
Ppu10I
XhoI
BsaBI
EcoRV
T7
ß-Glo β'
5000
BsrGI
Bpu1102I
Bpu10I
Eco47III
Tth111I
bla
4000
mB0AT1/pGHJ
1000
mB0AT1
5184 bps
2000
3000
ß-Glo 3'
SP6
BclI
SanDI
AflII
HindIII
BstEII
SbfI
SalI

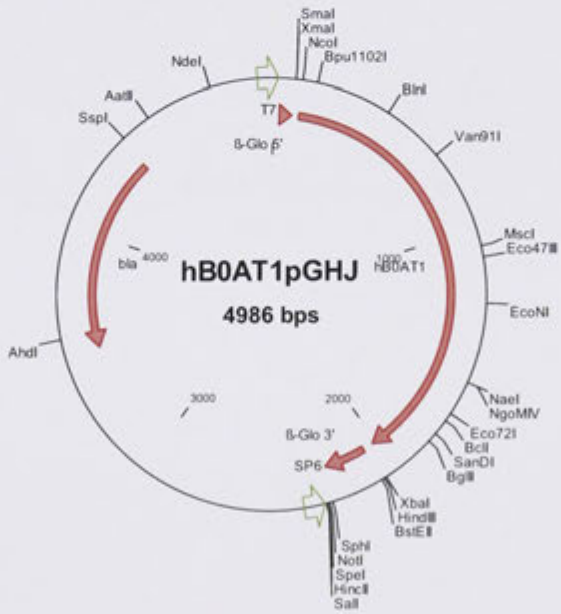
SmaI
XmaI
NcoI
Bpu1102I
NdeI
AatII
SspI
AhdI
T7
ß-Glo β'
BlnI
Van91I
MscI
Eco47III
EcoNI
bla
4000
hB0AT1pGHJ
1000
hB0AT1
4986 bps
3000
2000
ß-Glo 3'
SP6
NaeI
NgoMIV
Eco72I
BclI
SanDI
BglII
XbaI
HindIII
BstEII
SphI
NotI
SpeI
HincII
SalI

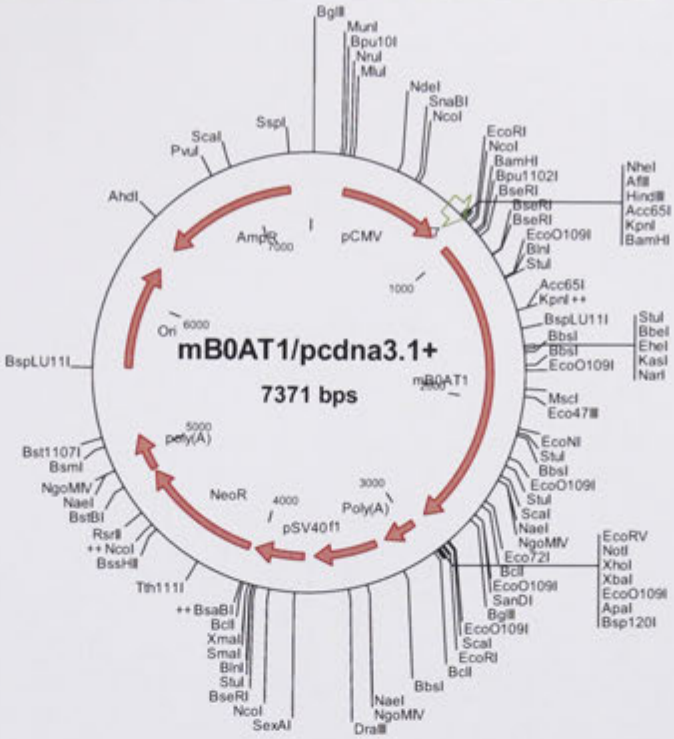
mB0AT1/pcdna3.1+
7371 bps
pCMV
mB0AT1
Poly(A)
pSV40f1
NeoR
Amp R
Ori
pA
BglII
MunI
Bpu10I
NruI
MluI
NdeI
SnaBI
NcoI
EcoRI
NcoI
BamHI
Bpu1102I
BseRI
NheI
AflII
HindIII
Acc65I
KpnI
BamHI
EcoO109I
BlnI
StuI
Acc65I
KpnI ++
BspLU11I
StuI
BbeI
BbsI
EheI
BbsI
KasI
EcoO109I
NarI
MscI
Eco47III
EcoNI
StuI
BbsI
EcoO109I
StuI
ScaI
NaeI
NgoMIV
Eco72I
EcoRV
NotI
XhoI
XbaI
EcoO109I
ApaI
Bsp120I
BclI
EcoO109I
SanDI
BglII
EcoO109I
ScaI
EcoRI
BclI
BbsI
NaeI
NgoMIV
DraIII
NcoI
SexAI
BseRI
StuI
BlnI
SmaI
XmaI
BclI
++BsaBI
Tth111I
BssHII
RsrII
++NcoI
BstBI
NaeI
NgoMIV
BsmI
Bst1107I
BspLU11I
AhdI
ScaI
PvuI
SspI
mB0AT2
pGHJ
5362 bps
T7
ß-Glo 5'
ß-Glo 3'
SP6
bla
NarI
KasI
EheI
BbeI
NdeI
BstAPI
EcoO109I
AatII
SmaI
XmaI
XbaI
XhoI
BsaBI
BstBI
BclI
BsmI
BsaAI
BglII
Bpu10I
Eco47III
HindIII
BstEII
SbfI
AccI
HincII
SalI
StuI
SapI
ScaI
BpmI
Ctr10I
BsaI

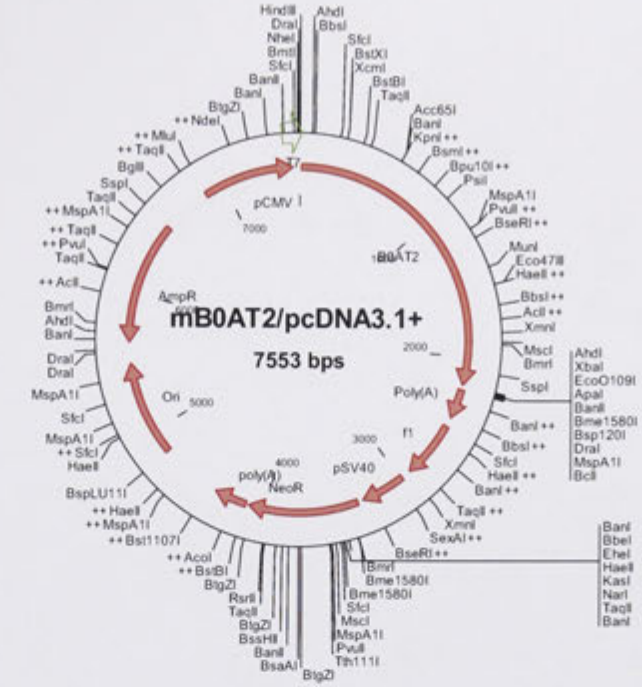
mB0AT2/pcDNA3.1+
7553 bps
pCMV
T7
mB0AT2
AmpR
Ori
Poly(A)
f1
pSV40
poly(A)
NeoR
2000
3000
4000
5000
7000

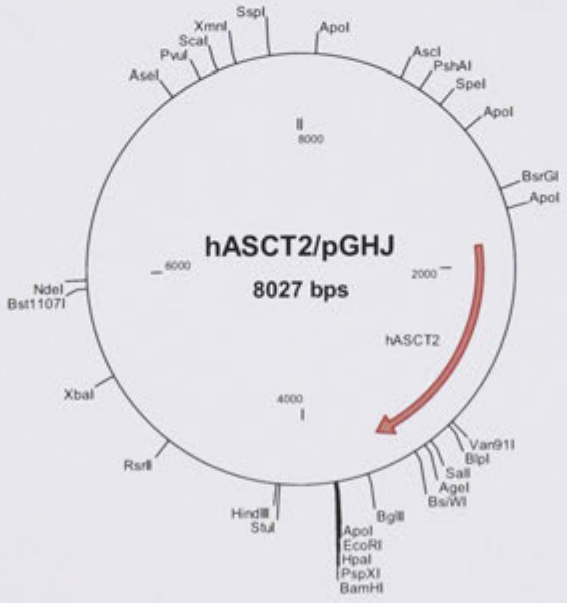
hASCT2/pGHJ
8027 bps
hASCT2
2000
4000
6000
8000

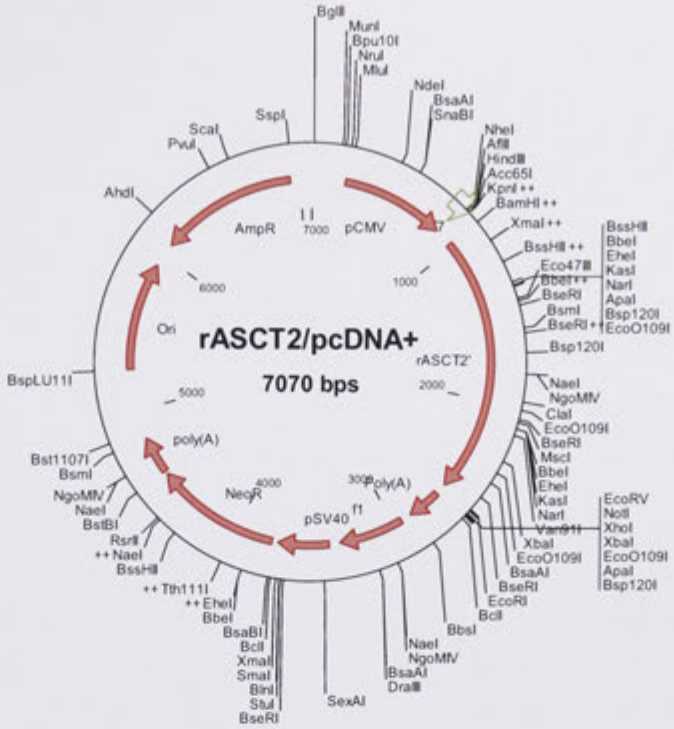
rASCT2/pcDNA+
7070 bps
AmpR
pCMV
rASCT2'
Ori
poly(A)
NeoR
Poly(A)
pSV40
f1
1000
2000
3000
4000
5000
6000
7000
BglII
MunI
Bpu10I
NruI
MluI
NdeI
BsaAI
SnaBI
NheI
AflII
HindIII
Acc65I
KpnI++
BamHI++
XmaI++
BssHII++
Eco47III
BseRI
BsmI
BseRI++
Bsp120I
NaeI
NgoMIV
ClaI
EcoO109I
BseRI
MscI
BbeI
EheI
KasI
NarI
XbaI
EcoO109I
BsaAI
BseRI
EcoRI
BclI
BbsI
NaeI
NgoMIV
BsaAI
DraIII
SexAI
BseRI
StuI
BlnI
SmaI
XmaI
BclI
BsaBI
BbeI
++EheI
++Tth111I
BssHII
++NaeI
RsrII
BstBI
NaeI
NgoMIV
BsmI
Bst1107I
BspLU11I
AhdI
PvuI
ScaI
SspI
BssHII
BbeI
EheI
KasI
NarI
ApaI
Bsp120I
EcoO109I
EcoRV
NotI
XhoI
XbaI
EcoO109I
ApaI
Bsp120I

Appendix B

Antibodies and their used dilutions

Antibody	Description	Raised in	Supplier
Primary antibodies			
Anti-mouse B^0AT1 N-term	Anti-mouse B^0AT1N-term (against GST fusion protein)	rabbit	Pineda
Anti-human B^0AT1 N-term	Anti-mouse B^0AT1N-term (against GST fusion protein)	chicken	Pineda
Anti-mouse B^0AT2 N-term	Anti-mouse B^0AT2 N-term (against GST fusion protein)	rabbit	Pineda
Anti-mouse B^0AT2 C-term	Anti-mouse B^0AT2 C-term (against GST fusion protein)	rabbit	Pineda
Anti-mouse ASCT2 N-term	Anti-mouse ASCT2 (against a ASCT2 N-term peptide)	rabbit	Pineda
Anti-human ASCT2 C-term	Anti-human ASCT2 (against a ASCT2 C-term peptide)	rabbit	Avissar laboratory
Anti-mouse CD98	Anti-mouse	rat	Pharmingen
LTL	Biotinylated Lotus Tetragonolobus lectin		Vector Laboratories
Secondary antibodies			
Alexa Fluor 488 (AF488) donkey anti-rabbit IgG	Alexa Fluor 488 conjugated to an anti-rabbit IgG	donkey	Invitrogen
Alexa Fluor 488 (AF488) goat anti-chicken IgG	Alexa Fluor 488 conjugated to an anti-chicken IgG	goat	Invitrogen
Texas Red Strepavidin	Texas Red conjugated to Strepavidin		Vector Laboratories
ECL Anti-rabbit IgG, horseradish peroxidise (HRP)	Horseradish peroxidase conjugated to a mouse IgG	mouse	Amersham

	Dilution for Western Blot analysis	
Detected protein	**Primary antibody**	**Secondary antibody**
B^0AT1	Anti-mouse B^0AT1 N-term 1:3,000	Anti-rabbit HRP 1:5,000
B^0AT2	Anti-mouse B^0AT2 N-term 1:3,000	Anti-rabbit HRP 1:5,000
ASCT2	Anti-mouse ASCT2 N-term 1:500	Anti-mouse HRP 1:2,000
ASCT2	Anti-human B^0AT1 N-term 1:1,000	Anti-mouse HRP 1:5,000
4F2	Anti-mouse CD98 1:500	Anti-mouse HRP 1:10,000

	Dilution for immunofluorescence studies with oocytes	
Detected protein	**Primary antibody**	**Secondary antibody**
B^0AT1	Anti-mouse B^0AT1N-term 1.200	AF488 donkey anti-rabbit 1:1000
B^0AT1	Anti-human B^0AT1 N-term 1:200	AF488 goat anti-chicken 1:1000
B^0AT2	Anti-mouse B^0AT2 N-term N/C1:200	AF488 donkey anti-rabbit 1:800

	Dilution for immunofluorescence studies on cells	
Detected protein	**Primary antibody**	**Secondary antibody**
B^0AT2	Anti-human B^0AT1 N-term 1:50	AF488 donkey anti-rabbit 1:600
ASCT2	Anti-mouse ASCT2 N-term 1:50	AF488 donkey anti-rabbit 1:800
ASCT2	Anti-human B^0AT1 N-term 1:50	AF488 donkey anti-rabbit 1:800

	Dilution for immunofluorescence studies on tissue sections	
Detected protein	**Primary antibody**	**Secondary antibody**
B^0AT1	B^0AT1 Nterm 1:500	AF488 donkey anti-rabbit 1:800
B^0AT2	B^0AT2 N-term 1:60	AF488 donkey anti-rabbit 1:800
LTL	Biotinylated Lotus Tetragonolobus lectin 1:400	Texas Red Streptavidin 1:300

Appendix C

Primers

Primer name	Sequence (5' → 3')	Purpose
		Primers used for PCR
B^0AT2 with *HindIIIs	CAGAAGCTTCCACCATGCCTAAGA	Generating B0AT2 with *HindIII at 5'-end
B^0AT2 with *XbaIa	CAGTCTAGACTACAAGTCAGACTC	Generating B0AT2 with *XbaI at 3'-end
		Primers used for RT PCR
Actin-sense	GCTCACCATGGATGATGATATCGC	Generating actin (1kb)
Actin antisense	GGAGGAGCAATGATCTTGATCTTC	Generating actin (1kb)
Mv7-3Nterm1s	ATGCCTAAGAATAGCAAAGTG	Generating B^0AT2 N-term
Mv7-3Nterm1a	TTGCAGCTTACTGTTCCAGGC	Generating B^0AT2 N-term
Mv7-3Cterm1s	CGTCGCTGCAACCTCATAGAT	Generating B^0AT2 C-term
Mv7-3Cterm1a	CAAGTCAGACTCTGGCATATC	Generating B^0AT2 C-term
		Primers used for sequencing
B02 into pcDNA a	CTCAGTGGAAGAGGTTTCTAAGAAG	Sequencing B^0AT2-pcDNA
B02 into pcDNA s	CAAGTGGTTCCCCAACACTGG	Sequencing B^0AT2-pcDNA
B02 in pcDNA seq s	GACTCAGTGGAAGAGGTTTCTAAG	Sequencing B^0AT2-pcDNA
pcDNA3.1 rev	TAGAAGGCACAGTCGAGG	Sequencing pcDNA
SP6	ATTAGGTGACACTATAG	Sequencing from the SP6 promotor
T7	TAATACGACTCACTATAGGG	Sequencing from the T7 promotor